Source identification of air pollutants in the Arctic, their seasonal and long-term trends using an atmospheric transport model and measurement data

David Arne Hirdman

Series of dissertations submitted to the
Faculty of Mathematics and Natural Sciences, University of Oslo
No. 980

ISSN 1501-7710

Cover: Inger Sandved Anfinsen.
Printed in Norway: AiT e-dit AS.

Produced in co-operation with Unipub.
The thesis is produced by Unipub merely in connection with the
thesis defence. Kindly direct all inquiries regarding the thesis to the copyright
holder or the unit which grants the doctorate.

Acknowledgements

The research presented in this thesis has been carried out at the Norwegian Institute for Air Research (NILU) in collaboration with the University of Oslo, and financial support from the Norwegian Research Council through the POLARCAT project. This support is gratefully acknowledged.

Throughout the project I have been fortunate to collaborate with a number of scientists both at the institute and abroad who have contributed to this work. I want to thank Prof. Jón Egill Kristjánsson for being my supervisor at UiO.

The staff at NILU and especially at the ATMOS department is greatly appreciated for their scientific input and unforgettable social companionship. A special thanks to Kristine "Kikki" Aasarød for keeping track of everything and taking care of my plants when I have been away.

I would like to express my gratefulness to people in the FLEXPART group and particularly to Harald Sodemann, John F. Burkhart and Sabine Eckhardt for their everlasting support and inspiration during all the different stages of this thesis.

Above all I want to gratefully recognize my head supervisor Dr. Andreas Stohl for his tireless and everlasting patience on top of all invaluable scientific comments, making me aim higher at every stage of this project.

I am grateful to Dr. Andreas Stohl, the head of the department Dr. Kjetil Tørseth, and the NILU administration for giving me the opportunity to finish my thesis by prolonging my position at NILU.

I deeply appreciate the unconditional support I have received from my family and friends.

Finally, I would like to express my sincere gratitude to Viktoria without whose loving patience, spending endless hours with me in my office when analyzing, and deliveries of the water of life (FILMJÖLK) from Sweden I would have been completely lost.

List of publications

This thesis comprises the work presented in the following three papers:

I. Hirdman D., Aspmo K., Burkhart J.F., Eckhardt S., Sodemann H., Stohl A.: Transport of mercury in the Arctic atmosphere: Evidence for a springtime net sink and summertime source , Geophys. Res. Lett., 36, L12814, doi: 10.1029/2009GL038345, 2009

II. Hirdman D., Sodemann H., Eckhardt S., Burkhart J.F., Jefferson A., Mefford T., Quinn P.K., Sharma S., Ström J., Stohl A.: Source identification of short-lived air pollutants in the Arctic using statistical analysis of measurement data and particle dispersion model output, Atmos. Chem. Phys, 10, 669-693, 2010.

III. Hirdman D., Burkhart J.F., Sodemann H., Eckhardt S., Jefferson A., Quinn P.K., Sharma S., Ström J., Stohl A.: Long-term trends of black carbon and sulphate aerosol in the Arctic: Changes in atmospheric transport and source region emissions, Atmos. Chem. Phys. Disc., 10, 12133-12184, 2010.

Content

1. Introduction **1**

2. The Arctic and Its Climate Sensitivity **2**
2.1. Radiative Balance 2
2.2. Atmopsheric Transport into the Arctic Troposphere 4
2.3. Arctic Haze and Other Types of Air Pollution Episodes 5
2.3.1 Arctic Haze 5
2.3.2 Light Absorbing Aerosols, Equivalent Black Carbon (EBC) 7
2.3.3 Light Scattering Aerosols 7
2.3.4 Sulphate 8
2.3.5 Tropospheric Ozone (O_3) 8
2.3.6 Gaseous Elemental Mercury (GEM) 8

3. Model **9**

4. Observations **11**
4.1. Measurement Sites 11
4.2. Measurement Data 12
4.3. Data and Model Output Averaging 14

5. Statistical Method **15**

6. Aim of the Papers and Broader Implications **16**

7. Conclusions **18**

8. Outlook **20**

9. References **21**

10. Summaries of the Individual Papers Presented in This Thesis **28**

Paper I-III **31**

1 Introduction

In the ongoing and lately intensified research on the global climate, the polar regions have received particular attention since some of the most visible changes have been observed there (Law and Stohl, 2007).

While current emissions in the high Arctic (north of 70°N) are negligible, recent geopolitical activities are increasing as a result of increased access to the region coincident with the decreasing extent of the Arctic sea ice. Arctic nations recognize the potential opportunities for exploitation of previously inaccessible natural resources such as minerals, oil, and gas beneath the sea bed of the Arctic Ocean. A recent report by Gautier et al. (2009) estimates that as much as 30% of the world's undiscovered gas and 13% of its undiscovered oil may be found here. A thinning and retreating sea ice has also reinvigorated interest in commercial realization of the northern sea route between the North Atlantic Ocean and the North Pacific Ocean (through the Northwest and Northeast Passage). Recent studies have supported both the feasibility and the economical benefit of such a route (Somanathan et al., 2009; Sou and Flato, 2009). Further, the interest of future Arctic prospects is not limited to the five Arctic countries (Canada, Denmark, Norway, Russia and USA). East Asian states such as China, Japan, North and South Korea would all benefit enormously from increased accessibility to the Arctic, providing shorter commercial shipping routes as well as the possibility of new fishing grounds along with other natural resources. China, an emerging world super power, is already preparing for an ice-free Arctic on several levels with, for example, ongoing bilateral dialogues with both Canada and Norway (Jakobson, 2010). But all these prospective economical benefits have associated environmental consequences. The introduction of new emission sources directly in the Arctic could, along with the clear direct effect on the composition of the atmosphere, pose a large threat to both the surface and marine environments such as the different mammal populations living within the Arctic (AMAP 2006,2007; Granier et al., 2006; Dalsøren et al., 2007; Lack et al., 2008; Huntington, 2009;).

The need for a more accurate way to identify and quantify potential source regions of species which affect the Arctic atmosphere is therefore great. It is important to know the relative importance if inner-Arctic sources versus transport of pollutants from lower latitudes into the Arctic.

As a part of the International Polar Year (IPY) an immense international science collaboration project was launched called POLARCAT (POLar study using Aircraft, Remote sensing, surface measurements and modelling of Climate, chemistry, Aerosols and Transport). The project objectives were to investigate the transport of air pollution (e.g. aerosols) from anthropogenic sources and boreal forest fires into the Arctic and address its effects on the atmospheric chemistry and climate. During several campaigns taking place at various locations in the Arctic during the spring and summer of 2008, well-coordinated observations were carried out using seven aircraft, a ship, a train, controlled meteorological balloons, and surface stations. In addition to the suite of *in situ* measurements, special satellite and numerical models products were developed. Regardless, however well-coordinated and equipped these campaigns are, they only capture a

snapshot of the atmospheric composition and are therefore only able to explain the specific sources of events encountered during the campaign (e.g. Warneke et al., 2009, 2010). To put these discoveries into a broader perspective in terms of seasonal and interannual variability, as well as the long-term importance of different source regions and the magnitude of influence over time, a complementary approach is required. The objectives of the work outlined in this dissertation specifically fill this void. By combining long-term measurement data of several species at 4 different observatories located across the Arctic, together with calculations from the Lagrangian dispersion model FLEXPART, I address these issues through a rigorous statistical analysis of the spatio-temporal variability of emission sensitivities and source regions over time.

2 The Arctic and Its Climate Sensitivity

The Arctic is a unique environment as a result of its generally cold temperatures, underlying snow and ice, and low height of the troposphere prohibiting to large extent transport influence from lower latitudes. It also experiences prolonged periods of darkness (winter) followed by periods of continuous light (summer). Due to its remote location the Arctic was for long believed also to be a pristine environment. Although early polar explorers such as Nordenskiöld (1883) and Nansen (1961) reported finding dark deposits on the snow in the 1880-1890's and Nansen furthermore speculated on distant sources of these deposits, this knowledge was thereafter forgotten until Mitchell (1957) in the late 1940's and 1950's reported about turbidity layers spotted in the Arctic atmosphere when flying reconnaissance flights for the U.S. Air Force. In the beginning of the 1970s' radiation measurements once again rediscovered the phenomenon and a more targeted research started to investigate its source (Rahn et al., 1977). Trajectory studies at the time suggested what "chemical fingerprinting" later confirmed, that the origin of the haze was anthropogenic. Nonetheless, it took until the late 1970s for scientists to realize that the haze was air pollution transported from the middle latitudes (Rahn et al., 1977; Rahn and McCaffrey, 1980; Iversen and Joranger, 1985; Barrie, 1986).

2.1 Radiative Balance

The radiative balance in the Arctic is delicate due to extreme contrasts in surface albedo between the highly reflective surfaces of snow and ice, and the dark and highly absorbing surface of the Arctic Ocean (Fig. 1). To this comes the influence from clouds, for which the effect may be both cooling through reflection of incoming solar radiation as well as warming by absorbing and reemitting or reflecting long and short-wave radiation, respectively, from the surface.

In winter, the longwave radiation completely dominates the radiative balance in the absence of sunlight interacting between the ice and snow covered surface and clouds and greenhouse gases in the atmosphere (left part of Fig. 1). In spring the sun returns, and with it, a whole new set of radiative interactions due to the entry of shortwave radiation to the atmosphere (middle and right part of Fig. 1). Some of the energy is

absorbed already in the upper atmosphere by gases, such as ozone, whereas large portions of it continues down where it may be reflected or absorbed by clouds or gases in the atmosphere. The fraction of the sunlight that reaches the Earth's surface may be reflected or absorbed. The ratio of reflected to incoming radiation at the surface is called albedo, and represents the reflectivity of the surface. When the sun strikes a snow-covered surface, up to 95% of the sunlight may be reflected, whereas sea ice reflects 30 to 40% of the incoming sunlight. Water surfaces, on the other hand, reflect only about 10% of the solar energy. The albedo of clouds is more complex as, their reflectivity depends on the thickness and microphysical properties and varies between 30-90%. Furthermore, the net change in albedo by clouds depends also on the reflectivity of the surface beneath them. A decreased extent of the Arctic sea ice due to a warming climate consequently results in a strong positive feedback increasing the warming.

The atmospheric life-time of the airborne pollutants are generally much longer in the Arctic than at lower latitudes due to slow removal processes in the Arctic atmosphere, thereby prolonging the time they directly and indirectly may affect the radiative balance. If later deposited on a snow or ice-covered surface the pollutant may continue to have an effect on the radiative balance by altering the surface's albedo as illustrated for the influence of black carbon (BC) in Fig. 1.

Due to these strong feedback mechanisms as well as large natural variability on different time-scales, the Arctic air temperatures have increased with a rate almost two times the global average over the past century (IPCC, 2007).

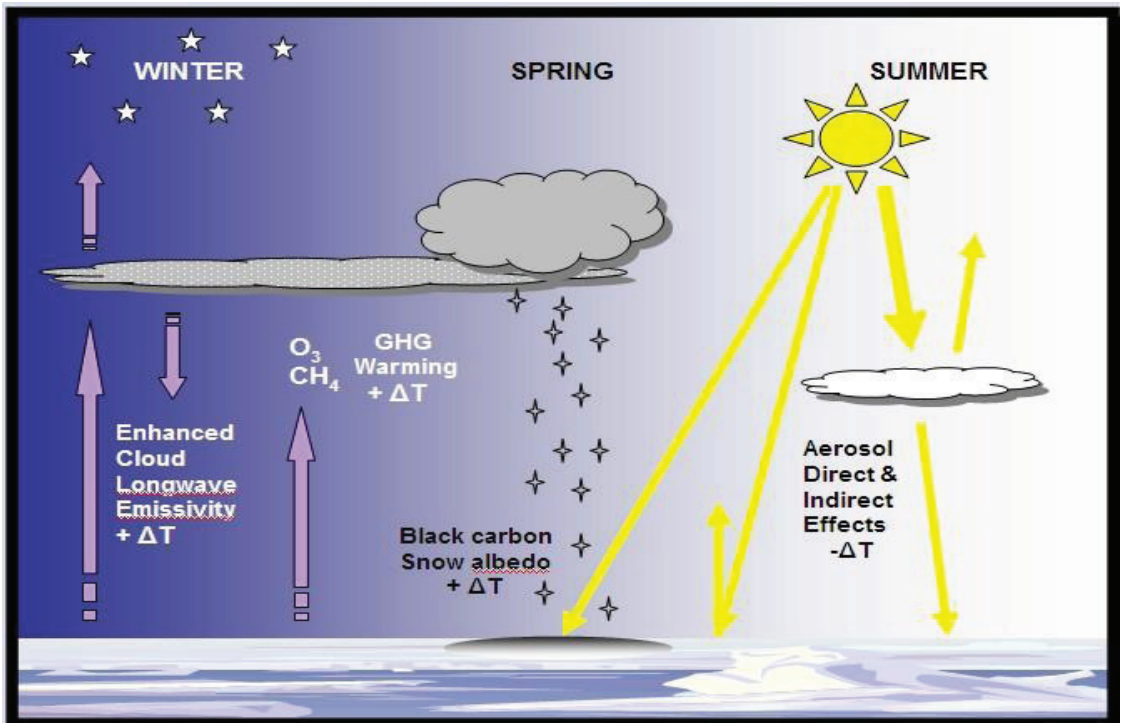

Figure 1. Schematic figure over the radiative balance of the Arctic atmosphere and its seasonal variation.

2.2 Atmospheric Transport into the Arctic Troposphere

One way of looking at atmospheric transport is from an isentropic perspective where the atmosphere consists of surfaces of constant potential temperature which form folded shells/domes over the Arctic, where the minimum value would be found in the boundary layer (Klonecki et al. 2003). The polar dome concept is just another way of looking at the Arctic front where temperature has a strong gradient. The Arctic front functions as a barrier against transport into the lower Arctic troposphere. In this kind of transport the transported air must have the same potential temperature as the destination. If this is not the case to begin with, it may get there by diabatic cooling through passage over colder surfaces, such as snow and ice covered land regions. These transport events are very episodic, and normally associated with synoptic blocking events (Raatz and Shaw 1984; Iversen and Joranger 1985). The required cooling makes the pathway over Northern Eurasia into the Arctic a predominant one. It is more difficult for pollutants emitted in other, warmer regions, to reach the Arctic troposphere than for pollutants emitted from source regions that are already north of the Arctic front or very close to it. This emphasizes relatively cold geographical regions such as Northern Eurasia (in winter) at the expense of regions further south that are too warm for air masses to reach the Arctic troposphere (Rahn 1981, Barrie 1986). In contrast, pollution from North America is transported out over the North Atlantic Ocean where the air is diabatically heated (Klonecki et al. 2003) and pollutants are frequently exposed to wet deposition processes in the development of cyclones travelling east towards Europe.

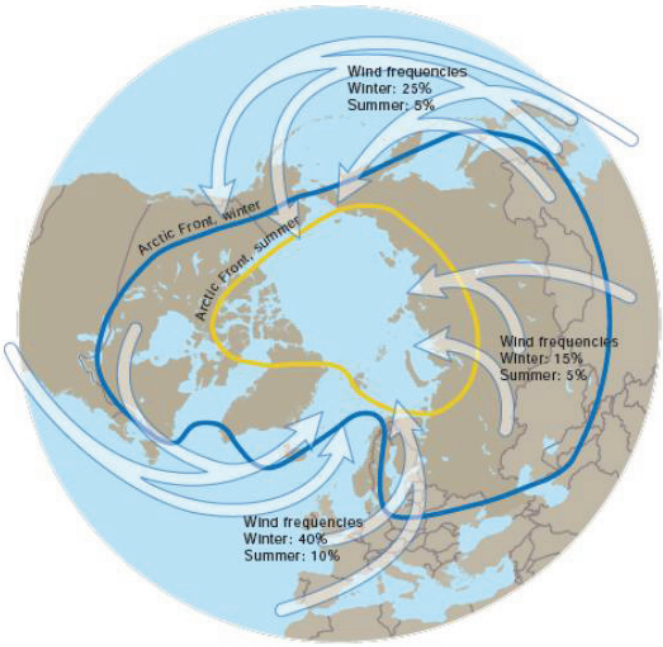

Figure 2. Mean position of the Arctic air mass in winter (January, in blue) and summer (July, in yellow), superimposed on the percentage frequency of major south-to-north transport routes into the Arctic (AMAP, 1998).

2.3 Arctic Haze and Other Types of Air Pollution Episodes

Recently, there has been renewed interest in Arctic air pollution because of its potential effects on climate. Warming is proceeding fastest in the Arctic due to strong feedbacks at high latitudes. While long-lived greenhouse gases undoubtedly are the strongest drivers of climate change, Quinn et al. (2008) argue that short-lived pollutants may also contribute to the Arctic warming and ice melt. The melt of snow/ice triggers further feedback mechanisms through a decrease of the albedo (Flanner and Zender, 2006; Flanner et al., 2007). BC changes the radiative balance in the Arctic through absorption of shortwave radiation in the atmosphere as well as by decreasing the surface albedo when deposited on snow or ice (Warren and Wiscombe, 1985; Hansen and Nazarenko, 2004). Tropospheric ozone (O_3) affects the Arctic atmosphere both locally by altering the radiation fluxes as well as more remotely by modulating heat transport into the Arctic (Shindell, 2007). Sulphate and nitrate aerosols cause scattering of shortwave radiation and also modify the optical properties of clouds (indirect aerosol effects) and like all aerosols they are subject to scavenging processes through dry and/or wet deposition which governs the distance they may be transported before being scavenged out (AMAP, 2006). While this shortwave scattering generally leads to a cooling of the surface, aerosols may also lead to increased thermal emissivity of thin Arctic clouds and, thus, a warming of the surface (Garrett and Zhao, 2006). Reductions in the concentration levels of short-lived pollutants could be an effective means to slow climate change in the Arctic (Quinn et al., 2008).

2.3.1 Arctic Haze

Arctic haze is a condition of reduced visibility (Fig. 3). When viewed away from the sun it appears greyish-blue, looking into the sun it appears reddish-brown. It typically has a layered structure but on average no distinct upper and lower boundaries, and produces none of the optical phenomena that would be expected if it were composed of ice crystals (Barrie, 1986). The haze is generally composed of sulphate and particulate organic matter and to a lesser extent ammonium, BC, nitrate, dust aerosols and distinct heavy metals (Quinn et al., 2007), and it is accompanied by enhanced concentrations of gaseous pollutants (Barrie, 1986). One of the striking things about Arctic haze is its strong seasonal variation. Both the optical effects of the haze and the concentrations of its major constituents have a pronounced winter-spring maximum and summer minimum. Rahn (1982), for instance has shown that the intensity of the haze, as expressed by its optical depth, or turbidity, is several times greater in spring than in summer.

26th of April 2006

2nd of May 2006

Figure 3. View from the Zeppelin station (top) during clear conditions on 26 April, and (bottom) during a severe episode of Arctic Haze on 2 May 2006. Image courtesy of Ann-Christine Engvall Stjernberg.

2.3.2 Light Absorbing Aerosols, Equivalent Black Carbon (EBC)

Light absorbing aerosols such as black carbon (BC), have gained great interest lately, due to their strong effect on the radiative balance in the Arctic, both as absorbers of short-wave radiation in the atmosphere as well as by decreasing the albedo if deposited on ice or snow (Fig. 4) (Hansen and Nazarenko, 2004; Flanner and Zender, 2006; Flanner et al., 2007). BC, in particular, is largely responsible for the light absorption effects of Arctic Haze aerosols (Polissar et al., 1999). Like other aerosols, BC also influences the microphysical properties of clouds (Garrett et al., 2002, Bréon et al., 2002). BC is produced through combustion of biomass, biofuel and fossil fuel (Klonecki et al., 2003; Stohl, 2006). Light absorbing aerosols have had a variety of different names in science as well as in media, e.g. soot and BC. To avoid future confusion with the terminology in this thesis I would like to explain the concept behind the term equivalent black carbon (EBC). EBC is the amount (mass) of black carbon which would absorb the equal quantity of light as the sample of measured light absorbing aerosols. Analyses involving measurement data of light absorbing aerosols will from now on be referred to as EBC measurements (see section 4.2).

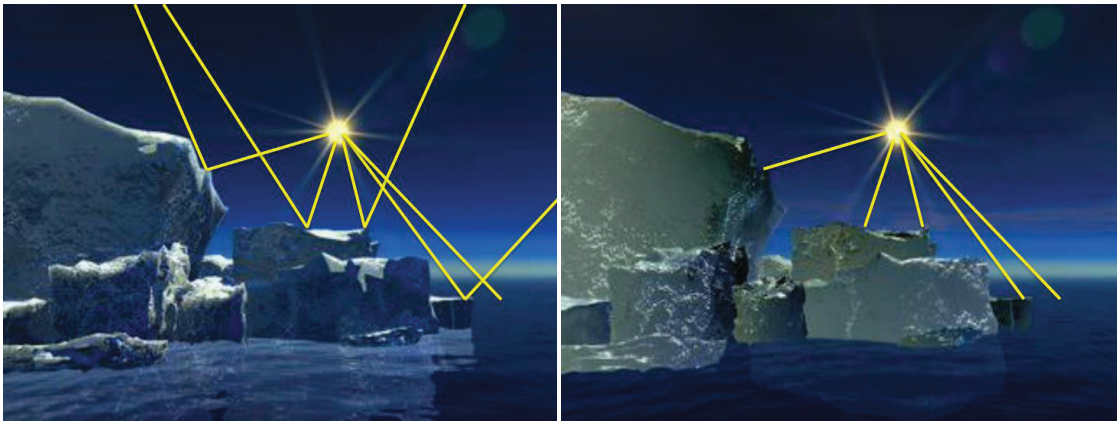

Figure 4. Snow and ice surfaces in the Arctic have a high albedo and thereby reflect light from the sun back to space (left panel). Light absorbing aerosols deposited on these surfaces decrease the albedo and thereby enhance the warming of the Arctic (right panel)(NASA).

2.3.3 Light Scattering Aerosols

Most aerosols predominantly scatter light instead of absorbing it (Charlson et al., 1992). The light scattering aerosols in the Arctic mainly consist of sulphate and sea-salt. In addition to scattering light which has a direct effect on the radiative balance, they influence the microphysical properties of clouds (Garrett et al., 2002, Bréon et al., 2002). As mentioned earlier the distribution of scattering aerosols in the Arctic is strongly influenced by dry and wet deposition (AMAP, 2006). Anthropogenic sources of light scattering aerosols include the industrial region of Norilsk in northern Russia with its smelters, as well as oil extraction facilities. Natural sources include desert dust, sea-salt and spontaneously burning sea cliffs such as the Smoking Hills in north-western Canada (Radke and Hobbs, 1989).

2.3.4 Sulphate

Sulphur dioxide oxidizes into sulphate in the atmosphere, which is acidic in nature. Due to the fact that sulphate is water soluble it is efficiently removed from the atmosphere by wet deposition and is therefore strongly affected by the amount, as well as type, of precipitation; on top of this is it also subject to dry deposition. Anthropogenic sources include oil and gas related activities (e.g. commercial shipping (Fuglestvedt et al., 2009; Bieltvedt Skeie et al., 2009)) as well as certain types of smelting industries mainly located in Russia. Natural sources include sea-salt and volcanoes as well as biogenic emissions related to forest fires.

2.3.5 Tropospheric Ozone (O_3)

Ozone is a potent greenhouse gas not only in the stratosphere but also in the troposphere and an important component in several physical and chemical processes. Tropospheric O_3 is a secondary pollutant controlled by photochemical production and loss processes involving species such as NO_x, carbon monoxide, methane, and non-methane volatile organic compounds (NMVOC) (Haagen-Smit, 1952; Seinfeld, 1988). In the absence of sunlight during the Arctic winter NO titration plays an important role in the destruction of O_3 near pollution sources. During the Arctic spring episodes of strong ozone depletion occur, which are termed ozone depletion events (ODE) and are caused by photochemical chain reaction involving Br and BrO (Barrie et al., 1988; Fan and Jacob, 1992; McConnell et al., 1992), which are thought to be emitted from sea ice. Anthropogenic sources of O_3 precursor species consist of production and combustion of fossil fuel, biofuel combustion, industrial processes, and anthropogenic biomass burning, whereas natural sources include wildfires, lightning, and biogenic emissions from soils and vegetation (Williams and Fehsenfeld, 1991; Quinn et al., 2008).

2.3.6 Gaseous Elemental Mercury (GEM)

Mercury (Hg) exists for the most part as gaseous elemental mercury (GEM) in the atmosphere, which under normal circumstances has an atmospheric lifetime of 6-24 months (Schroeder and Munthe, 1998). As a result GEM is quite evenly distributed since it can be transported over long distances. Hg is volatile in the environment due to its potential to be methylated and its capability to bioaccumulate in aquatic food webs (Steffen et al., 2008). In the Arctic spring, similar to the ODEs, depletion events of GEM occur and are consequently termed atmospheric mercury depletion events (AMDE). Current consensus is that the chemistry causing the AMDEs is similar to that which causes the ODEs (Lindberg et al., 2002; Ariya et al., 2002). An anthropogenic source of Hg is for instance the combustion of coal, whereas natural sources include volcanoes and wildfires.

3 Model

A crucial point in the development of appropriate emission reduction strategies are the source regions of Arctic air pollution which must be known quantitatively. Climate models and atmospheric chemistry transport models generally have problems reproducing the high observed Arctic haze aerosol concentrations (Hoyle et al., 2007). While there is some consensus on the major source regions of Arctic air pollutants, there are also considerable differences in the relative importance of different source regions between the various models (Shindell et al., 2008) and debate about the role of distant source regions like Southern Asia (Koch and Hansen, 2005; Stohl, 2006). In a situation where models are not fully conclusive, studies based on observations are very important. Calculated air mass trajectories have long been the tool of choice for identifying the source regions of observed pollutants, both in case studies of extreme events (Solberg et al., 1996) as well as for statistical analyses of large data sets (Polissar et al., 1999, 2001; Eneroth et al., 2003; Sharma et al., 2004, 2006). However, the accuracy of individual trajectories is limited, especially when long transport distances are involved and when measurements are taken in the turbulent boundary layer (Stohl, 1998). In the following studies we make use of the widely applied FLEXPART model, which is a Lagrangian particle dispersion model (LPDM) (Stohl et al., 1998; Stohl et al., 2005; Forster et al., 2007, see also http://transport.nilu.no/flexpart). FLEXPART calculates the trajectories of so-called tracer particles using the mean winds interpolated from the analysis fields plus parameterizations representing turbulence and convective transport. These processes, which are not included in standard trajectory models, are important for a realistic simulation of the transport of trace substances (Stohl et al., 2002). Including them makes the calculations more computationally demanding and increases the complexity of statistical analysis of the model results. However, Han et al. (2005) concluded that, for example, the reactive gaseous mercury (RGM) sources could be identified more precisely with LPDM output than with the trajectory model output. To our knowledge, no such model has ever been run backward in time from a measurement station over a decadal time period to allow for a statistical analysis of the transport of trace substances measured at the site. Here, we analyze measurements and LPDM calculations at three hourly intervals over a period of nine and eight years respectively for the first two papers and up to twenty-two years in the last paper where we conduct trend analysis.

FLEXPART calculates the trajectories of tracer particles using the mean winds interpolated from the analysis fields plus random motions representing turbulence. For moist convective transport, FLEXPART uses the scheme of Emanuel and Živković-Rothman (1999), as described and tested by Forster et al. (2007). This LPDM was validated with data from continental-scale tracer experiments (Stohl et al., 1998) and has been used in a large number of studies on long-range atmospheric transport (e.g., Stohl et al., 2003; Damoah et al., 2004; Eckhardt et al., 2007; Warneke et al., 2009, 2010).

FLEXPART can be run backward in time (Stohl et al., 2003; Seibert and Frank, 2004). Backward simulations from the Arctic observatories were made every 3 hours. During every 3-hour interval, 40000

particles were released at the measurement point and followed backward in time for 20 days to calculate an emission sensitivity (ES) function, called source-receptor-relationship by Seibert and Frank (2004). The ES value (in units of s m^{-3}) in a particular grid cell is proportional to the particle residence time in that cell and measures the simulated mixing ratio at the receptor that a source of unit strength (1 kg s^{-1}) in the cell would produce for a passive tracer. Of particular interest is the ES close to the surface, as most emissions occur near the ground. Thus, we calculate ES values for a so-called footprint layer 0-100 m above ground which form the basic input to our statistical analyses. For our three studies FLEXPART was run backward in time using operational analyses from the European Centre for Medium-Range Weather Forecasts (ECMWF, 2002) with 1°x1° resolution back to 2002. For earlier years the ERA-40 re-analysis data were used (Uppala et al., 2005) also with 1°x1° resolution. Analyses at 0, 6, 12 and 18 UTC and 3-hour forecasts at 3, 9, 15 and 21 UTC were used.

4 Observations

4.1 Measurement Sites

The measurement data used in the three studies come from four sites located in different parts of the Arctic: Alert, Canada (62,3°W, 82,5°N, 210 m.a.s.l.), Barrow, Alaska (156,6°W, 71,3°N, 11 m.a.s.l.), Summit, Greenland (38,4°W, 72,6°N, 3208 m.a.s.l.), and Zeppelin, Spitsbergen, Norway (11,9°E, 78,9°N, 478 m.a.s.l.). The Alert station is located on the north-eastern tip of Ellesmere Island (Helmig et al., 2007a). The surroundings, both land and ocean, are mainly ice or snow covered during 10 months of the year. Barrow station lies 8 km northeast from a small settlement on a small land tip, and it is surrounded by the Arctic Ocean on all sides except the south where there is Arctic tundra (Helmig et al., 2007a, 2007b). Hence, Barrow station is influenced by both maritime as well as continental air. Summit station is located on the top of the Greenland ice sheet, and surrounded by flat and homogeneous terrain for more than 100 km in all directions (Helmig et al., 2007a). The Zeppelin station is situated on a mountain ridge on the western coast of Spitsbergen, Svalbard. Contamination from the small nearby community of Ny Ålesund located at the coast is minimal, due to the usually stable stratification of the atmosphere and the location of the station 400 m. above the community. Air masses can arrive either from the ice-free North Atlantic Ocean or from the generally ice-covered Arctic Ocean.

Figure 4. Map of the Arctic and the four observatories from where measurement data have been used in these studies. The locations of the stations are marked with red stars.

4.2 Measurement Data

Gaseous Elemental Mercury (GEM): GEM measurements with 5 min time resolution were started at the Zeppelin station in February 2000. For more details on GEM measurements, see Berg et al. (2003).

Tropospheric Ozone (O_3): Surface O_3 concentrations are measured at all four sites using UV absorption instruments based on the absorption of UV radiation at 253.7 nm, all in agreement with the principle guidelines from the International Organization for Standardization (ISO) (ISO 13964:1998).

Equivalent Black Carbon (EBC): Aerosol light absorption measurements are conducted at all four sites. However, the time period over which measurements have been made differ widely. The instruments used are either aethalometers or particle soot absorption photometers (PSAPs) depending on station (Table 1). The light absorption is thereafter, in a non-straightforward way, converted into EBC assuming that all the light absorption is from black carbon (BC), where all the BC has the same light absorption efficiency. For the PSAPs this conversion is performed in the post-processing of the data while it is done internally in the aethalometers. However, both ways of converting aerosol light absorption into EBC relies on the same assumptions. For more detailed information about these measurements see Hirdman et al. (2010a, 2010b).

Aerosol Light Scattering: The aerosol light scattering coefficient is measured at Barrow using two independent nephelometer-based systems (Sheridan et al., 2001). The data are subject to the same filtering as the light absorption data, which means that only data from the "clean sector" are used here.

Sulphate: Measurements of sulphate and other inorganic ions at Alert, Barrow and Zeppelin, analyzed using ion chromatographic analyses on filter samples were available at daily or longer intervals (Table 1). The stations sample different particle size ranges on filters. At Zeppelin, particles smaller than about 10 μm are collected, at Alert, the total suspended particulates (TSP) are sampled, and at Barrow, sub- and super-micron particles are collected separately but in this study only the submicron measurements are used. Measured sulphate concentrations at Alert and Barrow were in both studies corrected for the influence from sea-salt by using measurements of sodium on the same filters and a ratio of sulphate to sodium in seawater. This was also done with the measured sulphate concentrations at Zeppelin for the first study, however, in order to extend the time period back to 1990 for Zeppelin in the second study, the measured sulphate concentrations used in this study were not corrected for the influence of sea-salt sulphate due to the fact that the required complementing analyses of sodium content in the filters started first in 1999. Due to the high altitude location of the Zeppelin station, the influence is limited to 16-22ng/m^3 or 9-18% on average of the measured annual mean concentration.

Atmospheric circulation indices: The daily North Atlantic Oscillation (NAO) index data used to study the correlation to cluster transport frequency were provided by the Climate Analysis Section, NCAR, Boulder, USA, Hurrell (1995). The seasonal values of the atmospheric circulation indices; NAO, Pacific-North American pattern (PNA) and Arctic Oscillation (here abbreviated as AOI in order not to confuse it with a

later defined transport cluster), used in the third paper (Hirdman et al. 2010b) were derived from monthly values. The monthly NAO and PNA index values were in turn derived using principal component analysis (Barnston and Livezey, 1987), while the AOI index was derived using empirical orthogonal functions (EOF) (Higgins et al., 2000).

Table 1. Measurement data used in the three studies included in the thesis. Further information on the instrumentation and data can be found in the listed references.

Station	Species	Time period	Time resolution	Data availability	References
Alert	EBC	1989-2008	1 h	75.7%	Sharma et al. (2004; 2006)
		2000-2006		84.3%	
Alert	Ozone	2000-2007	1 h	82.8	Worthy et al. (2003)
Alert	NSS sulphate	1985-2006	3-9 days	98.2%	Sirois and Barrie (1999)
		2000-2006	7 days	100%	
Barrow	EBC	1988-2008	1 h	58.8%	Sharma et al. (2006)
		2000-2007		50.9%	
Barrow	Ozone	2000-2006	1 h	94.7%	Helmig et al. (2007a)
Barrow	NSS sulphate	1997-2008	1-5 days	61.1%	Quinn et al. (1998)
		2000-2006		70.2%	
Summit	EBC	2003-2006	1 h	41.9%	Sharma et al. (2009)
Summit	Ozone	2000-2007	1 h	77.4%	Helmig et al. (2007a)
Zeppelin	EBC	2002-2007	1h	84.0%	Krecl et al. (2007)
		2002-2009		83.6%	
Zeppelin	GEM	2000-2008	1h	83.7%	Berg et al. (2003)
Zeppelin	Ozone	2000-2007	1 h	96.1%	Aas et al. (2008)
Zeppelin	NSS sulphate	2000-2006	24 h	97.1%	Aas et al. (2008)
Zeppelin	Total sulphate	1990-2008	24 h	94.7%	Aas et al. (2008)

4.3 Data and Model Output Averaging

The EBC, aerosol light scattering, GEM and O_3 data records from all stations have a time resolution of 1 hour. Data were averaged to match the model time resolution of 3 hours. For the daily sulphate measurements from Zeppelin, the 3-hourly model results were averaged to the corresponding sample length. The sample duration of sulphate measurements at Alert and Barrow varied and were therefore assumed to characterize the daily mean concentration over each sample period, after which then the 3-hourly model results were averaged to daily values. For sulphate, daily samples were taken at Zeppelin, whereas the sample duration at Alert was 3-9 days and at Barrow it varied between 1 and 5 days depending on season. In the correlation calculations using daily NAO indices, the 3-hourly model results were averaged to the corresponding sample length.

5 Statistical Method

The statistical method used to analyze the measurement data and the model results in the first two papers (Hirdman et al. 2009, 2010a) investigates where high and, respectively, low concentrations of the targeted pollutants are coming from and, thereby, infer their potential source regions. This is done by selecting either the top or the bottom 10% of the measured concentrations and calculating the average footprint emission sensitivity from the model calculations corresponding to this subset of the measurement data. This method was inspired by methods that had been developed to analyze pollution source regions using simple trajectory calculations (Stohl, 1996, 1998). Our method is nearly identical to the specific method of Ashbaugh (1983) and Ashbaugh et al. (1985) but takes advantage of the superior quality of particle dispersion model output compared to simple trajectories. To verify the statistical significance of the patterns identified we perform a bootstrap resampling analysis (Devore and Farnum, 1999) on the patterns in every grid cell, following Vasconcelos et al. (1996) who have used bootstrap resampling for trajectory statistics. Only values which are statistically significant at a level of 90% are retained. If a grid cell value falls outside of this confidence interval, a 9-point smoothing operator is employed that disperses information from neighbouring grid cells. After the smoothing, the bootstrapping is repeated and, if necessary, further smoothing is applied until all patterns pass the significance test. In order to confirm that the results by using this method is not sensitive to changes of the percentile threshold an analysis using the lowermost and uppermost quartiles instead of deciles was performed and the patterns identified were almost the same (Hirdman et al. 2010a).

In the third paper, (Hirdman et al. 2010b), a different approach was needed to investigate long-term trends of measured pollutants. We used a cluster analysis (Kalkstein et al., 1987) to semi-objectively classify the emission sensitivity patterns from FLEXPART into distinctly different groups of atmospheric transport. The classifications, done separately for every station, allowed us to study how the frequency of the different clusters has changed over time and, thus, how atmospheric transport to a station has changed. We also investigated how the measured concentrations of the different pollutants have changed for every transport cluster. These changes are likely due to changes of the emissions in the respective source regions associated with a transport cluster. This allows separating the effects of changes in atmospheric transport to the Arctic from effects of emission changes in a few important source regions, on the Arctic concentrations of certain pollutants.

6 Aim of the Papers and Broader Implications

The aim of my whole PhD thesis has been to develop a statistical way to combine and analyze measurement data with output from the Lagrangian dispersion model FLEXPART in order to more accurately:

a) Identify source regions of different air pollutants (especially short-lived ones) which affect the Arctic troposphere.

b) Understand the seasonal and long-term patterns associated with their emissions.

c) Evaluate the role of changes in transport processes on their observed variability.

This way of combining long-term measurements with a more advanced transport model will hopefully be seen as a minimum standard for future studies of this kind.

In the development of the method O_3 was a natural choice of species to begin with due to its strong depletion events in the Arctic spring. If to be successful it was crucial that the method could identify differences in transport of air with enhanced O_3 concentration compared with ones associated with low O_3 even though no chemistry is explicitly included in the model. Being successful in this, we sought also to investigate GEM since AMDEs are also caused by BrO. This investigation resulted in the first paper (Hirdman et al., 2009). In it we identify the seasonal changes in the atmospheric transport associated with high and respectively low concentrations of GEM as well as O_3 measured at Zeppelin, and thereby also the associated changes in source regions. In this study we observed that it in general was easier to distinguish specific source and sink regions for O_3 than GEM due to the great difference in their individual mean atmospheric lifetimes, and this insight helped us in the selection of specific species for the second paper.

The second paper (Hirdman et al., 2010a) was an extensive study of short-lived pollutants in the Arctic implementing available measurements of EBC, O_3, light scattering aerosols and sulphate from the four Arctic stations, Zeppelin (Svalbard, Norway), Summit (Greenland), Alert (Canada) and Barrow (Alaska, USA). For the investigation of the seasonal changes in source regions for these species, the period of 2000-2007 was chosen in order to have a relatively uniform set of recent measurement data from all stations. The length was chosen as a compromise between having a data set large enough to obtain statistically robust results and at the same time avoid using too long of a time period over which the emissions could have changed substantially in the major source regions.

A natural step from the second paper which identified the current source regions of several short-lived pollutants was to investigate the long-term evolution of some of these species using the full extent of the measurement data available at Alert, Barrow and Zeppelin (Summit was excluded due to the short time period over which the species of interest had been measured). In the third paper (Hirdman et al., 2010b) the analyses were further developed in order to make this kind of study feasible. The transport was clustered into six major transport pathways, where each cluster has specific characteristics in terms of mean

concentration of the different species, the change over time, as well as the overall influence at the different stations.

With this thesis I hope to increase the overall understanding of the sources and sinks of short-lived pollutants in the Arctic troposphere, their seasonal as well as long-term variation.

7 Conclusions

The main objective of this study in connection to the POLARCAT project has been to identify potential source regions of air pollutants reaching the Arctic troposphere in a more accurate way than has been done in the past. This was achieved by combining measurements from several Arctic stations with calculations from the LPDM FLEXPART. Our main conclusions from these studies are the following:

From transport climatologies based on 20-day backward calculations for Alert, Barrow and Zeppelin (all stations found in the Arctic boundary layer or lower part of the free troposphere), we conclude that the Arctic troposphere is highly sensitive to surface emissions in the Arctic but much less so to emissions outside the Arctic. In winter, the sensitivity extends to emissions in high-latitude Eurasia, whereas in summer the lower part of the Arctic troposphere is largely shielded off from continental emissions on the 20-day time scale. This has important consequences for potential increases in Arctic emissions. Should local sources in the Arctic (e.g., oil and gas drilling, shipping) increase in the future, they would contribute strongly to surface concentrations and deposition of short-lived pollutants in the Arctic, particularly in summer. In contrast, the high-altitude station Summit is more than an order of magnitude less sensitive to surface emissions in the Arctic than the lower altitude stations. This means that it would be less affected by Arctic emission increases. On the other hand, sensitivities to surface emissions in the southern parts of the northern hemisphere continents are higher for Summit than for the other stations. Accordingly, Summit is more sensitive to emissions at lower latitudes and much less sensitive to Arctic emissions than the other stations. Sources contributing to the pollutant loads measured at Summit and at the other stations are, thus, distinctly different. This also has important implications for the interpretation of pollution recorded in ice cores. Ice cores are obtained mostly at altitudes comparable to Summit and are, consequently, poorly representative of the situation close to the surface.

We observed that the annual mean concentrations of O_3 increase systematically with altitude from the lowest station, Barrow, to the highest, Summit. This increase is accompanied by an increasing fraction of air arriving from the stratosphere and increasing positive correlations between this calculated quantity and the observed O_3. Furthermore, at all stations, O_3-rich air masses have little surface contact during the previous 20 days. This indicates that while transport from the stratosphere is slow in the Arctic, it nevertheless has a large impact on observed surface O_3 throughout the year. When transport occurs from Eurasia, all stations show decreased O_3 concentrations in winter (due to titration of O_3 by nitric oxide) but enhanced ozone concentrations in summer (due to photochemical O_3 formation). When air travels across the Arctic Ocean in spring, all stations show decreased O_3 concentrations due to ozone depletion events. These depletion events are at Zeppelin well correlated to atmospheric mercury depletion events (AMDEs) observed in the measured GEM concentration. But whereas low-level transport across the Arctic Ocean also delivers low O_3 concentrations in summer, this type of transport is associated with the highest GEM concentrations in summer, especially at Zeppelin. This can be explained by reemission of previously deposited mercury when

snow melts in summer, and/or by the evasion of GEM from the ocean (which is supersaturated with dissolved gaseous mercury) when the sea ice breaks and direct contact between ocean and atmosphere is facilitated. We have, consequently, shown a link between mercury deposition in the Arctic in spring and its re-emission in summer.

Equivalent black carbon (EBC), sulphate and light scattering aerosols have similar potential source regions, and similarities are also seen in their long-term trends, at least for EBC and sulphate. For all three species high-latitude Eurasia is the major source region, however, there is no close correspondence between the sources of sulphate and light scattering aerosols. The Eurasian dominance as a source region for EBC holds true for all seasons but summer. During summertime more regional emissions dominate and the influence of boreal forest fires in Siberia is observed at Zeppelin whereas emissions from boreal influences forest fires in North America are identified for Alert and Barrow. At Barrow, this summertime influence from forest fires is also associated with enhancements of light scattering aerosols. Furthermore, in summer EBC concentrations are enhanced when the air descends from the free troposphere. This points toward boreal forest fires injecting emissions higher into the atmosphere or aged air masses from unresolved sources beyond the 20-day time scale considered in this study. However, we find no direct evidence that transport from Southern Asia or Southern North America is a source of EBC at the Arctic surface stations. When it comes to sulphate the high-latitude Eurasian influence primarily originates from two source regions, Eastern Europe and the metal smelting complexes at Norilsk. At Alert in fall and at Barrow in summer, high sulphate concentrations are also found when the air is transported from Eastern Asia and the North Pacific. This may indicate an anthropogenic source of the sulphate in Eastern Asia, but emissions from volcanoes on Kamchatka and the Aleutian Islands are equally likely sources.

Looking at decadal time series, we recognize a general and statistically significant downward trend in the measured concentrations of EBC as well as sulphate observed at Alert and Zeppelin but an insignificant downward or unclear long-term trend at Barrow for EBC and sulphate respectively. Despite the overall downward trend, there are indications that the EBC emissions from the eastern part of Northern Eurasia have increased in wintertime over the last decade, probably reflecting emission increases in China and other East Asian countries. There is large interannual variability in the measured EBC and sulphate concentrations at all stations, which masks trends over shorter periods. This points out the importance of continuous monitoring in the Arctic over long time periods. The interannual variation of the frequency of the different transport clusters is relatively well correlated to the annual North Atlantic Oscillation (NAO) index, which shows a downward trend since most of the measurements started. However, the changes in the atmospheric circulation are not large enough to cause substantial long-term trends of EBC and sulphate. Accordingly, changes in transport only explain a minor part of the long-term trends (0.3-7.2%). Therefore, the emission changes primarily in Northern Eurasia are driving the long-term downward trends of EBC and sulphate.

8 Outlook

I hope that this thesis will help to set a new standard in terms of how models and statistical tools can be used to analyze measurement data over longer periods of time, not only for the Arctic. There will, nevertheless, always be a need to further improve the methods used when analyzing the atmosphere. The models which are used for this will steadily improve their capability to describe the complexity of the atmosphere, where on recent example is through inverse modelling. However, improved models will not solve everything. We do recognize that a harmonization of the sampling instruments as well as of the measurements within the Arctic would greatly simplify data comparison. Another improvement for the coverage of the Arctic Basin would be if one or more stations would be placed in the central and eastern parts of northern Russia providing available long-term measurements. There is a heated debate going on now about the source regions of different pollutants entering the Arctic troposphere. This thesis will hopefully provide some answers, however, to learn more about the complex structure of the Arctic troposphere, its seasonal variation and thereby how representative the pollutants measured at the different ground stations are for the troposphere as a whole, measurements at different height are needed. There have been numerous campaigns over the years making these kinds of measurements, e.g. the recent airborne campaigns made within the POLARCAT project. These data sets will be able to give us some information on the vertical structure of the Arctic troposphere and by analyzing these data we can identify the source regions contributing to pollutants measured at different heights. However, airborne measurements generally suffer from two major shortcomings. Either they have a very poor time resolution (e.g. flask samples from balloons) or the time period of the data set is extremely limited (e.g. airplane campaigns). The result is that we will only collect short snapshots of the Arctic troposphere and its chemical composition. To be able to characterize the structure of contributing source regions to the Arctic troposphere in the vertical new measurements taken at different heights with good time resolution is needed in combination with the already existing ones. With the renewed focus that science connected to climate has received among politician globally I hope that there will be funding for such projects in a near future.

9 References

Aas, W., Solberg, S., Manø, S., and Yttri, K. E.: Monitoring of long range transported air pollutants, annual report for 2007, Norwegian Institute for Air Research, Kjeller, 2008.

AMAP: AMAP Assessment Report: Arctic Pollution Issues. Arctic Monitoring and Assessment Programme. xii+859p, 1998.

AMAP: AMAP Assessment Report: Arctic Pollution Issues. Arctic Monitoring and Assessment Programme, 2006.

AMAP: AMAP Assessment Report: Arctic Pollution Issues. Arctic Monitoring and Assessment Programme, 2007.

Ariya, P.A., Khalizov, A., and Gidas, A.: Reactions of Gaseous Mercury with Atomic and Molecular Halogens: Kinetics, Product Studies, and Atmospheric Implications, J. Phys. Chem. A, 106, 7310-7320, 2002.

Ashbaugh, L.: A statistical trajectory technique for determining air-pollution source regions, J.A.P.C.A., 33, 1096-1098, 1983.

Ashbaugh, L., Malm, W., and Sadeh, W.: A residence time probability analysis of sulfur concentrations at grand-canyon-national-park, Atmos. Environ., 19, 1263-1270, 1985.

Barnston, A.G., and Livezey, R.E.: Classification, seasonality and persistence of low-frequency atmospheric circulation patterns. Mon. Wea. Rev., 115**,** 1083-1126, 1987.

Barrie, L.: Arctic air-pollution - an overview of current knowledge, Atmos. Environ., 20, 643-663, 1986.

Barrie, L., Bottenheim, J., Schnell, R., Crutzen, P., and Rasmussen, R.: Ozone destruction and photochemical-reactions at polar sunrise in the lower arctic atmosphere, Nature, 334, 138-141, 1988.

Berg, T., Sekkesæter, S., Steinnes, E., Valdal, A.-K., and Wibetoe, G.: Springtime depletion of mercury in the European Arctic as observed at Svalbard, Sci. Total Env., 304, 43–51, 2003.

Bieltvedt Skeie, R., Fuglestvedt, J., Berntsen, T., Tronstad Lund, M., Myrhe, G., and Rypdal, K.: Global temperature change from the transport sectors: Historical development and future scenarios, Atmos. Environ., 43, 6260-6270, 2009.

Bréon, F.-M., Tanré, D., and Generosso, S.: Aerosol Effect on Cloud Droplet Size Monitored from Satellite, Science, 295, doi: 10.1126/science.1066434, 2002.

Charlson, R.J., Schwartz, S.E., Hales, J.M., Cess, R.D., Coakley, J.A., Hansen, J.E., and Hofmann, D.J.: Climate Forcing by Anthropogenic Aerosols, Science, 255, 423-430, 1992.

Dalsøren S.B., Endresen Ø., Isaksen I.S.A., Gravir G., Sørgård E.: Environmental impacts of the expected increase in sea transportation, with a particular focus on oil and gas scenarios for Norway and northwest Russia, J. Geophys. Res., 112, 2007.

Damoah, R., Spichtinger, N., Forster, C., James, P., Mattis, I., Wandinger, U., et al.: Around the world in 17 days— Hemispheric-scale transport of forest fire smoke from Russia in May 2003, Atmos. Chem. Phys., 4, 1311 –1321, 2004.

Devore, J., and Farnum, N.: Applied statistics for engineers and scientists, in, Duxbury Press, 315-318, 1999.

Eckhardt, S., Breivik, K., Manø, S., and Stohl, A.: Record high peaks in PCB concentrations in the Arctic atmosphere due to long-range transport of biomass burning emissions, Atmos. Chem. Phys. 7, 4527-4536, 2007.

Emanuel, K.A., Živković-Rothman, M.: Development and evaluation of a convection scheme for use in climate models, J. Clim., 17, 218-237, 1999.

Eneroth, K., Kjellstrom, E., and Holmen, K.: A trajectory climatology for Svalbard; investigating how atmospheric flow patterns influence observed tracer concentrations, Phys. Chem. Earth., 28, 1191-1203, 2003.

Fan, S.-M., and Jacob, D.J.: Surface ozone depletion in the Arctic spring sustained by bromine reactions on aerosols, Nature, 359, 1992.

Flanner, M.G. and Zender, C.S.: Linking snowpack microphysics and albedo evolution, J. Geophys. Res., 111, doi: 10.1029/2005JD006834, 2006.

Flanner, M.G., Zender, C.S., Randerson, J.T., Rasch, P.J.: Present-day climate forcing and response from black carbon in snow, J. Geophys. Res., 112, doi: 10.1029/2006JD008003, 2007.

Forster, C., Stohl, A., and Seibert, P.: Parameterization of convective transport in a lagrangian particle dispersion model and its evaluation, J. Appl. Meteorol. and Climatology, 46, 403-422, 2007.

Fuglestvedt, J., Berntsen, T., Eyering, V., Isaksen, I., Lee, D.S., and Sausen, R.: Shipping Emissions: From Cooling to Warming of Climate - and Reducing Impacts on Health, Environ. Sci. Technol., 43, 9057-9062, 2009.

Garrett T.J., Radke, L.F., and Hobbs, P.V.: Aerosol Effects on Cloud Emissivity and Surface Longwave Heating in the Arctic, J. Atmos. Sci., 59, 769-778, 2002.

Garrett, T., and Zhao, C.: Increased arctic cloud longwave emissivity associated with pollution from mid-latitudes, Nature, 440, 787-789, 2006.

Gautier D.L., Bird K.J., Charpentier R.R., Grantz A., Houseknecht D.W., Klett T.R. et al.: Assessment of undiscovered oil and gas in the Arctic, Science, 324, 2009.

Granier C., Niemeier U., Jungclaus J.H., Emmons L., Hess P., Lamarque J.-F. et al.: Ozone pollution from future ship traffic in the Arctic northern passages, Geophys. Res. Lett. , 33, 2006.

Haagen-Smit, A. J.: Chemistry and physiology of Los Angeles smog, Ind. Eng. Chem., 44, 1342–1346, 1952.

Han, Y., Holsen, T., Hopke, P., and Yi, S.: Comparison between back-trajectory based modeling and lagrangian backward dispersion modeling for locating sources of reactive gaseous mercury, Environ. Sci. Technol., 39, 1715-1723, 2005.

Hansen, J., and Nazarenko, L.: Soot climate forcing via snow and ice albedos, Proceedings of the National Academy of Sciences of the United States of America, 101, 423-428, doi: 10.1073/pnas.2237157100, 2004.

Helmig, D., Oltmans, S., Carlson, D., Lamarque, J., Jones, A., Labuschagne, C. et al.: A review of surface ozone in the polar regions, Atmos. Environ., 41, 5138-5161, 2007a.

Helmig, D., Oltmans, S., Morse, T., and Dibb, J.: What is causing high ozone at Summit, Greenland?, Atmos. Environ., 41, 5031-5043, 2007b.

Higgins, R.W., Leetmaa, A., Xue, Y., and Barnston, A.: Dominant factors influencing the seasonal predictability of U.S. precipitation and surface air temperature. J. Climate, 13, 3994-4017, 2000.

Hirdman, D., Aspmo, K., Burkhart J.F., Eckhardt, S., Sodemann, H., Stohl, A.: Transport of mercury in the Arctic atmosphere: evidence for a spring-time net sink and summer-time source, Geophys. Res. Lett., 36, doi: 10.1029/2009GL038345, 2009.

Hirdman, D., Sodemann, H., Eckhardt S., Burkhart J.F., Jefferson A., Mefford, T., et. al.: Source identification of short-lived air pollutants in the Arctic using statistical analysis of measurement data and particle dispersion model output, Atmos. Chem. Phys., 10, 669-693, 2010a.

Hirdman, D., Burkhart J.F., Sodemann, H., Eckhardt S., Jefferson A., Quinn, P.K., et. al.: Long-term trends of black carbon and sulphate aerosol in the Arctic: Changes in atmospheric transport and source region emissions, submitted to Atmos. Chem. Phys. Disc., 10, 12133-12184, 2010b.

Hoyle, C., Berntsen, T., Myhre, G., and Isaksen, I.: Secondary organic aerosol in the global aerosol - chemical transport model OSLO CTM2, Atmos. Chem. Phys., 7, 5675-5694, 2007.

Huntington, H.P.: A preliminary assessment of threats to arctic marine mammals and their conservation in the coming decades, Marine Policy, 33, 77-82, 2009.

Hurrell, J.W.: Transient Eddy Forcing of the Rotational Flow during Northern Winter, J. Atmos. Sci., 52, 2286-2301, 1995.

Iversen, T., and Joranger, E.: Arctic air-pollution and large-scale atmospheric flows, Atmos. Environ., 19, 2099-2108, 1985.

IPCC (Intergovernmental Panel on Climate Change): Summary for Policymakers, Contribution of Working Group I to the 4th Assessment Report, 2007.

Jakobson, L.: China prepares for an Ice-Free Arctic, SIPRI Insight on Peace and Security, 2, 2010.

Kalkstein, L. S., Tan, G., and Skindlov, J. A.: An evaluation of three clustering procedures for use in synoptic climatological classification, J. Climate and Applied Meteorology 26, 717-730, 1987.

Klonecki, A., Hess, P., Emmons, L., Smith, L., Orlando, J., and Blake, D.: Seasonal changes in the transport of pollutants into the Arctic troposphere-model study, J. Geophys. Res., 108, 2003.

Koch, D., and Hansen, J.: Distant origins of arctic black carbon: A Goddard Institute for Space Studies modelE experiment, J. Geophys. Res., 110, doi: 10.1029/2004JD005296, 2005.

Krecl, P., Strom, J., and Johansson, C.: Carbon content of atmospheric aerosols in a residential area during the wood combustion season in Sweden, Atmos. Environ., 41, 6974-6985, 2007.

Lack D., Lerner B., Granier C., Baynard T., Lovejoy E., Massoli P. et al.: Light absorbing carbon emissions from commercial shipping, Geophys. Res. Lett., 35, 2008.

Lalonde, J. D., A. J. Poulain, and M. Amyot (2002), The Role of Mercury Redox Reactions in Snow on Snow-to-Air Mercury Transfer, Environ. Sci. Technol, 36, 174–178.

Law, K., and Stohl, A.: Arctic air pollution: Origins and impacts, Science, 315, 1537-1540, 2007.

Lindberg, S.E., Brooks, S., Lin, C.-J., Scott, K.J., Landis, M.S., Stevens, R.K., et al.: Dynamic oxidation of gaseous mercury in the Arctic troposphere at polar sunrise, Environ. Sci. Tech., 36, 1245–1256, 2002.

McConnell, J.C., Henderson, G.S., Barrie, L., Bottenheim, J., Niki, H., Langford, C.H., and Templeton, E.M.J.: Photochemical bromine production implicated in Arctic boundary-layer ozone depletion, Nature, 355, 150–152, 1992.

Mitchell, J. M.: Visual range in the polar regions with particular reference to the Alaskan Arctic, J. Atmos. Terr. Phys., 17, 1957.

Nansen, F.: Blant sel og bjørn, H. Aschehoug & CO, Oslo, 1961.

Nordenskiöld, A. E.: Nordenskiöld on the inland ice of Greenland, Science, 2, 8, 1883.

Polissar, A., Hopke, P., Paatero, P., Kaufmann, Y., Hall, D., Bodhaine, B. et al.: The aerosol at Barrow, Alaska: Long-term trends and source locations, Atmos. Environ., 33, 2441-2458, 1999.

Polissar, A., Hopke, P., and Harris, J.: Source regions for atmospheric aerosol measured at Barrow, Alaska, Environ. Sci. Technol., 35, 4214-4226, 2001.

Quinn, P.K., Coffman, D.J., Kapustin, V.N., Bates, T.S., and Covert, D.S.: Aerosol optical properties in the marine boundary layer during ACE 1 and the underlying chemical and physical aerosol properties, J. Geophys. Res., 103, 16547-16563, 1998.

Quinn, P., Shaw, G., Andrews, E., Dutton, E., Ruoho-Airola, T., and Gong, S.: Arctic haze: Current trends and knowledge gaps, Tellus series B-Chemical and Physical Meteorology, 59, 99-114, 2007.

Quinn, P., Bates, T., Baum, E., Doubleday, N., Fiore, A., Flanner, M. et al.: Short-lived pollutants in the arctic: Their climate impact and possible mitigation strategies, Atmos. Chem. Phys., 8, 1723-1735, 2008.

Raatz, W., and Shaw, G.: Long-range tropospheric transport of pollution aerosols into the alaskan arctic, J. Clim. Appl. Meteorol., 23, 1052-1064, 1984.

Radke, L. F., Hobbs, P. V.: Arctic hazes in summer over Greenland and the North American Arctic. III: A contribution from natural burning of carbonaceous materials and pyrites, J. Atmos. Chem., 9, 161-167, 1989.

Rahn, K., Borys, R., and Shaw, G.: Asian source of Arctic haze bands, Nature, 268, 713-715, 1977.

Rahn, K. A., and McCaffrey, R. J.: On the origin and transport of the winter Arctic aerosol, University of Rhode Island, 486-503, 1980.

Rahn, K.: Relative importances of North-America and Eurasia as sources of Arctic aerosol, Atmos. Environ., 15, 1447-1455, 1981.

Rahn, K. A.: On the causes, characteristics and potential environmental effects of aerosol in the Arctic atmosphere, The Arctic Ocean, the Hydrographic Environment and Fate of Pollutants, 163-195, 1982.

Schroeder, W. H., and Munthe, J.: Atmospheric mercury – an overview, Atmos. Environ., 32, 809–822, 1998.

Seibert, P., and Frank, A.: Source-receptor matrix calculation with a lagrangian particle dispersion model in backward mode, Atmos. Chem. Phys., 4, 51-63, 2004.

Seinfeld, J. H.: Ozone air quality models: A critical review, J. Air Pollut. Control Assoc., 38, 616–645, 1988.

Sharma, S., Lavoue, D., Cachier, H., Barrie, L., and Gong, S.: Long-term trends of the black carbon concentrations in the Canadian Arctic, J. Geophys. Res., 109, doi: 10.1029/2003JD004331, 2004.

Sharma, S., Andrews, E., Barrie, L., Ogren, J., and Lavoue, D.: Variations and sources of the equivalent black carbon in the high Arctic revealed by long-term observations at Alert and Barrow: 1989-2003, J. Geophys. Res., 111, doi: 10.1029/2005JD006581, 2006.

Sharma, S., Ishizawa, M., Chan, D., Lavoué, D., Leaitch, R., Worthy, D. et al: Synoptic Transport of Anthropogenic BC to the Arctic, NOAA annual meeting, Boulder, Colorado, 2009.

Sheridan, P. J., Delene, D. J., and Ogren, J. A.: Four years of continuous surface aerosol measurements from the Department of Energy's Atmespheric Radiation Measurement Program Southern Great Plains Cloud and Radiation Testbed site, J. Geophys. Res., 106, 20735-20747, 2001.

Shindell, D.: Local and remote contributions to Arctic warming, Geophys. Res. Lett. , 34, 2007.

Shindell, D., Chin, M., Dentener, F., Doherty, R., Faluvegi, G., Fiore, A. et al.: A multi-model assessment of pollution transport to the Arctic, Atmos. Chem. Phys., 8, 5353-5372, 2008.

Sirois, A., and Barrie, L.: Arctic lower tropospheric aerosol trends and composition at alert, Canada: 1980-1995, J. Geophys. Res., 104, 11599-11618, 1999.

Somanathan, S., Flynn, P., Szymanski, J,: The Northwest Passage: A simulation, Transportation Research part A-Policy and Practice, 43, 127-135, 2009.

Sou, T., Flato, G.: Sea Ice in the Canadian Arctic Archipelago: Modeling the Past (1950-2004) and the Future (2041-60), J. Clim., 22, 2181-2198, 2009.

Steffen, A., Douglas, T., Amyot, M., Ariya, P., Aspmo, K., Berg, T., et al.: A synthesis of atmospheric mercury depletion event chemistry in the atmosphere and snow, Atmos. Chem. Phys., 8, 1445-1482, 2008.

Stohl, A.: Trajectory statistics – A new method to establish source-receptor relationships of air pollutants and its application to the transport of particulate sulfate in Europe, Atmos. Environ., 30, 579-587, 1996.

Stohl, A.: Computation, accuracy and applications of trajectories - a review and bibliography, Atmos. Environ., 32, 947-966, 1998.

Stohl, A., Hittenberger, M., and Wotawa, G.: Validation of the lagrangian particle dispersion model FLEXPART against large-scale tracer experiment data, Atmos. Environ., 32, 4245-4264, 1998.

Stohl, A., Eckhardt, S., Forster, C., James, P., Spichtinger, N., and Seibert P.: A replacement for single back trajectory calculations in the interpretation of atmospheric trace substance measurements, Atmos. Environ., 36, 4635-4648, 2002.

Stohl, A., Forster, C., Eckhardt, S., Spichtinger, N., Huntrieser, H., Heland, J., et al.: A backward modeling study of intercontinental pollution transport using aircraft measurements. J. Geophys. Res. 108, 4370, doi:10.1029/2002JD002862, 2003.

Stohl, A., Forster, C., Frank, A., Seibert, P., and Wotawa, G.: Technical note: The lagrangian particle dispersion model FLEXPART version 6.2, Atmos. Chem. Phys., 5, 2461-2474, 2005.

Stohl, A.: Characteristics of atmospheric transport into the arctic troposphere, J. Geophys. Res., 111, doi: 10.1029/2005JD006888, 2006.

Vasconcelos, L., Kahl, J., Liu, D., Macias, E., and White, W.: A tracer calibration of back trajectory analysis at the Grand Canyon, J. Geophys. Res., 101, 19329-19335, 1996.

Warneke, C., Bahreini, R., Brioude, J., Brock, C.A., de Gouw, J.A., Fahey, D.W. et al.: Biomass burning in Siberia and Kazakhstan as an important source for haze over Alaskan Arctic in April 2008, Geophys. Res. Lett., 36, doi: 10.1029/2008GL036194, 2009.

Warneke, C., Froyd, K.D., Brioude, J., Bahreini, R., Brock, C.A., Cozic, J., et al.: An important contribution to springtime Arctic aerosol from biomass burning in Russia, Geophys. Res. Lett., 37, doi: 10.1029/2009GL041816, 2010.

Warren, S., and Wiscombe, W.: Dirty snow after nuclear-war, Nature, 313, 467-470, 1985.

Williams, E.J., and Fehsenfeld, F.C.: Measurement of soil nitrogen oxide emissions at three North American ecosystems, J. Geophys. Phys., 96, 1033-1042, 1991.

Worthy, D. E., Platt, J. A., Kessler, R., Ernst, M., and Racki, S.: The greenhouse gases measurement program, measurement procedures and data quality, in: Canadian baseline program; summery of progress to 2002, edited by: Canada, M. S. O., 97-120, 2003.

10 Summaries of the Individual Papers Presented in This Thesis:

Paper I:

Hirdman D., Aspmo K., Burkhart J.F., Eckhardt S., Sodemann H., and Stohl A.

Transport of mercury in the Arctic atmosphere: Evidence for a springtime net sink and summer-time source

Geophysical Research Letter, 36, L12814, doi: 10.1029/2009GL038345, 2009

Abstract: In the Arctic, atmospheric concentrations of gaseous elemental mercury (GEM) can decrease strongly in spring when mercury is deposited to the snow. Some studies suggest mercury can accumulate in the snow while others suggest rapid re-emission after atmospheric mercury depletion events. We have combined measurements of GEM at the Arctic site Zeppelin (Ny Ålesund, Spitsbergen) with the output of the Lagrangian particle dispersion model FLEXPART, for a statistical analysis of the GEM source and sink regions. We find that the Arctic is a strong net sink region for GEM in April and May, suggesting that mercury accumulates in the Arctic snow pack. For summer, we find the Arctic to be a GEM source, indicating reemission of previously deposited mercury when the snow and/or ice melts, or evasion from the ocean through sea ice leads and polynyas. Our results are corroborated by a related analysis of ozone source and sink regions.

Paper II:

Hirdman D., Sodemann H., Eckhardt S., Burkhart J.F., Jefferson A., Mefford T., Quinn P.K., Sharma S., Ström J., and Stohl A.

Source identification of short-lived air pollutants in the Arctic using statistical analysis of measurement data and particle dispersion model output

Atmospheric Chemistry and Physics, 10, 669-693, 2010

Abstract: As a part of the IPY project POLARCAT (Polar Study using Aircraft, Remote Sensing, Surface Measurements and Models, of Climate Chemistry, Aerosols and Transport), this paper studies the sources of equivalent black carbon (EBC), sulphate, light-scattering aerosols and ozone measured at the Arctic stations Zeppelin, Alert, Barrow and Summit during the years 2000-2007. These species are important pollutants and climate forcing agents, and sulphate and EBC are main components of Arctic haze. To determine where these substances originate, the measurement data were combined with calculations using FLEXPART, a Lagrangian particle dispersion model. The climatology of atmospheric transport from surrounding regions on a twenty-day time scale modelled by FLEXPART shows that the stations Zeppelin, Alert and Barrow are highly sensitive to surface emissions in the Arctic and to emissions in high-latitude Eurasia in winter. Emission sensitivities over southern Asia and southern North America are small throughout the year. The high-altitude station Summit is an order of magnitude less sensitive to surface emissions in the Arctic whereas emissions in the southern parts of the northern hemisphere continents are more influential relative to the other stations. Our results show that for EBC and sulphate measured at Zeppelin, Alert and Barrow, northern Eurasia is the dominant source region. For sulphate, Eastern Europe and the metal smelting industry in Norilsk are particularly important. For EBC, boreal forest fires also contribute in summer. No evidence for any substantial contribution to EBC from sources in southern Asia is found. European air masses are associated with low ozone concentrations in winter due to titration by nitric oxides, but are associated with high ozone concentrations in summer due to photochemical ozone formation. There is also a strong influence of ozone depletion events in the Arctic boundary layer on measured ozone concentrations in spring and summer. These results will be useful for developing emission reduction strategies for the Arctic.

Paper III:

Hirdman D., Burkhart J.F., Sodemann H., Eckhardt S., Jefferson A., Quinn P.K., Sharma S., Ström J., and Stohl A.

Long-term trends of black carbon and sulphate aerosol in the Arctic: Changes in atmospheric transport and source region emissions

Atmospheric Chemistry and Physics Discussion, 10, 12133-12184, 2010.

Abstract: As a part of the IPY project POLARCAT (Polar Study using Aircraft, Remote Sensing, Surface Measurements and Models, of Climate, Chemistry, Aerosols and Transport) and building on previous work (Hirdman et al., 2010), this paper studies the long-term trends of both atmospheric transport as well as equivalent black carbon (EBC) and sulphate for the three Arctic stations Alert, Barrow and Zeppelin. We find a general downward trend in the measured EBC concentrations at all three stations, with a decrease of -2.1±0.4 ng m^{-3} yr^{-1} (for the years 1989-2008) and -1.4±0.8 ng m^{-3} yr^{-1} (2002-2009) at Alert and Zeppelin respectively. The decrease at Barrow is, however, not statistically significant. The measured sulphate concentrations show a decreasing trend at Alert and Zeppelin of -15±3 ng m^{-3} yr^{-1} (1985-2006) and -1.3±1.2 ng m^{-3} yr^{-1} (1990-2008) respectively, while the trend at Barrow is unclear.

To reveal the influence of different source regions on these trends, we used a cluster analysis of the output of the Lagrangian particle dispersion model FLEXPART run backward in time from the measurement stations. We have investigated to what extent variations in the atmospheric circulation, expressed as variations in the frequencies of the transport from four source regions with different emission rates, can explain the long-term trends in EBC and sulphate measured at these stations. We find that the long-term trend in the atmospheric circulation can only explain a minor fraction of the overall downward trend seen in the measurements of EBC (0.3-7.2%) and sulphate (0.3-5.3%) at the Arctic stations. The changes in emissions are dominant in explaining the trends. We find that the highest EBC and sulphate concentrations are associated with transport from Northern Eurasia and decreasing emissions in this region drive the downward trends. Northern Eurasia (cluster: NE, WNE and ENE) is the dominant emission source at all Arctic stations for both EBC and sulphate during most seasons. In wintertime, there are indications that the EBC emissions from the eastern parts of Northern Eurasia (ENE cluster) have increased over the last decade.


GEM
reemission
strongly
months
likely
ng
low
gaseous
accumulates
measured
Ocean
sink
Lindberg
events
results
contrast
R10
R90
emission
atmospheric
strong
evasion
troposphere
net
measurements
suggest
emissions
lowest
et
statistical
found
contact
al
May
AMDEs
winter
analysis
RP
Zeppelin
ocean
highest
associated
masses
ozone
surface
FLEXPART
low-level
spring
high
O3
little
anthropogenic
ice
Figure
depletion
snow
deposited
mercury
grid
transport
patterns
sources
regions
also
Hg
air
summer
atmosphere
previously
across
data
values
average
concentrations
April
model
leads
studies
source
sea
indicating
indicates
Europe
Arctic

GEOPHYSICAL RESEARCH LETTERS, VOL. 36, L12814, doi:10.1029/2009GL038345, 2009

Transport of mercury in the Arctic atmosphere: Evidence for a spring-time net sink and summer-time source

D. Hirdman,[1] K. Aspmo,[1] J. F. Burkhart,[1] S. Eckhardt,[1] H. Sodemann,[1] and A. Stohl[1]

Received 25 March 2009; revised 20 May 2009; accepted 27 May 2009; published 26 June 2009.

[1] In the Arctic, atmospheric concentrations of gaseous elemental mercury (GEM) can decrease strongly in spring when mercury is deposited to the snow. Some studies suggest mercury can accumulate in the snow while others suggest rapid reemission after atmospheric mercury depletion events. We have combined measurements of GEM at the Arctic site Zeppelin (Ny Ålesund, Spitsbergen) with the output of the Lagrangian particle dispersion model FLEXPART, for a statistical analysis of GEM source and sink regions. We find that the Arctic is a strong net sink region for GEM in April and May, suggesting that mercury accumulates in the Arctic snow pack. For summer, we find the Arctic to be a GEM source, indicating reemission of previously deposited mercury when the snow and/or ice melts, or evasion from the ocean through sea ice leads and polynyas. Our results are corroborated by a related analysis of ozone source and sink regions. **Citation:** Hirdman, D., K. Aspmo, J. F. Burkhart, S. Eckhardt, H. Sodemann, and A. Stohl (2009), Transport of mercury in the Arctic atmosphere: Evidence for a spring-time net sink and summer-time source, *Geophys. Res. Lett.*, *36*, L12814, doi:10.1029/2009GL038345.

1. Introduction

[2] Mercury (Hg) is emitted to the atmosphere by a variety of natural (volcanoes, wildfires, etc.) and anthropogenic (e.g., combustion of coal) sources. While anthropogenic Hg emissions have decreased over North America and Europe during the 1990s, emissions in Asia have increased strongly and China is now the country with the by far largest Hg emissions worldwide [*Pacyna et al.*, 2006]. In the atmosphere, Hg exists predominantly as gaseous elemental mercury (GEM) which under normal conditions has an atmospheric lifetime of 6-24 months [*Schroeder and Munthe*, 1998]. Consequently, GEM can be transported over long distances and is quite uniformly distributed in a hemisphere but has substantial interhemispheric concentration differences. GEM can be converted to various oxidized compounds in the gas or particulate phase, which have a much shorter atmospheric lifetime than GEM. These compounds can be deposited rapidly to the Earth's surface but previously deposited Hg can also be remitted by evasion of GEM.

[3] During so-called atmospheric mercury depletion events (AMDEs), which occur in the Arctic during the spring, GEM concentrations can decrease substantially, despite the otherwise long lifetime of GEM [*Schroeder et al.*, 1998]. AMDEs are accompanied by ozone (O_3) depletion events (ODEs), which are caused by strong emissions of halogen compounds and a catalytic cycling of ozone-destroying halogen atoms and radicals [*McConnell et al.*, 1992], now often termed bromine explosions. Reactions with Br atoms or BrO radicals also oxidize GEM to reactive gaseous mercury, which is then deposited to snow or ice in the Arctic [*Lindberg et al.*, 2002]. The fate of Hg in the snow pack, however, is still heavily discussed. Some studies suggest that Hg deposited during AMDEs in spring accumulates in the snow and is later released with melt water in a form that is available to biota [e.g., *Lindberg et al.*, 2002]. Other studies suggest that in the snow Hg is reduced and remitted to the atmosphere as GEM within a few days after deposition, without any sign of accumulation in the snow pack [e.g., *Lalonde et al.*, 2002; *Steffen et al.*, 2002]. GEM concentrations in the Arctic are highest in summer, which has been attributed to release of Hg previously deposited in spring [*Steffen et al.*, 2005] and/or evasion of GEM from the ocean through open leads [*Aspmo et al.*, 2006].

[4] In this study, we present a statistical analysis of the source regions of GEM observed at an Arctic observatory. We demonstrate strong overall influence of AMDEs on spring-time GEM levels, indicating that a substantial amount of GEM must be removed from the atmosphere at least for some months. In addition, we show that measured GEM concentrations in summer are systematically enhanced by GEM emissions in the Arctic, either by reemission of previously deposited Hg during melting, or from the ocean.

2. Methods

[5] For our analysis, we use measurement data from the research station Zeppelin (11.9°E, 78.9°N, 478 m asl). The station is situated in an unperturbed Arctic environment on a ridge of Zeppelin mountain on the western coast of Spitsbergen. The station is accessible via cable car from the nearby small settlement of Ny Ålesund located near sea level. Contamination of the measurements by emissions from the settlement is minimal because of the altitude difference and the generally stable atmospheric stratification. The station is ideally located for our purpose because air masses arriving with a southwesterly flow from the ice-free North Atlantic Ocean provide a strong contrast to the air masses arriving from the ice-covered Arctic Ocean. Hourly O_3 concentrations were recorded by UV absorption spectrometry (API 400A). GEM measurements with 5 min time resolution were started in February 2000 using a Tekran gas phase mercury analyzer (Model 2537A; Tekran Inc., Toronto, Canada). For more details on GEM measurements at Zeppelin, see *Berg et al.* [2003]. All GEM (and O_3) data obtained during the years 2000–2008 (2000–2007, for

[1]Norwegian Institute for Air Research, Kjeller, Norway.

0094-8276/09/2009GL038345$05.00

O_3) were averaged to 3 hours, to fit with the time resolution of our model results.

[6] To identify the sources of the measured GEM, we use 3-hourly backward simulations with the Lagrangian particle dispersion model FLEXPART [*Stohl et al.*, 1998, 2005]. FLEXPART was driven with 3-hourly operational meteorological data from the European Centre for Medium-Range Weather Forecasts with $1^\circ \times 1^\circ$ resolution. The model calculates the trajectories of tracer particles using the mean winds from the analysis fields with additional random motions representing turbulence [*Stohl and Thomson*, 1999] and convection [*Forster et al.*, 2007]. During every 3-hour interval, 40000 particles were released at the measurement point and followed backward for 20 days to calculate an emission sensitivity S on a $1^\circ \times 1^\circ$ grid, under the assumption that removal processes can be neglected. S (in units of s m^{-3}) in a particular grid cell is proportional to the particle residence time in that cell and measures the simulated concentration at the receptor that a source of unit strength (1 kg s^{-1}) in the cell would produce. We use the S distribution in a 100 m layer adjacent to the surface (so-called footprint layer) as input to our statistical analyses of surface sources and sinks.

[7] We use a statistical method to identify possible source and sink regions of GEM based on the measurement data and the model output. The method is similar to older methods based on trajectory calculations [*Ashbaugh*, 1983; *Ashbaugh et al.*, 1985] but takes advantage of the superior quality of FLEXPART emission sensitivity fields compared to simple trajectories, which ignore turbulence and convection. We relate every one of M measurements to a corresponding modeled footprint emission sensitivity field S and calculate the average

$$S_T(i,j) = \frac{1}{M}\sum_{m=1}^{M} S(i,j,m), \quad (1)$$

where i, j are grid indices of S. Then we select the subset of the data with the $L = \frac{M}{10}$ highest 10% (or, respectively, lowest 10%) of measured GEM concentrations and calculate

$$S_P(i,j) = \frac{1}{L}\sum_{l=1}^{L} S(i,j,l), \quad (2)$$

where the suffix P can be either 10 or 90 and indicates the percentile. The ratio

$$R_P(i,j) = \frac{L}{M}\frac{S_P(i,j)}{S_T(i,j)}, \quad (3)$$

with P being again either 10 or 90, can then be used for identifying grid cells that are likely sources (or sinks) of GEM. If air mass transport patterns were the same for the data subset and for the full data set, we would expect $R_P(i,j) = 0.1$ for all i, j. Information on sources and sinks of GEM are contained in the deviations from this expected value. When using the top decile of the data, for instance, $R_{90}(i,j) > 0.1$ means that high measured GEM concentrations are associated preferentially with high S values in grid cell (i,j), indicating a likely source, whereas $R_{90}(i,j) < 0.1$ indicates a possible sink or at least the absence of a source. Conversely, when using the lowest decile of the data, $R_{10}(i,j) > 0.1$ indicates a likely sink in grid cell (i,j), and $R_{10}(i,j) < 0.1$ a source.

[8] Not all features of R_P are statistically significant. Particularly where S_T values are low, spurious R_P values can occur. Therefore, we limit the calculation of R_P to grid cells where $S_T > 5 \cdot 10^{-9}$ s m^{-3}. We furthermore employ a bootstrap resampling analysis [*Devore and Farnum*, 1999] to identify non-significant values at the 90% level, which are then iteratively removed by smoothing the R_P field until all values are statistically significant. Bootstrapping was also used by *Vasconcelos et al.* [1996] to determine statistical significance of trajectory statistics.

3. Results

[9] In Figure 1 we show R_P fields for both the highest and the lowest 10% of all GEM data, for three different seasons. In winter, high GEM concentrations (Figure 1a) are associated with transport especially from Europe where R_{90} values exceed 0.25, indicating direct transport of anthropogenic GEM emissions. The R_{10} values in winter (Figure 1d) are below 0.1 almost everywhere. This indicates that air masses associated with low GEM concentrations avoid surface contact and, therefore, must descend from above the boundary layer. The highest R_{10} values (still mostly not exceeding 0.1) are found over the Arctic where there are no emission sources. Given that China has the largest anthropogenic GEM emissions, one would expect China to appear as a source region. However, transport from China is too infrequent on the 20-day time scale of the FLEXPART calculations to be represented in our statistics.

[10] In spring, the picture changes dramatically, especially for the low GEM concentrations. While the R_{90} values are again highest over the middle latitudes (Figure 1b), the lowest 10% of the GEM data are strongly associated with transport across the sea-ice-covered Arctic Ocean at low altitudes (Figure 1e). This is also exactly the area where elevated BrO concentrations are seen in satellite observations during bromine explosions in spring [see, e.g., *Lindberg et al.*, 2002]. Values of $R_{10} > 0.5$ over the Arctic mean that, during spring, low-level transport across the sea ice almost always leads to AMDEs that can be observed at Zeppelin.

[11] In summer, the situation reverses compared to spring. Now high R_{90} values can be found over the Arctic Ocean (Figure 1c), indicating that air masses receive GEM emissions during low-level transport across the Arctic Ocean. On the other hand, no clear GEM sink regions can be found in the $R_{10} < 0.1$ patterns and surface contact in the Arctic is rather avoided (Figure 1f).

[12] For our statistical analyses, we have selected the months of the year for which the seasonal patterns are most pronounced. March is somewhat similar to April and May but the spring-time pattern is not yet fully established. June is a month where both the top and the bottom percentile of GEM concentrations are associated with frequent low-level transport across the Arctic, indicating a switch from the Arctic being a GEM sink to the Arctic being a GEM source. September–November are transition months where no clear R_P patterns can be found.

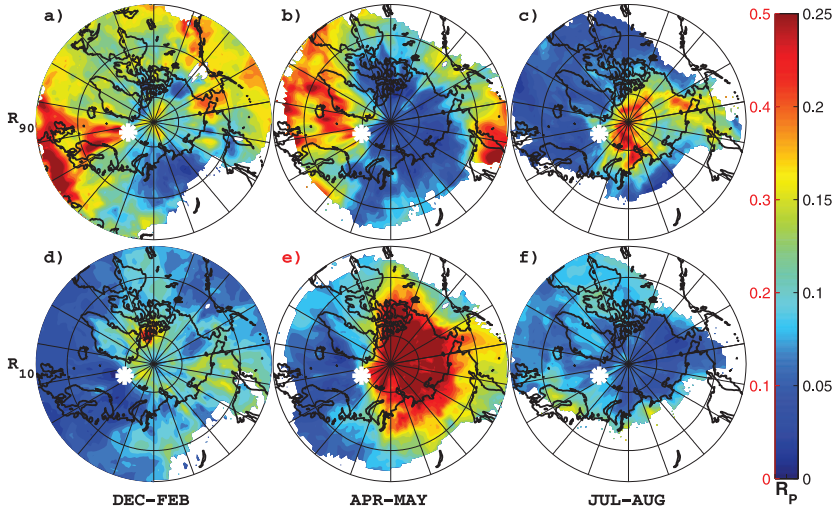

Figure 1. Fields of (a–c) R_{90} and (d–f) R_{10} for GEM measurements at the Zeppelin station during the years 2000–2008, for December–February (Figures 1a and 1d), April–May (Figures 1b and 1e) and July–August (Figures 1c and 1f). Right scale of color bar applies to Figures 1a–1d and 1f, left scale applies to Figure 1e. The white asterisk marks the location of the Zeppelin station. Areas where S_T is below the threshold are plotted white.

[13] Note that our results are insensitive to changes in the data thresholds. Using the top and bottom 20% of the data, for instance, yields almost identical patterns. We have also employed a different statistical analysis that is not based on percentiles but uses the entire dataset and weighs the individual S fields with the corresponding measured GEM concentrations. Again, the Arctic appeared as a sink of GEM in spring and a source in summer. Finally, we have determined the 10% cases with the highest (intense Arctic surface contact) and 10% cases with the lowest (little or no Arctic surface contact) footprint S values aggregated over the entire Arctic Ocean and calculated their respective mean GEM concentrations. This reveals that in April and May air masses having intense surface contact in the Arctic are associated with 33% lower average GEM concentrations (1.21 ± 0.19 ng m^{-3}) than air masses having little or no surface contact in the Arctic (1.83 ± 0.32 ng m^{-3}). In contrast, in July and August, the average GEM concentrations are higher for air masses having intense surface contact in the Arctic (1.81 ± 0.17 ng m^{-3}) than for air masses having little or no contact with the Arctic surface (1.60 ± 0.17 ng m^{-3}). In all other months, differences between these two types of air masses are less than 0.07 ng m^{-3}, except for November (0.13 ng m^{-3}).

[14] Our results for spring indicate a net removal of GEM by AMDEs on the seasonal timescale. While past studies have shown that reemission of GEM from the snow pack or sea ice can occur [e.g., *Lalonde et al.*, 2002; *Steffen et al.*, 2002], according to our results not all Hg deposited can be remitted in spring. If all deposited Hg were remitted in the same season, the Arctic would also be associated with high R_{90} values. Furthermore, no net effect on average GEM concentrations would be seen for air masses with intense surface contact in the Arctic. Since we see a 33% reduction of average GEM concentrations and no GEM concentrations in the top decile for these air masses, our results suggest a net removal of GEM from the atmosphere in the Arctic during spring. This strongly supports the idea that a substantial fraction of Hg removed during AMDEs indeed accumulates in the snow [e.g., *Lindberg et al.*, 2002] and is in agreement with a study conducted at Barrow [*Brooks et al.*, 2006] that showed that during a two-week spring period 60% of the deposited Hg was re-emitted as GEM while 40% remained in the snow.

[15] It is tempting to interpret the GEM source in the Arctic in summer as reemission of Hg deposited during spring. The Arctic GEM source maximizes in July and August and is not evident anymore in September when the ice-free ocean area is larger, possibly indicating that the GEM source is associated with a high rate of melting of snow and sea ice in the Arctic in summer. It has also been shown that underneath the sea ice the surface waters of the Arctic Ocean are supersaturated with dissolved gaseous mercury [*Andersson et al.*, 2008]. The sea ice normally prevents evasion of Hg into the atmosphere, but *Aspmo et al.* [2006] have shown that large Hg fluxes can occur through open leads and polynyas when the sea ice breaks in summer. Thus, the probably more likely explanation for the large GEM source in the Arctic in summer is evasion from the ocean.

[16] To further support the validity of our results, we repeated our statistical analysis for O_3. Ozone depletion events in spring are highly correlated to those of GEM, but O_3 as no important Arctic sources in summer. Figure 2d shows that in winter low O_3 concentrations are associated with transport from Europe, a result of O_3 titration by anthropogenic nitric oxide emissions. High O_3 concentrations in winter (Figure 2a) and spring (Figure 2b) are

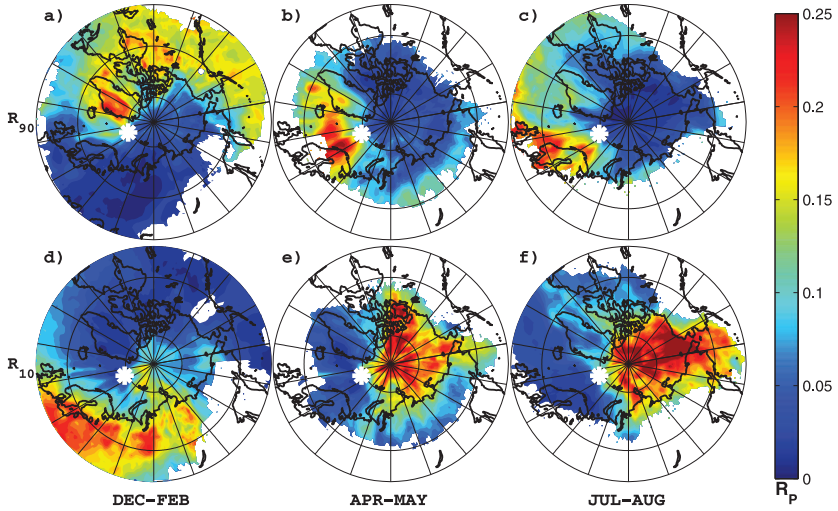

Figure 2. Same as Figure 1 but for ozone for the years 2000–2007.

associated primarily with downward transport from the free troposphere. In winter, this can be seen most clearly by values $R_{90} > 0.2$ over the high topography of Greenland and values $R_{90} < 0.05$ over most low-lying regions (especially those with frequent transport to Zeppelin, not shown). Thus, air masses rich in O_3 tend to have little surface contact.

[17] In spring, low O_3 concentrations are associated with low-level transport across the Arctic Ocean (Figure 2e), indicating the common occurrence of ODEs and AMDEs. In contrast to GEM, however, low O_3 concentrations in summer are associated even more strongly with transport across the Arctic (Figure 2f). In the absence of nitrogen oxide sources, O_3 is quickly destroyed in the relatively moist Arctic boundary layer even without involving halogen chemistry. Furthermore, O_3 formation over the continents in spring and summer (as seen by high R_{90} values over Europe in Figures 2b and 2c) creates a marked contrast to the largely emission-free Arctic. In summary, our results for O_3 show the expected seasonally varying source and sink regions: Europe turning from a sink in winter to a source in summer, the Arctic being a sink during spring and summer, and downward transport from the free troposphere being a source throughout the year, and particularly during winter and spring. This lends confidence also to the source and sink areas we have identified in our analysis of the GEM data.

4. Conclusions

[18] We have used measurements of gaseous elemental mercury (GEM) and ozone at the Arctic measurement site Zeppelin, Ny Ålesund, on Spitsbergen in combination with a Lagrangian particle dispersion model to perform a statistical analysis of the source and sink regions of GEM and ozone. Our conclusions from this study are as follows:

[19] 1. In winter, transport of anthropogenic GEM emissions from mid-latitude source regions (especially Europe) leads to the highest observed GEM concentrations at Zeppelin. Low GEM concentrations are associated with downward transport of air masses from the free troposphere.

[20] 2. In April and May, high measured GEM concentrations are associated with transport from mid-latitude source regions. Low GEM concentrations are strongly associated with low-level transport across the Arctic Ocean, providing evidence for the influence of atmospheric mercury depletion events (AMDEs) at Zeppelin as reported previously [*Berg et al.*, 2003]. Average GEM concentrations in air masses with strong Arctic Ocean surface contact are 33% lower than in air masses having little or no such contact, showing a net removal of GEM from the air during April and May. Apparently, not all mercury deposited during AMDEs can be reemitted as GEM during the same season. This supports the view that mercury accumulates in the snow pack during spring [*Lindberg et al.*, 2002; *Brooks et al.*, 2006]. Only a fraction of the mercury deposited during AMDEs can be immediately reemitted as suggested by *Lalonde et al.* [2002].

[21] 3. In July and August, the highest measured GEM concentrations are associated with strong surface contact over the Arctic Ocean. This can be explained by reemission of previously deposited mercury when snow melts in summer, and/or by the evasion of GEM from the ocean (which is supersaturated with dissolved gaseous mercury) when the sea ice breaks and direct contact between ocean and atmosphere is facilitated.

[22] 4. A statistical analysis for ozone revealed that in spring low ozone concentrations are found in air masses having ice contact, indicating a common occurrence of ODEs and AMDEs. However, in summer ozone continues to be low in air masses with surface contact in the Arctic Ocean, as expected. For ozone, it is also seen that Europe acts as a sink region in winter (explained by ozone titration) and as a source region in summer (explained by photochemical ozone formation). These easily interpretable

results for ozone support the validity of our statistical transport analyses.

[23] **Acknowledgments.** Two anonymous reviewers provided thoughtful comments on the paper. We thank ECMWF and met.no for access to the ECMWF archives. Funding for this study was provided by the Norwegian Research Council through the POLARCAT project.

References

Andersson, M. E., J. Sommar, K. Gardfeldt, and O. Lindqvist (2008), Enhanced concentrations of dissolved gaseous mercury in the surface waters of the Arctic Ocean, *Mar. Chem.*, *110*, 190–194.

Ashbaugh, L. L. (1983), A statistical trajectory technique for determining air pollution source regions, *J. Air Pollut. Control Assoc.*, *33*, 1096–1098.

Ashbaugh, L. L., W. C. Malm, and W. Z. Sadeh (1985), A residence time probability analysis of sulfur concentrations at Grand Canyon National Park, *Atmos. Environ.*, *19*, 1263–1270.

Aspmo, K., C. Temme, T. Berg, C. Ferrari, P.-A. Gauchard, X. Fain, and G. Wibetoe (2006), Mercury in the atmosphere, snow and melt water ponds in the North Atlantic Ocean during Arctic summer, *Environ. Sci. Technol.*, *40*, 4083–4089.

Berg, T., S. Sekkester, E. Steinnes, A.-K. Valdal, and G. Wibetoe (2003), Springtime depletion of mercury in the European Arctic as observed at Svalbard, *Sci. Total Environ.*, *304*, 43–51.

Brooks, S. B., A. Saiz-Lopez, H. Skov, S. E. Lindberg, J. M. C. Plane, and M. E. Goodsite (2006), The mass balance of mercury in the springtime arctic environment, *Geophys. Res. Lett.*, *33*, L13812, doi:10.1029/2005GL025525.

Devore, J., and N. Farnum (1999), *Applied Statistics for Engineers and Scientists*, pp. 315–318, Duxbury, Pacific Grove, Calif.

Forster, C., A. Stohl, and P. Seibert (2007), Parameterization of convective transport in a Lagrangian particle dispersion model and its evaluation, *J. Appl. Meteorol. Climatol.*, *46*, 403–422.

Lalonde, J. D., A. J. Poulain, and M. Amyot (2002), The role of mercury redox reactions in snow on snow-to-air mercury transfer, *Environ. Sci. Technol.*, *36*, 174–178.

Lindberg, S. E., S. Brooks, C.-J. Lin, K. J. Scott, M. S. Landis, R. K. Stevens, M. Goodsite, and A. Richter (2002), Dynamic oxidation of gaseous mercury in the Arctic troposphere at polar sunrise, *Environ. Sci. Technol.*, *36*, 1245–1256.

McConnell, J. C., G. S. Henderson, L. Barrie, J. Bottenheim, H. Niki, C. H. Langford, and E. M. J. Templeton (1992), Photochemical bromine production implicated in Arctic boundary-layer ozone depletion, *Nature*, *355*, 150–152.

Pacyna, E. G., J. M. Pacyna, F. Steenhuisen, and S. Wilson (2006), Global anthropogenic mercury emission inventory for 2000, *Atmos. Environ.*, *40*, 4048–4063.

Schroeder, W. H., and J. Munthe (1998), Atmospheric mercury—An overview, *Atmos. Environ.*, *32*, 809–822.

Schroeder, W. H., K. G. Anlauf, L. A. Barrie, J. Y. Lu, A. Steffen, D. R. Schneeberger, and T. Berg (1998), Arctic springtime depletion of mercury, *Nature*, *394*, 331–332.

Steffen, A., W. Schroeder, J. Bottenheim, J. Narayan, and J. D. Fuentes (2002), Atmospheric mercury concentrations: Measurements and profiles near snow and ice surfaces in the Canadian Arctic during Alert 2000, *Atmos. Environ.*, *36*, 2653–2661.

Steffen, A., W. Schroeder, R. Macdonald, L. Poissant, and A. Konoplev (2005), Mercury in the Arctic atmosphere: An analysis of eight years of measurements of GEM at Alert (Canada) and a comparison with observations at Amderma (Russia) and Kuujjuarapik (Canada), *Sci. Total Environ.*, *342*, 185–198.

Stohl, A., and D. J. Thomson (1999), A density correction for Lagrangian particle dispersion models, *Boundary Layer Meteorol.*, *90*, 155–167.

Stohl, A., M. Hittenberger, and G. Wotawa (1998), Validation of the Lagrangian particle dispersion model FLEXPART against large scale tracer experiment data, *Atmos. Environ.*, *32*, 4245–4264.

Stohl, A., C. Forster, A. Frank, P. Seibert, and G. Wotawa (2005), Technical note: The Lagrangian particle dispersion model FLEXPART version 6.2., *Atmos. Chem. Phys.*, *5*, 2461–2474.

Vasconcelos, L. A.d.P., J. D. W. Kahl, D. Liu, E. S. Macias, and W. H. White (1996), A tracer calibration of back trajectory analysis at the Grand Canyon, *J. Geophys. Res.*, *101*, 19,329–19,335.

K. Aspmo, J. F. Burkhart, S. Eckhardt, D. Hirdman, H. Sodemann, and A. Stohl, Norwegian Institute for Air Research, Instituttveien 18, N-2027 Kjeller, Norway. (dhi@nilu.no)


absorption
related
Europe
layer
found
BC
America
free
data
Ocean
paper
shows
measurements
throughout
transport
statistical
Eastern
R10
show
observed
patterns
pollution
cell
boreal
higher
low
et
stations
calculations
winter
fires
well
continental
percentile
contact
stratosphere
emission
influence
study
fields
pollutants
lower
ozone
method
ice
sulphate
due
Alaska
Thus
calculated
masses
measurement
scavenging
period
sensitive
Eurasia
troposphere
light
also
concentrations
similar
different
increased
aerosols
likely
results
sensitivities
events
Arctic
Zeppelin
loss
haze
Pacific
small
Stohl
surface
using
northern
particle
primarily
enhanced
Asia
spring
may
RP
EBC
R90
trajectory
potential
Canada
much
air
emissions
year
O3
lowest
days
mean
oil
aerosol
changes
highest
measured
Summit
time
CT
Source
However
regions
decide
southern
stratospheric
values
summer
boundary
generally
sources
high
grid
sensitivity
shown
species
Atlantic
strong
fall
almost
used
region
Greenland
FLEXPART
particles
resolution
Norilsk
located
indicating
Fig
al
North
scattering
Barrow
studies
forest
station
analysis
model
Alert
associated
atmospheric
footprint
maximum

Atmos. Chem. Phys., 10, 669–693, 2010
www.atmos-chem-phys.net/10/669/2010/

Atmospheric Chemistry and Physics

Source identification of short-lived air pollutants in the Arctic using statistical analysis of measurement data and particle dispersion model output

D. Hirdman[1], H. Sodemann[1], S. Eckhardt[1], J. F. Burkhart[1], A. Jefferson[2,3], T. Mefford[2,3], P. K. Quinn[4], S. Sharma[5], J. Ström[6], and A. Stohl[1]

[1]Norwegian Institute for Air Research (NILU), Norway
[2]National Oceanic & Atmospheric Administration (NOAA) Earth System Research Laboratory (ESRL) Global Monitoring Division, USA
[3]Cooperative Institute for Research in Environmental Sciences, University of Colorado, USA
[4]National Oceanic & Atmospheric Administration (NOAA) Pacific Marine Environmental Lab (PMEL), USA
[5]Environment Canada, Science and Technology Branch, Climate Research Directorate, Canada
[6]Norwegian Polar Institute, Tromsø, Norway

Received: 11 August 2009 – Published in Atmos. Chem. Phys. Discuss.: 24 September 2009
Revised: 8 January 2010 – Accepted: 13 January 2010 – Published: 25 January 2010

Abstract. As a part of the IPY project POLARCAT (Polar Study using Aircraft, Remote Sensing, Surface Measurements and Models, of Climate Chemistry, Aerosols and Transport), this paper studies the sources of equivalent black carbon (EBC), sulphate, light-scattering aerosols and ozone measured at the Arctic stations Zeppelin, Alert, Barrow and Summit during the years 2000–2007. These species are important pollutants and climate forcing agents, and sulphate and EBC are main components of Arctic haze. To determine where these substances originate, the measurement data were combined with calculations using FLEXPART, a Lagrangian particle dispersion model. The climatology of atmospheric transport from surrounding regions on a twenty-day time scale modelled by FLEXPART shows that the stations Zeppelin, Alert and Barrow are highly sensitive to surface emissions in the Arctic and to emissions in high-latitude Eurasia in winter. Emission sensitivities over southern Asia and southern North America are small throughout the year. The high-altitude station Summit is an order of magnitude less sensitive to surface emissions in the Arctic whereas emissions in the southern parts of the Northern Hemisphere continents are more influential relative to the other stations. Our results show that for EBC and sulphate measured at Zeppelin, Alert and Barrow, northern Eurasia is the dominant source region. For sulphate, Eastern Europe and the metal smelting industry in Norilsk are particularly important. For EBC, boreal forest fires also contribute in summer. No evidence for any substantial contribution to EBC from sources in southern Asia is found. European air masses are associated with low ozone concentrations in winter due to titration by nitric oxides, but are associated with high ozone concentrations in summer due to photochemical ozone formation. There is also a strong influence of ozone depletion events in the Arctic boundary layer on measured ozone concentrations in spring and summer. These results will be useful for developing emission reduction strategies for the Arctic.

Correspondence to: D. Hirdman
(dhi@nilu.no)

1 Introduction

In the late 19th century, some of the early Arctic explorers noticed "dirty" deposits on the ice and snow in remote areas of the Arctic and speculated on their origin (Nordenskiöld, 1883; Nansen, 1961; Garrett and Verzella, 2008). Around the year of 1894, Nansen hypothesized that these deposits must have been transported via the atmosphere from faraway source regions but he did not relate them to air pollution. While it cannot be proven that these old reports of "dirty snow" were indeed caused by air pollution, this is a likely explanation. A historical ice-core record of black carbon (BC) shows that BC concentrations over Greenland peaked around

1910 (McConnell et al., 2007). Even though BC concentrations now are likely much lower than in the beginning of the 20th century current pollution events can indeed cause a visible discoloration of the snow (Stohl et al., 2007) and similar discolorations might have been observed already by Nordenskiöld (1883) and Nansen (1961) in the late 1800s. The anecdotal evidence for air pollution in the Arctic was forgotten and the Arctic was long considered a pristine place, until pilots flying over the North American Arctic in the 1950s observed widespread haze (Greenaway, 1950; Mitchell, 1957) that could be seen every winter and early spring. It took until the 1970s for scientists to realize that the haze was air pollution transported from the middle latitudes (Rahn et al., 1977; Rahn and McCaffrey, 1980; Iversen and Joranger, 1985; Barrie, 1986).

Arctic haze is a condition of reduced visibility. When viewed away from the sun it appears greyish-blue, looking into the sun it appears reddish-brown. It typically has a layered structure but on average no distinct upper and lower boundaries, and produces none of the optical phenomena that would be expected if it were composed of ice crystals (Barrie, 1986). The haze is generally composed of sulphate and particulate organic matter and to a lesser extent ammonium, BC, nitrate, dust aerosols and distinct heavy metals (Quinn et al., 2007), and it is accompanied by enhanced concentrations of gaseous pollutants (Barrie, 1986). One of the striking things about Arctic haze is its strong seasonal variation. Both the optical effects of the haze and the concentrations of its major constituents have a pronounced winter-spring maximum and summer minimum. Rahn (1982), for instance has shown that the intensity of the haze, as expressed by its optical depth, or turbidity, is several times greater in spring than in summer.

Recently, there has been renewed interest in Arctic air pollution because of its potential effects on climate. Warming is proceeding fastest in the Arctic due to strong feedbacks at high latitudes. While long-lived greenhouse gases undoubtedly are the strongest drivers of climate change, Quinn et al. (2008) argue that short-lived pollutants may also contribute to the Arctic warming and ice melt. The melt of snow/ice triggers further feedback mechanisms through a decrease of the albedo (Flanner and Zender, 2006; Flanner et al., 2007). BC changes the radiative balance in the Arctic through absorption of shortwave radiation in the atmosphere as well as by decreasing the surface albedo when deposited on snow or ice (Warren and Wiscombe, 1985; Hansen and Nazarenko, 2004). Tropospheric ozone (O_3) affects the Arctic atmosphere both locally by altering the radiation fluxes as well as more remotely by modulating heat transport into the Arctic (Shindell, 2007). Sulphate and nitrate aerosols cause scattering of shortwave radiation and also modify the optical properties of clouds (indirect aerosol effects). While this generally leads to a cooling of the surface, aerosols may also lead to increased thermal emissivity of thin Arctic clouds and, thus, a warming of the surface (Garrett and Zhao, 2006). Reductions in the concentration levels of short-lived pollutants could be an effective means to slow climate change in the Arctic (Quinn et al., 2008). However, in order to develop appropriate emission reduction strategies, the source regions of Arctic air pollution must be known quantitatively.

Surfaces of constant potential temperature form folded shells over the Arctic with minimum values in the boundary layer (Klonecki et al., 2003; Stohl, 2006). If transport occurs along isentropes, the potential temperature in pollution source regions must be the same as in the layers where Arctic Haze is found (Raatz and Shaw, 1984; Iversen and Joranger, 1985). This isentropic transport emphasizes relatively cold geographical regions such as Northern Eurasia (in winter) in contrast to regions further south that are too warm for air masses to reach the Arctic lower troposphere on a direct transport route (Rahn, 1981; Barrie, 1986).

Current emissions in the high Arctic (north of 70° N) are negligible. However, Gautier et al. (2009) suggests that 30% of the world's undiscovered gas and 13% of undiscovered oil may be found in the Arctic. If these resources are exploited, emissions in the Arctic could increase strongly and this would probably have a dramatic impact on Arctic pollutant concentrations near the surface. Furthermore, with retreating Arctic sea ice in summer, commercial shipping in the Arctic may become feasible. Several studies suggest a large potential influence of these emissions on O_3 and BC concentrations in the Arctic (Granier et al., 2006; Dalsøren et al., 2007; Lack et al., 2008).

Climate models and atmospheric chemistry transport models generally have problems reproducing the high observed Arctic haze aerosol concentrations (Hoyle et al., 2007). While there is some consensus on the major source regions of Arctic air pollutants, there are also considerable differences in the relative importance of different source regions between the various models (Shindell et al., 2008) and discussions about the role of distant source regions like Southern Asia (Koch and Hansen, 2005; Stohl, 2006). In a situation where models are not fully conclusive, studies based on observations are very important. Calculated air mass trajectories have long been the tool of choice for identifying the source regions of observed pollutants, both in case studies of extreme events (Solberg et al., 1996) as well as for statistical analyses of large data sets (Polissar et al., 1999, 2001; Eneroth et al., 2003; Sharma et al., 2004, 2006). However, the accuracy of individual trajectories is limited, especially when long transport distances are involved and when measurements are taken in the turbulent boundary layer (Stohl, 1998).

For this study, a Lagrangian particle dispersion model (LPDM) was employed for a statistical analysis of the source regions of various observed pollutants. LPDM calculations are more accurate than trajectory calculations which ignore atmospheric turbulence and convection (Stohl et al., 2002; Han et al., 2005). The major advantage is however that LPDM calculations are also more quantitative because the model output can be combined with emission fluxes from

appropriate inventories to derive modelled source contributions which can be compared with measured data of long-lived species, thus allowing validation of the simulated transport (Stohl et al., 2006, 2007).

This paper is structured as follows: in Sect. 2, the methods used will be described. Subsequently, in Sect. 3.1, the climatology of atmospheric transport towards the four Arctic observatories, Zeppelin (Spitsbergen, Norway), Alert (Canada), Barrow (Alaska) and Summit (Greenland) will be presented. In Sect. 3.2, the potential source regions of several observed parameters (equivalent BC (EBC), sulphate, light scattering aerosols and O_3) will be investigated for the years 2000–2007. Finally, conclusions will be drawn.

2 Methods

2.1 Measurement sites

The measurement data used in this study comes from four sites located in different parts of the Arctic (Fig. 1): Zeppelin, Spitsbergen, Norway (11.9° E, 78.9° N, 478 m a.s.l.), Alert, Canada (62.3° W, 82.5° N, 210 m a.s.l.), Barrow, Alaska (156.6° W, 71.3° N, 11 m a.s.l.) and Summit, Greenland (38.4° W, 72.6° N, 3208 m a.s.l.). Zeppelin station is situated on a mountain ridge on the western coast of Spitsbergen. Due to the usually stable stratification of the atmosphere contamination from the small nearby community of Ny Ålesund located at the coast is minimal. Air masses can arrive either from the ice-free North Atlantic Ocean or from the generally ice-covered Arctic Ocean. Alert station is located the furthest north of all the Arctic stations on the north-eastern tip of Ellesmere Island (Helmig et al., 2007a). The surroundings, both land and ocean, are mainly ice or snow covered during 10 months of the year. Barrow station lies 8 km northeast from a small settlement on a small land tip, and it is surrounded by the Arctic Ocean on all sides except south where there is Arctic tundra (Helmig et al., 2007a, b). Hence, Barrow station is influenced by both maritime as well as continental air. Summit station is located on the top of the Greenland glacial ice sheet, and surrounded by very flat and homogeneous terrain for more than 100 km in all directions (Helmig et al., 2007a).

2.2 Measurement data

Measured concentrations of EBC (derived from the aerosol light absorption coefficient), sulphate, the aerosol light scattering coefficient and O_3 are used in this study. Sulphate and BC are important components of Arctic haze, with sulphate being responsible mainly for the light-scattering effects and BC primarily responsible for the light absorption effects of Arctic haze aerosol (Polissar et al., 1999). Both components can also exist in an internal aerosol mixture and can in addition influence cloud microphysical properties. O_3 is a secondary pollutant and a strong greenhouse gas which contributes to warming of the Arctic (Shindell, 2007).

Table 1 summarizes the measurement data used here. The EBC, aerosol light scattering and O_3 data records from all stations have a time resolution of 1 h. Data were averaged to match the model time resolution of 3 h (see Sect. 2.2). For sulphate, daily samples were taken at Zeppelin, whereas the sample duration at Alert was 7 days and at Barrow it varied between 1 and 5 days depending on season. The 3-hourly model results were averaged to the corresponding sample length. Particularly for Alert and Barrow the sampling length for sulphate is often too long to resolve individual transport events, which limits the statistical analysis of source regions as will be discussed in further detail in Sect. 3.2.2.

The information on light absorbing particles is collected with particle soot absorption photometers (PSAP) at Zeppelin and Barrow and with aethalometers at Alert and Summit. PSAP measurements are reported as the particle light absorption coefficient σ_{ap} (Bond et al., 1999), whereas aethalometer output is reported directly as BC concentrations through an internal conversion using an assumed mass absorption efficiency. Conversion between σ_{ap} and BC is not straightforward. It requires the assumptions that all the light absorption measured is from BC, and that all BC has the same light absorption efficiency. Therefore, PSAP data are reported as EBC, where σ_{ap} values have been converted approximately to BC mass concentration using a value of $10\,m^2\,g^{-1}$, typical of aged BC aerosol (Bond and Bergstrom, 2006). The conversion to BC in the aethalometers is done internally but relies on the same assumptions, so these data will be referred to as EBC as well.

PSAP measurements have been made at Barrow since October, 1997, as part of the standard NOAA/ESRL/GMD aerosol optical measurements system design (Delene and Ogren, 2002). The measurements at Zeppelin are performed using a custom built PSAP that is based on the same measurement principle. The responses of both the PSAPs and the aethalometer depend on the loading of particles on the filter and on the amount of light that the particles scatter (Bond et al., 1999; Weingartner et al., 2003; Arnott et al., 2005). The Barrow and Zeppelin PSAP data were corrected for these dependencies according to the procedure described by Bond et al. (1999), while no corrections were applied to the aethalometer measurements from Alert and Summit. To avoid local contamination by emissions from the town of Barrow is the Barrow PSAP data routinely screened where only values were used when the wind direction fell within the "clean-air sector" from 0–130° (Bodhaine, 1995). This screening very likely also affects how representative these data are when analyzing potential source regions, which will be discussed in Sect. 3.2.1. At Summit, the diesel generator and the camp are local pollution sources. Thus, data were used only when the air masses approach from the "clean-air sector" (111–248°) in agreement with an earlier study by Kahl et al. (1997).

Table 1. Measurement data used in this study. Further information on the instrumentation and data can be found in the listed references.

Station	Species	Time period	Time resolution	Data availability	References
Zeppelin	EBC	2002–2007	1 h	84.0%	Krecl et al. (2007)
Zeppelin	Ozone	2000–2007	1 h	96.1%	Aas et al. (2008)
Zeppelin	NSS sulphate	2000–2006	24 h	97.1%	Aas et al. (2008)
Alert	EBC	2000–2006	1 h	84.3%	Sharma et al. (2004, 2006)
Alert	Ozone	2000–2007	1 h	82.8	Worthy et al. (2003)
Alert	NSS sulphate	2000–2006	7 days	100%	Sirois and Barrie (1999)
Barrow	EBC	2000–2007	1 h	50.9%	Sharma et al. (2006)
Barrow	Ozone	2000–2006	1 h	94.7%	Helmig et al. (2007a)
Barrow	NSS sulphate	2000–2006	1–5 days	70.2%	Sirois and Barrie (1999)
Barrow	Light scattering aerosols	2000–2007	1 h	53.0%	Sheridan et al. (2001)
Summit	EBC	2003–2006	1 h	41.9%	Sharma et al. (2009)
Summit	Ozone	2000–2007	1 h	77.4%	Helmig et al. (2007a)

Sulphate and other inorganic ions were measured at Zeppelin, Alert and Barrow by ion chromatography analysis on filter samples taken at daily or longer intervals (Table 1). Measured sulphate concentrations were corrected for the influence from sea-salt by using measurements of sodium on the same filters and a ratio of sulphate to sodium in seawater. The stations sample different particle size ranges when measuring sulphate. At Zeppelin, particles smaller than about 10 μm are collected, at Alert, the total suspended particulates (TSP) are sampled, and at Barrow, sub- and super-micron particles are collected separately but in this study only the submicron measurements are used.

The light scattering coefficient is measured at Barrow using two independent nephelometer-based systems (Sheridan et al., 2001). The data are subject to the same filtering as the light absorption data, which means that only data from the "clean sector" are used here.

Surface ozone concentrations are measured using UV absorption instruments based on the absorption of UV radiation at 253.7 nm, all in agreement with the principle guidelines from the International Organization for Standardization (ISO) (ISO 13964:1998).

The time period considered in this study (2000–2007) was chosen such that a relatively uniform set of recent measurement data from the four Arctic stations was available. Some data sets do not extend much further back in time. The time period is also a compromise between having available a large enough data set for obtaining robust statistical results and to avoid using a too long time period, over which emission changes in the major source regions could be substantial. The time period is representative in respect to atmospheric transport over the last two decades which will be presented in a follow-up paper where also the effects of emission changes over decadal periods are studied.

2.3 Model calculations

To date, trajectory models have been the most broadly used tools for the statistical analysis of the atmospheric transport of trace substances to measurement sites. We make use of the widely applied Lagrangian particle dispersion model (LPDM) FLEXPART (Stohl et al., 1998, 2005; Forster et al., 2007). FLEXPART calculates the trajectories of so-called tracer particles using the mean winds interpolated from the analysis fields plus parameterizations representing turbulence and convective transport. These processes, which are not included in standard trajectory models, are important for a realistic simulation of the transport of trace substances (Stohl et al., 2002). Including them makes the calculations more computationally demanding and the statistical analysis of the model results becomes more complex. However, Han et al. (2005) concluded that the reactive gaseous mercury (RGM) sources could be identified more precisely with LPDM calculations than with the trajectory model calculations.

FLEXPART was run backward in time using operational analyses from the European Centre for Medium-Range Weather Forecasts (ECMWF, 2002) with $1° \times 1°$ resolution for the period 2002–2007. For earlier years the ERA-40 re-analysis data were used (Uppala et al., 2005) also with $1° \times 1°$ resolution. Analyses at 00:00, 06:00, 12:00 and 18:00 UTC and 3-h forecasts at 03:00, 09:00, 15:00 and 21:00 UTC were used. During every 3-h interval, 40 000 particles were released at the measurement point and followed backward for 20 days. The choice of 20 days is somewhat subjective, but it is comparable to the atmospheric lifetimes of most of the species studied in this paper and therefore should be long enough to capture transport from the most relevant source regions.

In backward mode, FLEXPART calculates an emission sensitivity function S, called source-receptor-relationship by

Seibert and Frank (2004). The S value (in units of s m^{-3}) in a particular grid cell is proportional to the particle residence time in that cell and measures the simulated concentration at the receptor that a source of unit strength (1 kg s^{-1}) in the cell would produce for an inert tracer which is not affected by chemical or other removal processes. The emission sensitivity S close to the surface is of particular interest, as most emissions occur near the ground. Thus, S values are calculated for a so-called footprint layer 0–100 m above ground. S can be folded with emission distributions of any species to calculate receptor concentrations of that species under the assumption that the substance is inert. However, here concentrations are not calculated but instead S is used directly.

2.4 Statistical analyses

The statistical method for analysing the measurement data and the model results is basically the same as the trajectory residence time analysis of Ashbaugh (1983) and Ashbaugh et al. (1985) but takes advantage of the superiority of the FLEXPART S fields compared to simple trajectories as described in Hirdman et al. (2009). It explores where high and, respectively, low concentrations of the targeted pollutants are coming from and, thereby, infer their potential source regions. M model calculations were matched with M corresponding measured concentrations. From the gridded footprint emission sensitivity field *S(i,j,m)*, where i and j are the indices of the model output grid and m=1,... M are the observation numbers, the average footprint emission sensitivity S_{T} is calculated as

$$S_{\mathrm{T}}(i,j) = \frac{1}{M}\sum_{m=1}^{M} S(i,j,m) \tag{1}$$

S_{T} can also be interpreted as a flow climatology that shows the regions where air masses arriving at a station are likely to have been within the boundary layer during the 20 days prior to arrival. Next, we select the $L = M/10$ highest (or, alternatively, the lowest) 10% of the measured concentrations and calculate the average footprint emission sensitivity

$$S_P(i,j) = \frac{1}{L}\sum_{l=1}^{L} S(i,j,l) \tag{2}$$

only for this data subset, where the percentile P is either 10 or 90. Both S_P and S_{T} peak near the observatory as emission sensitivities generally decrease with distance from the station. This bias is removed by calculating the relative fraction R_P, where

$$R_P = \frac{L}{M}\frac{S_P}{S_{\mathrm{T}}} \tag{3}$$

and with P still being either 10 or 90, this may then be used for identifying grid cells that are likely sources (or sinks) for the parameter of interest. If the measured species were completely unrelated to air mass transport patterns then the data subset and the full data set would look the same and $R_P(i,j)$=0.1 would be expected for all i,j. The deviation from this expected value contains information on sources and sinks. When using the top decile of the measurement data, $R_{90}(i,j) > 0.1$ indicates that high measured concentrations are preferentially associated with transport through grid cell (i,j), making (i,j) a potential source. Conversely, $R_{90}(i,j) < 0.1$ indicates that cell (i,j) is less likely to be a source. On the contrary, when applying this to the lowest decile of the measurement data, $R_{10}(i,j) > 0.1$ indicates a likely sink in grid cell (i,j), and $R_{10}(i,j) < 0.1$ a source or at least the absence of a sink.

Not all features of the R_P field are statistically significant. Particularly where S_{T} values are low (indicating rare transport towards the receptor even for the full data set), spurious R_P values may occur. To remove spurious values $R_P(i,j)$ is only calculated in grid cells where $S_{\mathrm{T}}(i,j) > 1\times10^{-9}$ s m^{-3}. This threshold is a compromise between the need to remove spurious values and the desired large spatial coverage. To verify the statistical significance of the remaining R_P patterns, a bootstrap resampling analysis was performed (Devore and Farnum, 1999) analogous to that used by Vasconcelos et al. (1996a) for trajectory statistics. This technique does not assume any specific distribution of the data. For every bootstrap resampling, one S field is removed and a new R_P map is created. This leads to M+1 R_P maps from which a mean distribution for each grid cell can be derived. Only R_P values that are statistically significant at the 90% significance level are retained. If a R_P value falls outside of this confidence interval, a 9-point smoothing operator is employed that disperses information from neighbouring grid cells. After the smoothing, the bootstrapping is repeated and, if necessary, further smoothing is applied. These steps are repeated until all R_P values pass the significance test. While the remaining features are all statistically significant, the interpretation must nevertheless be done carefully as there may still be systematic effects that cannot be accounted for by the bootstrapping. In a study based on back trajectories, Vasconcelos et al. (1996b) noticed that the angular resolution of the statistical analysis is better than its radial resolution. For example, transport from a clean region may be shielded from identification if a closer pollution source lies into the same direction as viewed from the station. Overall, however, the method is well suited for identifying the origin of clean and polluted air masses, respectively, arriving at the measurement stations (Hirdman et al., 2009).

The time period which is considered in the study (2000–2007) has been chosen in order to present our analysis on a complete and uniform set of recent measurement data from these Arctic stations as possible, where some data sets do not extend much further back in time. In the compromise between obtaining robust statistical results and the necessity of a cut off at some point to avoid including changes in emissions from the major source regions, the specific time period was considered to be adequate. It is beyond the scoop of this

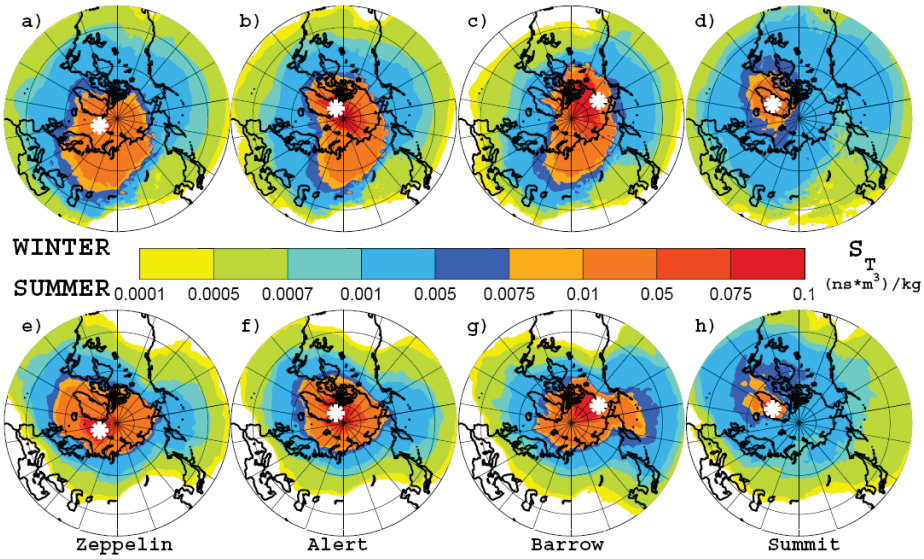

Fig. 1. Transport climatologies (S_T), for winter (top row) and summer (bottom row) and for the Arctic stations: Barrow, Alert, Zeppelin and Summit for the years 2000–2007. The stations locations are marked with a white asterisk.

paper to address changes in the emission strengths but this will be investigated in a follow-up paper.

3 Results

3.1 Transport climatologies

General transport climatologies are compared by plotting the total footprint sensitivity S_T for the different measurement stations (Fig. 1). S_T shows the overall sensitivity to surface emissions during the last 20 days of transport and, thus, indicates where surface sources can potentially influence the measurements. Plots of S_T can also be interpreted as flow-climatologies where high values indicate frequent transport reaching the station.

High S_T values for all low-altitude surface stations are primarily limited to the Arctic (Fig. 1, here in orange/red). Thus, emissions within the Arctic can strongly influence pollutant concentrations at all stations, while emissions of the same strength outside the Arctic would have a much smaller impact. However, there is a strong seasonal variation. In winter (DJF), relatively high S_T values extend towards northern Eurasia. This is consistent with our understanding of atmospheric transport patterns in the Arctic, with winter-time low-level transport into the Arctic occurring primarily from Eurasia (Rahn and McCaffrey, 1980; Carlson, 1981; Barrie, 1986; Klonecki et al., 2003; Stohl, 2006; Quinn et al., 2007; Law and Stohl, 2007; Shindell et al., 2008). In summer (JJA), high S_T values are confined to the Arctic Ocean basin and sharply decrease near the continental coasts, indicating that air masses from the relatively warmer land masses are less likely to reach the Arctic stations on a 20-day timescale. As a result, sources near the continental coasts potentially have a much larger influence on the Arctic than sources located in the continental interior. Pollution sources within the Arctic itself, which are currently quite limited, would have by far strongest influence on Arctic pollutant concentrations. For instance, increased commercial shipping with the retreat of the sea ice in summer could lead to strongly elevated concentrations of BC, O_3 and other pollutants in the Arctic (Granier et al., 2006; Dalsøren et al., 2007; Lack et al., 2008).

Alert (Fig. 1b, f) is the station most isolated from continental source regions due to its location deep within the Arctic. Compared to Alert, Barrow (Fig. 1c, g) samples more air masses from the North American sector of the Arctic and Zeppelin (Fig. 1a, e) samples more air from the European sector of the Arctic. All three stations are sensitive also to emissions from northern Siberia.

Transport to the Summit station (Fig. 1d, h) is distinctly different. Because of Summit's high altitude, the air has surface contact mostly over Greenland itself, whereas S_T elsewhere is low. Thus, measurements at Summit are representative for the Arctic free troposphere. Summit is also special since the remaining continental influence is mostly located over North America and Europe, whereas Siberia has relatively little influence. When considering also emission

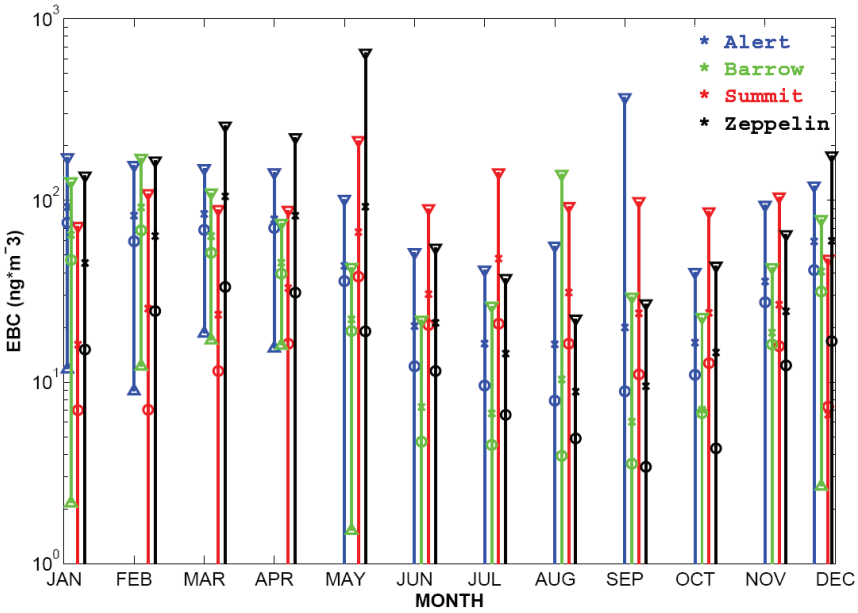

Fig. 2. Monthly averaged concentrations of measured EBC at Alert (blue), Barrow (green), Summit (red) and Zeppelin (black) during the years 2000–2007 (2000–2006 for Alert, 2003–2006 for Summit and 2002–2007 for Zeppelin). The EBC is plotted on a logarithmic scale. The mean concentration is marked with a cross, the median with a circle and bars indicate ±1 standard deviation. Notice that symbols for Barrow, Summit and Zeppelin are slightly offset in time for clarity of presentation.

sensitivities above the footprint layer (lowest 100 m), Summit is influenced quite strongly by transport from North America (not shown) in agreement with the isobaric trajectory study by Kahl et al. (1997). This implies that sources that can emit above the boundary layer (e.g., boreal forest fires) could affect the pollution levels at Summit more strongly than at the low-altitude surface sites. It is also important to notice that while S_T values in high-latitude regions are much lower than for the other stations, the S_T values at lower latitudes are higher. For instance, S_T values in northern Siberia are an order of magnitude lower for Summit than for Alert. In, contrast, over the southern United States and southern ChinaS_T values for Summit are higher than for Alert. This can be understood in the framework of the polar dome concept (Carlson, 1981; Stohl, 2006), where air masses from warm low-latitude areas rise isentropically as they are transported northwards. Summit, because of its high altitude, is more likely to sample these air masses than the other Arctic stations. This implies that aerosol reconstructions from inland Greenland ice cores (McConnell et al., 2007) must be interpreted cautiously because these ice cores will not be representative for the Arctic boundary layer but rather for the Arctic free troposphere and more southerly latitudes.

3.2 Source regions

A natural step after looking at the general atmospheric transport reaching the Arctic stations during different seasons of the year is to couple these transport calculations to the variety of species measured at these sites.

3.2.1 Equivalent black carbon

The measured EBC concentrations experience a clear seasonal variation with a minimum during the late summer months for all low-altitude stations (Fig. 2). For these stations, transport from lower latitudes is infrequent and removal processes such as wet scavenging by precipitation are most effective in summer, explaining the much lower summer concentrations. Summit shows a smaller but opposite seasonal variation with a maximum in late spring and early summer (Fig. 2). Summit continues sampling air from lower latitudes even in summer (Fig. 1) and is less impacted by wet scavenging by drizzle below the Arctic stratus cloud deck. Thus, the different seasonal EBC variation at Summit, is a possible explanation. Annual arithmetic mean concentrations are about the same for Barrow (32.0 ng m^{-3}) and Summit (29.6 ng m^{-3}) while at Alert (47.1 ng m^{-3}) and at Zeppelin (45.1 ng m^{-3}) higher mean concentrations are

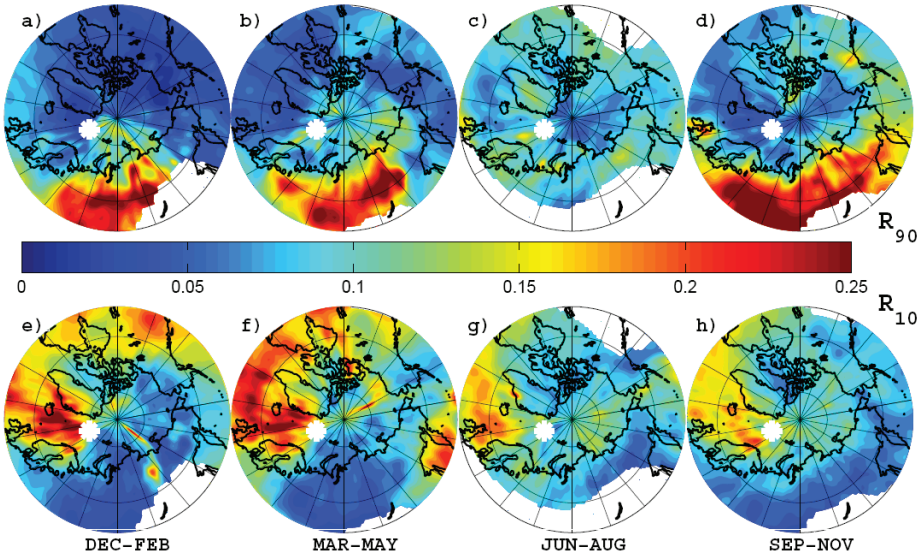

Fig. 3. Fields of R_{90} (top row) and R_{10} (bottom row) for measurements of EBC at the Zeppelin station during the years 2002–2007, for December–February (far left column), March–May (middle left column), June–August (middle right column) and September–November (far right column). The location of the Zeppelin station is marked by a white asterisk. White areas have been excluded from the analysis because S_T is too low.

measured. At the latter two stations, values are somewhat higher than reported in earlier studies (Sharma et al., 2006; Eleftheriadis et al., 2009). This may be due to using a different instrument at Zeppelin for this study than in Eleftheriadis et al. (2009) and a different period of investigation for Alert than in Sharma et al. (2006).

In Fig. 3 we show R_P fields for both the highest and the lowest 10% of all EBC data measured at Zeppelin, for all for seasons. In winter, high EBC concentrations (Fig. 3a) are associated with transport especially from the central parts of Northern Eurasia where R_{90} values exceed 0.2. Also at Alert and Barrow, are high R_{90} values in winter completely dominated by long-range transport from Northern Eurasia (Figs. 4a and 5a), in agreement with the earlier work of Worthy et al. (1994), Polissar et al. (1999, 2001), Sharma et al. (2004, 2006) and Eleftheriadis et al. (2009). None of these stations "sees" significant influence of transport from North America or South East Asia for the top decile of EBC concentrations during winter. Episodes associated with the lowest decile of the EBC data (Figs. 3e, 4e and 5e) show transport from source free regions, or over regions where the transported air would experience strong scavenging by precipitation such as over the North Atlantic Ocean for Zeppelin and Alert or the western Pacific Ocean for Barrow.

The R_{90} and R_{10} patterns in spring (MAM) are generally similar to winter for Zeppelin, Alert and Barrow (Figs. 3b,f, 4b, f and 5b, f). Two exceptions are that high R_{10} values are more related to transport from the North Pacific Ocean for Alert (Fig. 4f), and from the North Atlantic Ocean for Barrow.

During the summer, the picture changes completely. Notice first that R_{90} values are below 0.1 almost everywhere. This indicates that surface contact is unlikely to have occurred when EBC values are high. Thus, high EBC concentrations mostly descend from the free troposphere, consistent with the higher concentrations measured at Summit during summer (see Fig. 2). For Zeppelin (Fig. 3c), the R_{90} field is noisy but elevated R_{90} values are noticeable over northeastern Siberia indicating the influence of frequent boreal forest fires in this region (Kasischke et al., 2005). At Alert (Fig. 4c), there is a small influence from forest fires in Alaska which is consistent with earlier conclusions of significant influences downwind from forest fires in Alaska and Canada (Forster et al., 2001; Stohl et al., 2006). For Barrow (Fig. 5c), high R_{90} values occur over Alaska south of the station which can only be caused by boreal forest fires. Examining individual years, the pattern is particularly strong in 2004 (not shown) and the location of the highest R_{90} values coincides very well with the location of the severe boreal forest fires in that year (Stohl et al., 2006).

In fall (SON), R_{90} patterns for Zeppelin, Alert and Barrow are again similar to the winter situation, with the highest

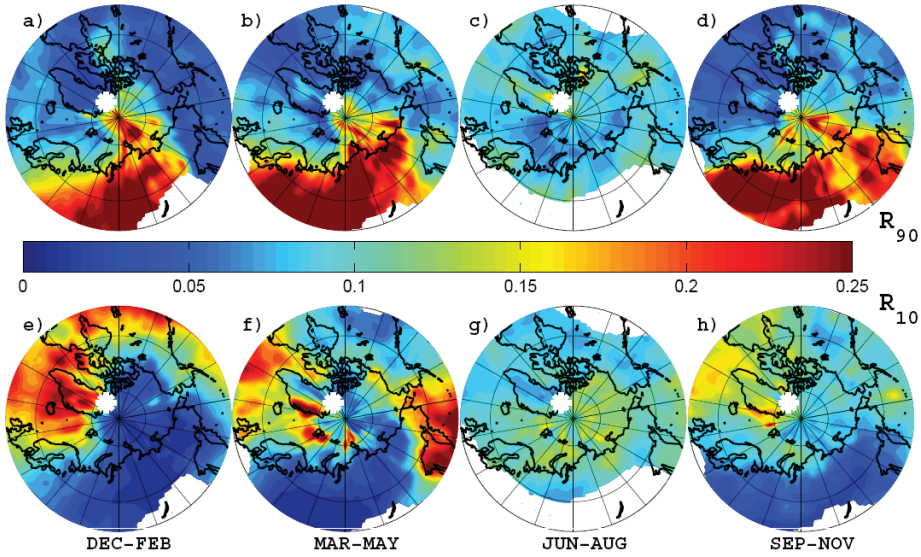

Fig. 4. Same as Fig. 3 but for the Alert station during the years 2000–2006.

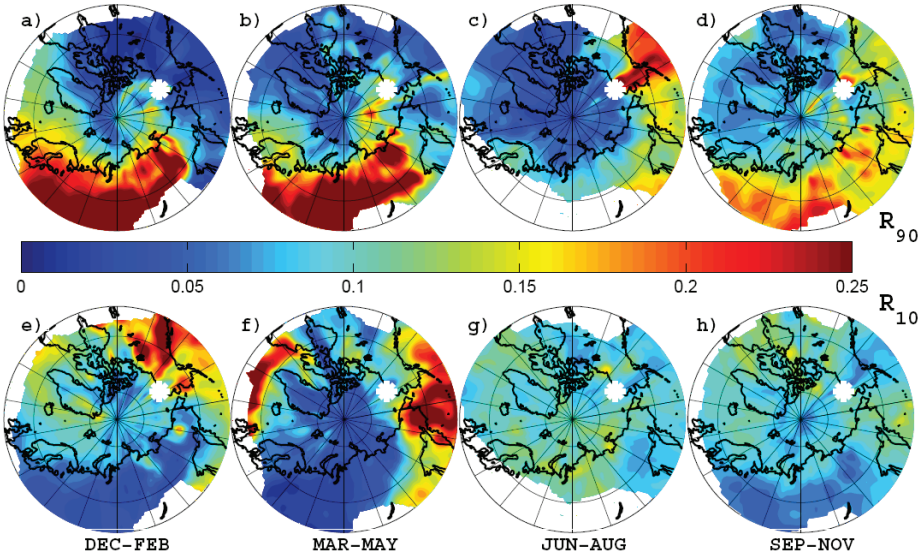

Fig. 5. Same as Fig. 3 but for the Barrow station during the years 2000–2007.

values found over Northern Eurasia (Figs. 3d, 4d, 5d). The largest difference is that R_{90} values over East Asia are enhanced compared to the winter situation.

The R_P fields for Summit differ from the other stations (Fig. 6). First of all, they are noisier because of lower S_T values, than for the other stations, and also because less data are available. In winter, larger R_{90} values are associated with

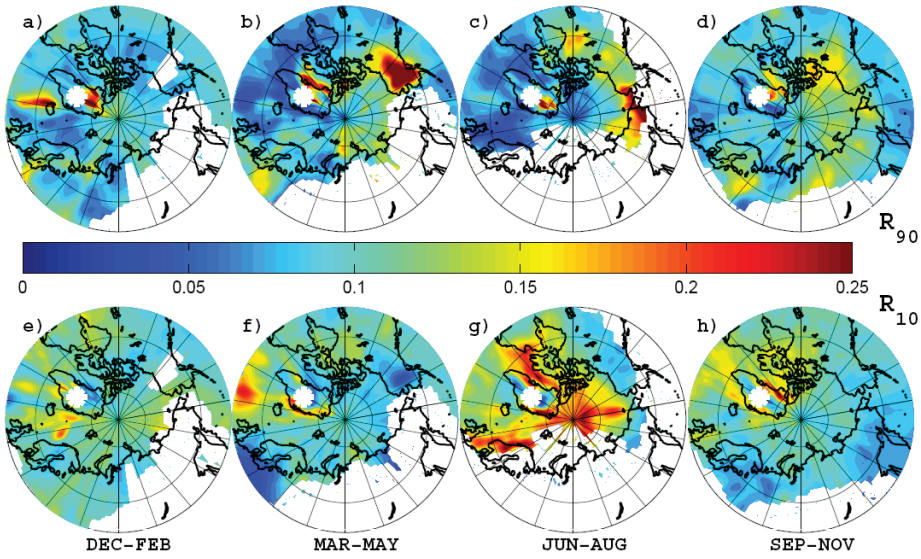

Fig. 6. Same as Fig. 3 but for the Summit station during the years 2003–2006.

transport from Iceland and to some extent also from Central Europe (Fig. 6a) while the R_{10} values show increased surface contact over the Norwegian Sea and the North Atlantic Ocean (Fig. 6e). In spring, the R_{90} patterns demonstrate increased sensitivity over Alaska (Fig. 6b), probably related to early forest fires and Eastern Europe as well as over the Greenland west coast where some of the larger settlements are located. Low EBC concentrations are during spring associated with transport from the North Atlantic Ocean (Fig. 6f). In summer, enhanced R_{90} values are found over the continental regions on both sides of Bering Strait as well as over the north central parts of Canada (Fig. 6c), which likely is associated with forest fires. Low EBC concentrations are related to transport from the surrounding seas, e.g. the Arctic Ocean, Davis Strait and the Norwegian Sea (Fig. 6g). In fall, increased R_{90} values are associated with transport from Eastern Europe, North-Central Eurasia and North-Eastern Canada (Fig. 6d) while the bottom decile of the EBC measurement data are related to transport from the North Atlantic Ocean and Baffin Bay (Fig. 6h). The increased R_{90} values over the Greenland glacial ice sheet during all seasons might be associated with local contamination or descent of aged EBC-rich air from higher levels of the atmosphere, which are likely to be in the footprint layer over the ice sheet.

Discussion

In summer, R_{90} maxima are seen above regions with frequent boreal forest fires, which seem to be the major source of EBC during that season. Elsewhere, R_{90} values are below 0.1 almost everywhere for all stations (in particular for Barrow). In the summer, the Arctic front retreats so far to the north that the Arctic stations see very little direct low-level transport from the surrounding continents. In addition, scavenging processes in the Arctic boundary layer are very efficient because of frequent drizzle (Stohl, 2006). Thus, episodes of high EBC values observed in summer are often associated with air masses that have had almost no surface contact and have instead descended from the free troposphere. As airborne campaigns in the 1980s (Brock et al., 1989) and more recently during POLARCAT have shown, free tropospheric air masses in the Arctic are rich in fire emissions (Warneke et al., 2009; Engvall et al., 2009; Paris et al., 2009). Intense fires can inject pollution directly into the free troposphere and even into the low stratosphere (Fromm et al., 2005) and, thus, would not necessarily be detectable as sources in the R_{90} fields, which are based on footprint emission sensitivities. However, contributions from aged anthropogenic emissions that have been emitted more than 20 days before the measurement may also contribute to an enhanced EBC background that arrives at the stations via the free troposphere.

During seasons other than summer, Northern Eurasia is the dominant EBC source region for all seasons and all stations except Summit. No clear indication of EBC transport from South East Asia can be seen. This is in contrast to some model studies, which attribute a large fraction of BC to South Asia even for the Arctic surface (Koch and Hansen, 2005). Also no influence from North America could be detected,

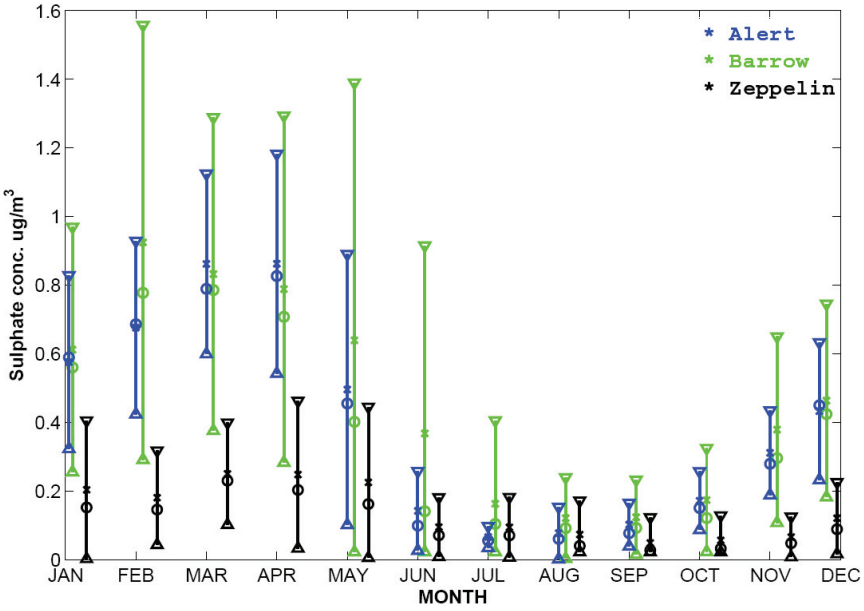

Fig. 7. Monthly averaged concentrations of non-sea-salt sulphate at Alert (blue), Barrow (green) and Zeppelin (black) during the years 2000–2006. The mean concentration is marked with a cross, the median with a circle and the bars indicate variance of ±1 standard deviation. Notice that symbols for Barrow and Zeppelin are slightly offset in time for clarify of presentation.

except for Barrow during the fall when there is some influence from southerly sources in Alaska and for Summit in spring and fall. The apparent lack of influence from North America seen at Barrow might not be entirely representative for this part of the Arctic since episodes with direct transport from most North American source regions have mostly been removed by the data screening to avoid local contamination. However, the results for the other stations confirm the overall small influence of North America anthropogenic sources on the Arctic EBC concentrations.

One important question is to what extent the results depend on the choice of a particular percentile threshold. In the appendix, we show for one example that our results are robust against changes in that threshold, and that an alternative method using all the data gives consistent results. This holds for all stations and all parameters studied.

3.2.2 Sulphate

Monthly mean concentrations of sulphate measured at all three stations show a clear minimum in late summer to early fall (Fig. 7), which is due to more effective scavenging processes and the northward retreat of the Arctic front, as already discussed for EBC. The annual mean concentrations of non-sea-salt (NSS) sulphate at Alert (0.40 $\mu g\,m^{-3}$) and Barrow (0.47 $\mu g\,m^{-3}$), are roughly three times as high as the annual mean concentration at Zeppelin (0.14 $\mu g\,m^{-3}$). The difference is largest from October until May and is most likely the result of a stronger impact of wet scavenging at the Zeppelin station, which is influenced by low pressure systems arriving from the North Atlantic Ocean. To a limited extent, differences may also reflect the different particle size cut-offs used for sampling aerosol on the filters at the various stations.

For the Zeppelin station, R_{90} values are enhanced over northern Eurasia throughout the year (Fig. 8). During winter (Fig. 8a), R_{90} values are moderately enhanced throughout northern Eurasia. During the summer when the Arctic front has retreated furthest north and the lower Arctic atmosphere is nearly closed off from continental influence, high values of R_{90} are observed only over Scandinavia and the northern region of Russia (Fig. 8c). In all seasons except for winter, there are two R_{90} maxima: one over Eastern Europe and the other over Central Siberia. This distribution of sources is consistent with the sulphur sources for the Arctic identified in a numerical model study by Iversen (1989). The first maximum indicates transport of sulphate-rich air from Eastern Europe and particularly the Kola Peninsula, whereas the second maximum appears to be due primarily to transport from the metal smelting industry in Norilsk. Norilsk stands out as the worldwide strongest maximum in maps of satellite-observed sulphur dioxide total columns (Khokhar et

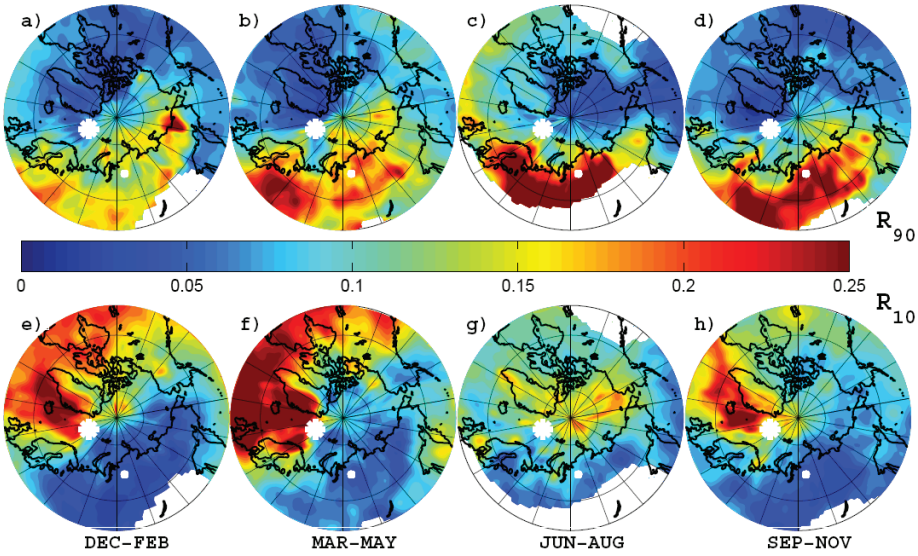

Fig. 8. Fields of R_{90} (top row) and R_{10} (bottom row) for non-sea-salt sulphate measured at the Zeppelin station during the years 2000–2006, for December–February (far left column), March-May (middle left column), June–August (middle right column) and September–November (far right column). The location of the Zeppelin station is marked by a large white asterisk, and a small white dot marks the location of the industrialized city of Norilsk. White areas have been excluded from the analysis because S_T is too low.

al., 2005). It is likely that this strong but distant point source cannot be fully resolved by our method. Possibly most of the R_{90} enhancements over central Siberia might actually be associated with transport from Norilsk.

High R_{10} values for Zeppelin are found over ocean areas throughout the year (Fig. 8e–h), especially over the North Atlantic where wet scavenging by precipitation is most efficient. At the same time, no high R_{90} values are found over North America, confirming that NSS sulphate originating from there gets scavenged before reaching the European Arctic (Rahn, 1982). In summer, R_{10} values are also high over the Arctic Ocean, indicating sulphate removal by scavenging processes (Behrenfeldt et al., 2008). The results shown in Fig. 8 are not sensitive to changes of the percentile threshold as shown in the appendix.

At Alert (Fig. 9), the time resolution of the sulphate measurements is 7 days. The coarse time resolution impacts the transport analysis by making it difficult to detect individual transport events. As a result, source regions are not well demarcated. Nevertheless, high R_{90} values can be found over Norilsk in spring and summer (Fig. 9b, c). In winter, the R_{90} maximum is displaced slightly to the east of Norilsk, and transport of high sulphate concentrations from Eastern Europe is indicated as well (Fig. 9a). The maximum over north-western Canada cannot easily be explained but might be related to oil production activities. In fall (Fig. 9d), the highest R_{90} values are found over eastern Asia, probably indicating some influence from emissions in China and/or from volcanoes on the Kamchatka Peninsula. Note that transport even from north-eastern China is too infrequent on the 20-day time scale of FLEXPART calculations to be resolved in these statistics.

At Barrow (Fig. 10), the time resolution of the measurements ranges from 1 to 5 days, with shortest sampling durations used during the Arctic haze season in spring. Throughout the year, R_{90} values are elevated in the vicinity of Norilsk, again indicating the importance of this source for the entire Arctic. Transport from Eastern Europe also causes high sulphate concentrations at Barrow throughout the year (Fig. 10a–d). The maximum over south-western Canada in spring corresponds well with the location of the great oil sand fields in Alberta, and its large petroleum industry. In summer, high R_{90} values can be found from eastern Asia across the entire northern North Pacific Ocean (Fig. 10c). This might indicate an influence from anthropogenic emissions in Asia or from ships travelling between North America and Asia (Dalsøren et al., 2007). Another possible source is volcanic emissions on Kamchatka and the Aleutian Islands. Notice that smaller R_{90} maxima over the Aleutian Islands can be found also during other times of the year, for instance in spring (Fig. 10b).

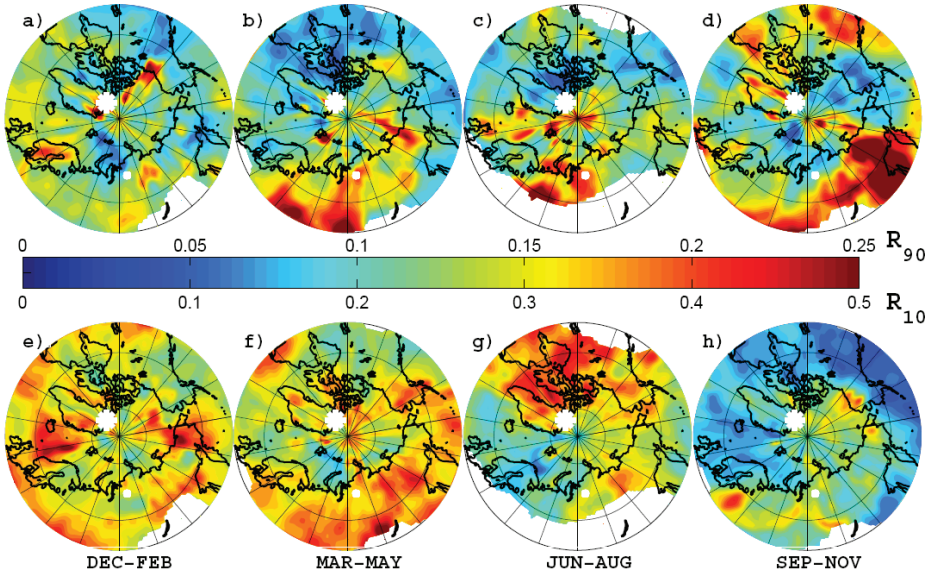

Fig. 9. Same as Fig. 8 but for the Alert station. The upper scale on the colour bar applies to panels **(a–d)**, and the lower scale applies to panels **(e–h)**.

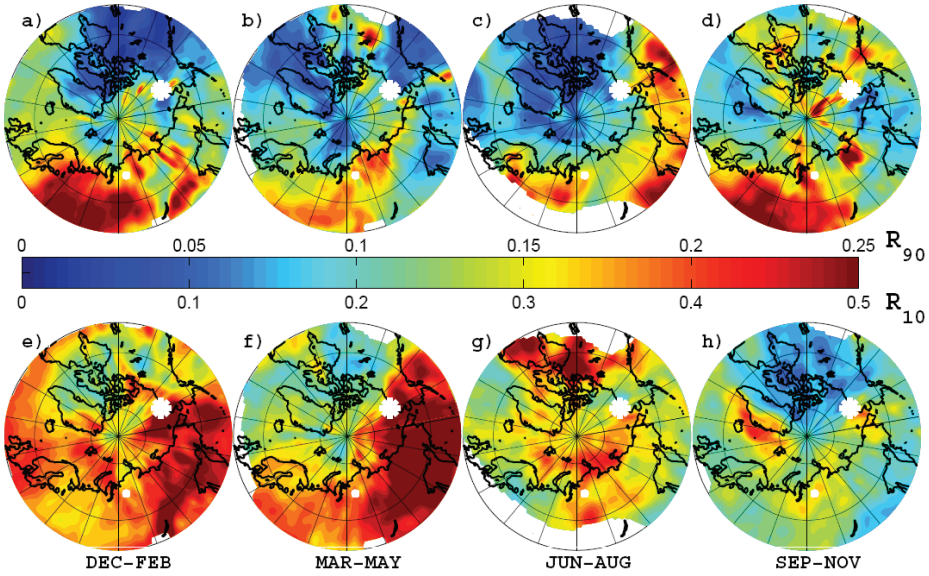

Fig. 10. Same as Fig. 8 but for the Barrow station. The upper scale on the colour bar applies to panels **(a–d)**, and the lower scale applies to panels **(e–h)**.

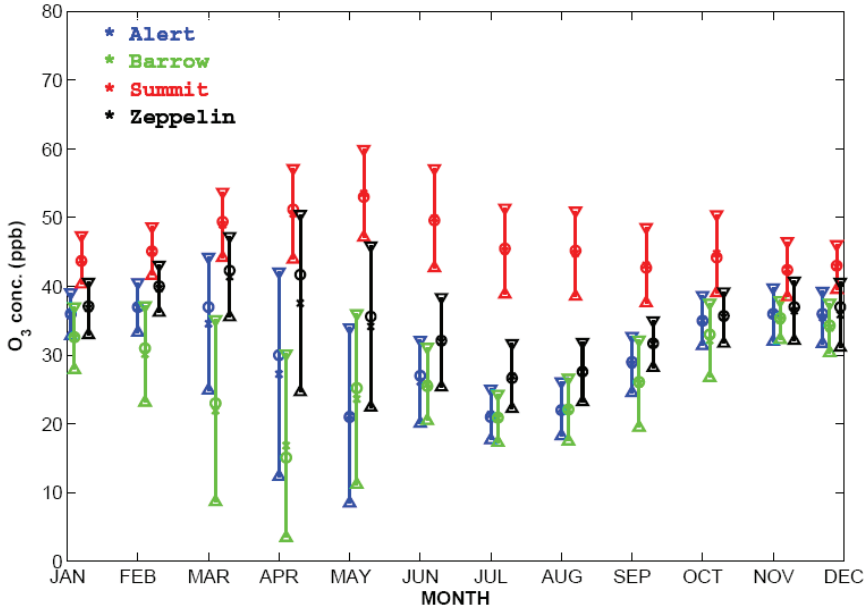

Fig. 11. Monthly ozone at Alert (blue), Barrow (green), Summit (red) and Zeppelin (black) during the years 2000–2007 (2000–2006 for Barrow). The mean concentration is marked with a cross, the median with a circle and the bars indicate the range ±1 standard deviation. Notice that symbols for Barrow, Summit and Zeppelin are slightly offset in time for clarify of presentation.

3.2.3 Light scattering aerosols

Since light scattering aerosol data were only available for one station (Barrow), results will only be briefly discussed here. For the lowest decile of the data (not shown), the R_{10} patterns are very similar to those for EBC during winter and spring (see Fig. 5e, f), while the patterns during summer and fall are more pronounced over source free regions such as the Hudson Bay and the North Pacific Ocean. For the R_{90} values, in spring results are similar to EBC with increased R_{90} values over North-Central Eurasia and in summer with a pronounced source region associated with the boreal forest fires (not shown). In winter increased R_{90} values are associated with transport from the southern parts of Canada. During all times of the year, the increased R_{90} values are found along the coastline of eastern Alaska and western Canada. Surprisingly, these maxima are not at all identified for the NSS sulphate data, probably indicating that much of the light scattering is caused by organic aerosols. According to the R_{90} results, possible sources for these light-scattering aerosols include oil extracting facilities at Prudhoe Bay and in western Canada, as well as the Smoking Hills (Radke and Hobbs, 1989), a continuous source of smoke. However, as discussed in Sect. 3.2.1, the extensive screening of the Barrow aerosol data could also affect the analysis.

3.2.4 Ozone

Hirdman et al. (2009) already have presented an O_3 source region analysis for Zeppelin. However, Hirdman et al. (2009) studied mercury and discussed O_3 results only briefly to support the mercury analysis. In this paper, we present a full statistical analysis of O_3 for all four observatories. Annual mean O_3 concentrations increase with the station's altitude: 26.7±9.9 for Barrow (11 m a.s.l.), 30.1±8.9 for Alert (210 m a.s.l.), 34.6±7.6 for Zeppelin (478 m a.s.l.), and 46.3±7.3 ppb for Summit (3208 m a.s.l.). These concentrations are in good agreement with earlier reports (Oltmans et al., 2006; Helmig et al., 2007b). The vertical gradient is indicative of a high-altitude source and a low-altitude sink of O_3. Seasonal variations are also different (Fig. 11): Summit shows a maximum in late spring, which may be indicative of a stratospheric source peaking at this time of the year (Helmig et al., 2007b). In spite of that, the TOPSE campaign also revealed strong photochemical activity in spring (Browell et al., 2003). In contrast, concentrations at Barrow and Alert are lowest at this time of the year, related to O_3 depletion events (see below). All stations show low values in summer when the Arctic lower troposphere is most isolated both from mid-latitude precursor sources and from the stratosphere.

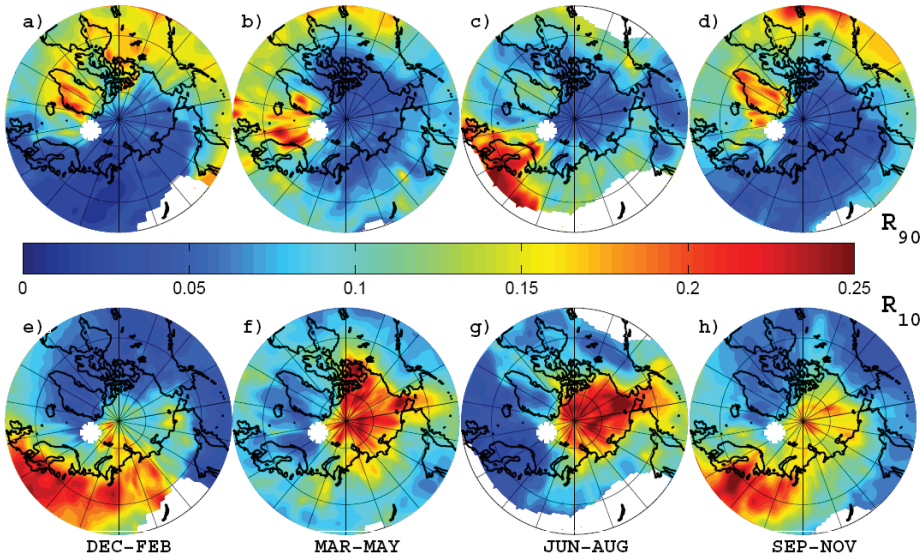

Fig. 12. Fields of R_{90} (top row) and R_{10} (bottom row) for surface ozone measurements at the Zeppelin station during the years 2000–2007, for December–February (left column), March–May (middle-left column), June–August (middle-right column) and September–November (right column). The location of the Zeppelin station is marked by a white asterisk. White areas have been excluded from the analysis because S_T is too low.

Since O_3 is a secondarily formed reactive trace gas, the interpretation of sources and sinks is less direct than for primary species. High R_{90} values may indicate regions of precursor gas emissions, regions of preferential O_3 formation or lack of O_3 destruction by deposition or titration.

Figure 12 shows the R_P fields for high and low O_3 events observed at Zeppelin in winter, spring, summer and fall. In winter, R_{10} values are highest over Eurasia (Fig. 12e). There, in the absence of sunlight, O_3 is titrated by reaction with nitric oxide emitted from anthropogenic sources (Morin et al., 2008) leading to low O_3 concentrations at Zeppelin. R_{90} values are generally well below 0.1 over the regions from where the transport reaching the station is most frequent (see Fig. 1), namely the Arctic Ocean and Eurasia where R_{90} values approach zero (Fig. 12a). Thus, high O_3 concentrations are almost never associated with air masses having surface contact (an exception are high R_{90} values found over the remote low latitudes from where transport is infrequent). Instead, the high O_3 concentrations are primarily associated with descent of air masses from above the boundary layer, which have no surface contact prior to arrival. The high R_{90} values over the elevated topography of Greenland in Fig. 12a also show the downward transport from the free troposphere (Fig. 1a).

In spring, R_{10} values are highest within the Arctic Ocean basin (Fig. 12f), in agreement with earlier studies (Solberg et al., 1996; Eneroth et al., 2007; Bottenheim et al., 2009). Notice the strong decrease in the R_{10} values following almost exactly the coastlines. The high R_{10} values over the Arctic Ocean coincide well with the regions where satellites observe high concentrations of bromine monoxide (BrO) (Simpson et al., 2007), suggesting that the low O_3 values are caused primarily by ozone depletion events (ODEs) during the polar sunrise (Barrie et al., 1988; Anlauf et al., 1994; Bottenheim et al., 1990, 2002, 2009). Hirdman et al. (2009) found the same pattern for gaseous elemental mercury (GEM), which also reacts with Br and BrO, indicating a common sink process for O_3 and GEM. As in winter, the R_{90} values along the major transport pathways are well below 0.1 (Fig. 12b), indicating little surface contact except for air masses descending from Greenland. High R_{90} values just off Scandinavia might indicate transport of photochemically formed O_3 from Europe.

In summer, high R_{90} values for O_3 can be found over the continental land masses (Fig. 12c), especially Europe, highlighting the importance of photochemical O_3 formation (Honrath et al., 2004). Notice in particular the sharp contrast to the winter situation when titration by nitric oxide emissions destroys the O_3 in this region (Fig. 12e). R_{10} values are still the highest in oceanic air masses, indicating that the Arctic lower troposphere continues to act as an O_3 sink in summer (Fig. 12g). In fact, ODEs with $O_3 < 10$ ppb do occur

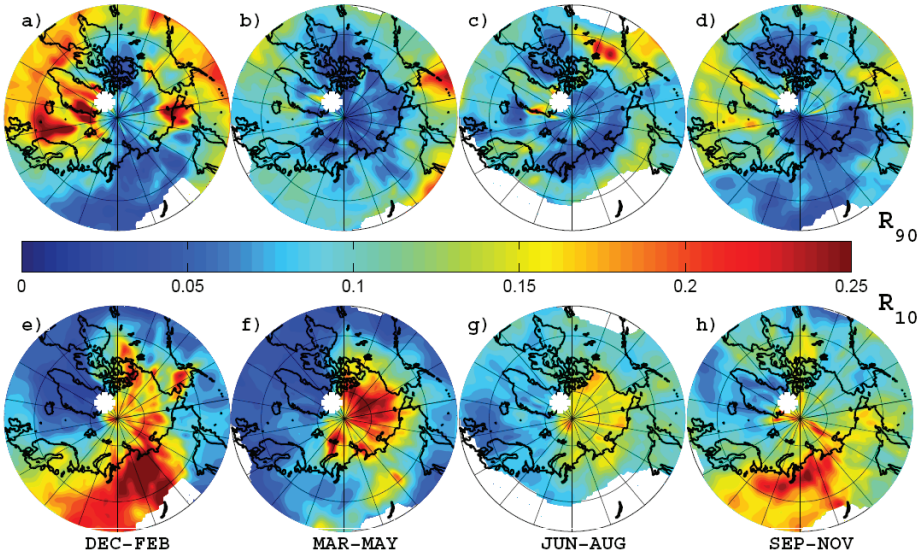

Fig. 13. Same as Fig. 12 but for the Alert station during the years 2000–2007.

at Zeppelin occasionally in early summer, which is in agreement with recent measurements on board of a trans-polar drifting station (Bottenheim et al., 2009).

Fall (Fig. 12d, h) is a time of transition. R_{10} values are elevated both over the Arctic Ocean alike to spring and summer but also over Eurasia, indicating the return to winter-time O_3 titration. The R_{90} patterns do already show strong similarities with the winter conditions.

The results for Alert (Fig. 13) are similar to those for Zeppelin (Fig. 12). However there are two main differences. First of all, Europe does not act as a source for anthropogenic O_3 formation during summer, but instead there are strongly enhanced R_{90} values over north-western Canada where the country's greatest petroleum production fields from oil sand are located (Fig. 13c). This region also experiences frequent forest fires, which can lead to substantial O_3 formation (Wotawa and Trainer, 2000; Forster et al., 2001). Secondly the R_{90} values (Fig. 13a, b, d) show a stronger influence coming from the North Atlantic and North Pacific Oceans than for Zeppelin.

At Barrow, in winter (Fig. 14e) low O_3 occurs due to titration mainly over Eurasia and high O_3 are generally coupled with transport from the North Pacific Ocean (Fig. 14a). In spring, the low O_3 concentrations are again primarily associated with ODEs over the Arctic Ocean (Fig. 14f), while high R_{90} values primarily are found over Eastern Asia and over the North Pacific downwind of Eastern Asia (Fig. 14b). This is consistent with the fact that pollution outflow from Asia has its largest influence on western North America in spring (Forster et al., 2004). In summer, O_3 concentrations in the top decile (R_{90}) are mainly associated with transport from nearby areas in Alaska/Canada and distant regions in Eurasia (Fig. 14c). The local North American source in Fig. 14c could be associated with O_3 formed from anthropogenic precursor emissions from the oil fields at Prudhoe Bay and/or in boreal forest fires. Interestingly, low O_3 concentrations in summer are not associated with transport from the Arctic Ocean but instead with transport mainly from the central North Pacific Ocean (Fig. 14g). Correspondingly, no ODEs are observed at Barrow in summer and the lowest measured O_3 concentrations are consistent with a North Pacific Ocean boundary-layer origin (Watanabe et al., 2005). In fall, high O_3 descends mostly from above the boundary layer (Fig. 14d), while the R_{10} patterns mark the transition between summer and winter (Fig. 14h).

At Summit, R_{90} values are well below 0.1 almost everywhere and throughout the year (Fig. 15a–d), confirming that high O_3 concentrations are primarily associated with air masses which had little or no surface contact. The exception is transport of photochemically formed O_3 from Europe in spring and summer and to some extent also in fall (Fig. 15b, c, d). Transport of photochemical pollution from Europe to Summit is known to occur occasionally (Helmig et al., 2007b). In contrast, the low O_3 concentrations at Summit are associated with uplift of air masses from the same regions that cause low-O_3 events at the other stations: Eurasia in winter (Fig. 15e), related to titration; the Arctic Ocean in spring (Fig. 15f), related to ODEs; and from both the Arctic

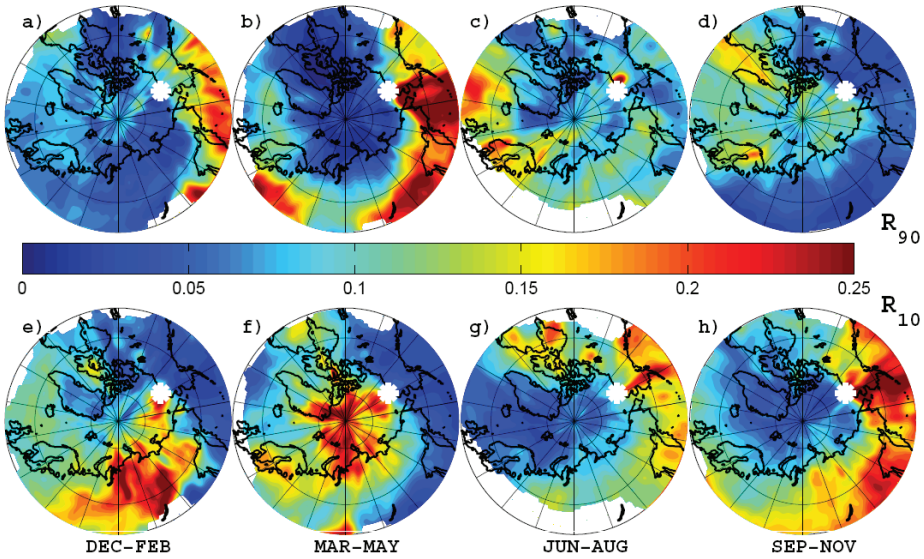

Fig. 14. Same as Fig. 12 but for the Barrow station during the years 2000–2006.

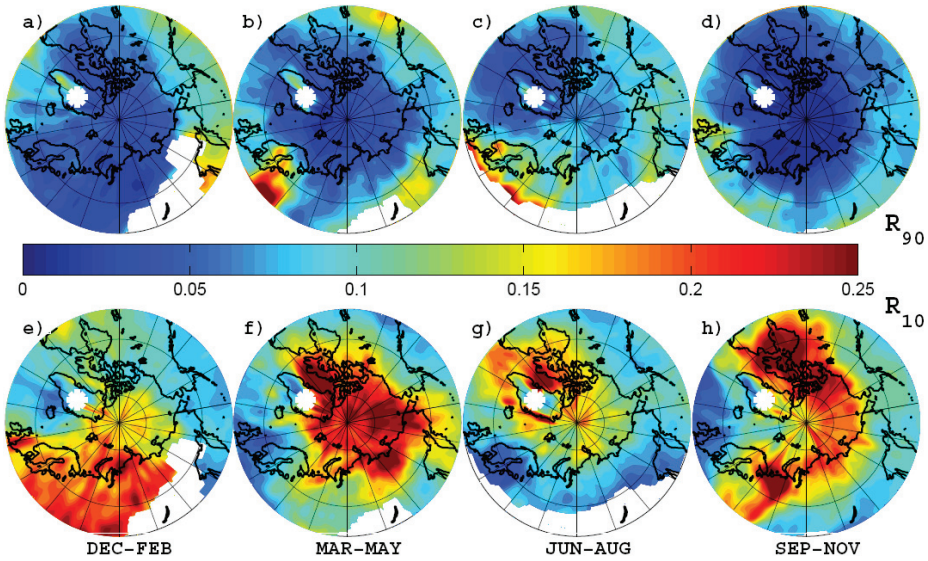

Fig. 15. Same as Fig. 12 but for the Summit station during the years 2000–2007.

Ocean and high-latitude land areas in fall. It is quite remarkable that these surface sinks are well detected even at the high altitude of Summit.

The above analysis shows that at all stations most of the high O_3 concentrations occur in air masses having little surface contact, which is suggestive either of a stratospheric source or of a free-tropospheric photochemical source. In

Table 2. The mean fraction (%) of air intruding from the stratosphere averaged over 10 and 20 days back in time, for the uppermost and lowermost decile of O_3 concentrations, and for the different seasons, as well as the Pearson correlation coefficient r_{20} for the correlation between measured O_3 and the fraction of air intruding from the stratosphere averaged over 20 days back in time. All the r_{20} values are statistically significantly different from zero.

Station →		Zeppelin			Alert			Barrow			Summit		
Season ↓		10	20	r_{20}	10	20	r_{20}	10	20	r_{20}	10	20	r_{20}
Winter	High O_3	0.0	0.9	0.24	0.0	0.7	0.32	0.0	0.1	0.15	0.4	2.2	0.44
	Low O_3	0.0	0.2		0.0	0.0		0.0	0.0		0.1	0.8	
Spring	High O_3	0.0	0.5	0.54	0.0	0.6	0.32	0.1	1.3	0.41	2.8	5.4	0.38
	Low O_3	0.0	0.0		0.0	0.0		0.0	0.1		0.2	0.5	
Summer	High O_3	0.0	0.4	0.42	0.0	0.1	0.20	0.0	0.1	0.05	0.0	1.1	0.18
	Low O_3	0.0	0.0		0.0	0.0		0.0	0.1		0.0	0.4	
Fall	High O_3	0.0	0.9	0.34	0.4	1.0	0.32	0.0	0.2	−0.18	1.9	4.5	0.53
	Low O_3	0.1	0.4		0.0	0.3		0.2	0.9		0.1	1.0	

order to quantify the stratospheric influence the fraction of particles which have been transported from above the thermal tropopause to the station as a function of time backward was calculated (with FLEXPART). Table 2 gives the seasonal averages of this stratospheric influence for the different stations averaged over transport times of 10 and 20 days, respectively, and for the O_3 concentrations in the top and bottom decile, respectively. For the low-altitude stations (Alert, Barrow, Zeppelin), the fraction of particles arriving from the stratosphere on both time scales is very small (typically 1% or less even for the 20-days time scale) indicating that the stratospheric influence on Arctic surface air is small on these time scales (Stohl, 2006). The Summit station experiences the largest influence from the stratosphere due to its high-altitude location (3208 m a.s.l.). At all stations, the stratospheric influence is larger for the high O_3 concentrations than for the low O_3 concentrations. By calculating Pearson's correlation coefficient (r_{20}) between measured O_3 and the stratospheric influence averaged over 20 days back, a positive correlation for all four stations throughout the year was found (except for Barrow during fall). The correlation normally peaks in spring (r_{20}=0.4±0.1) which coincides with the season of the year where the strongest influence from the stratosphere would be expected because of relatively frequent stratospheric intrusions (Stohl, 2006) and high O_3 concentrations in the lowermost stratosphere. The correlation shows a relation with the station altitude such that the highest r_{20} values are found for Summit followed by Zeppelin, Alert and last Barrow (Table 2). In summary, while intrusions of stratospheric air are rare on the timescales considered, especially for low-altitude sites, transport from the stratosphere does appear to have a substantial influence on surface O_3 concentrations in the Arctic.

4 Conclusions

In this paper we have employed a novel method to combine the calculations from a Lagrangian particle dispersion model, FLEXPART, and measurement data from four Arctic stations (Zeppelin, Alert, Barrow and Summit) in a statistical analysis of the source regions of short-lived pollutants. The calculated sensitivities have been normalized to surface emissions when observed pollutant concentrations were in the top (or lowest) decile with the emission sensitivities for the entire data set to reveal the regions from where high (or low) pollutant concentrations originate. The results are robust against changes of the percentile thresholds used. The calculated emission sensitivities have also been used as flow climatologies to reveal the overall air mass origins for the different stations. Our main findings from this study are:

– Transport climatologies based on 20-day backward calculations for Zeppelin, Alert and Barrow show that these stations are highly sensitive to surface emissions in the Arctic. In winter, they are also sensitive to emissions in high-latitude Eurasia, whereas in summer these Arctic surface stations are largely shielded off from continental emissions on the 20-day time scale. Should local sources in the Arctic (e.g., oil and gas drilling, shipping) increase in the future, they would contribute strongly to surface concentrations of pollutants in the Arctic, particularly in summer. Emission sensitivities over southern Asia and southern North America are extremely small throughout the year. The high-altitude station Summit is more than an order of magnitude less sensitive to surface emissions in the Arctic than the lower altitude stations. In contrast, sensitivities to surface emissions in the southern parts of the Northern Hemisphere continents are higher than for the other stations. This shows that potential pollution source regions

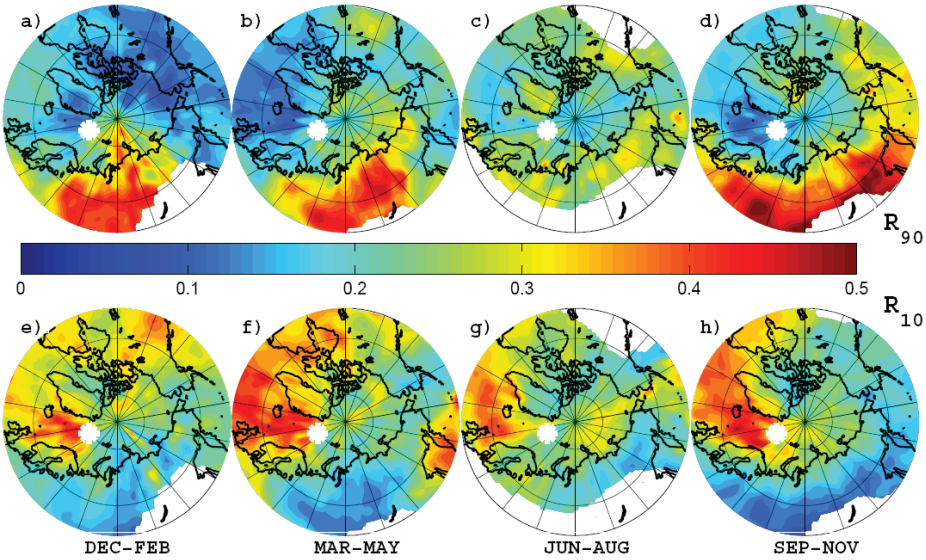

Fig. A1. Fields of R_{75} (top row) and R_{25} (bottom row) for measurements of EBC at the Zeppelin station during the years 2002–2007, for December–February (far left column), March–May (middle left column), June–August (middle right column) and September–November (far right column). The location of the Zeppelin station is marked by a white asterisk. White areas have been excluded from the analysis because S_T is too low.

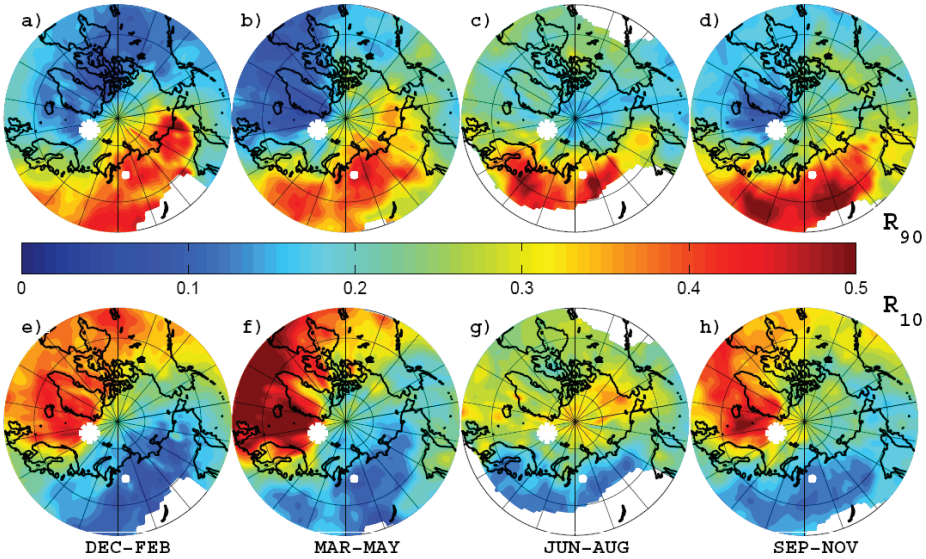

Fig. A2. Fields of R_{75} (top row) and R_{25} (bottom row) for non-sea-salt sulphate measured at the Zeppelin station during the years 2000–2006, for December–February (far left column), March–May (middle left column), June–August (middle right column) and September–November (far right column). The location of the Zeppelin station is marked by a large white asterisk, and a small white dot marks the location of the industrialized city of Norilsk. White areas have been excluded from the analysis because S_T is too low.

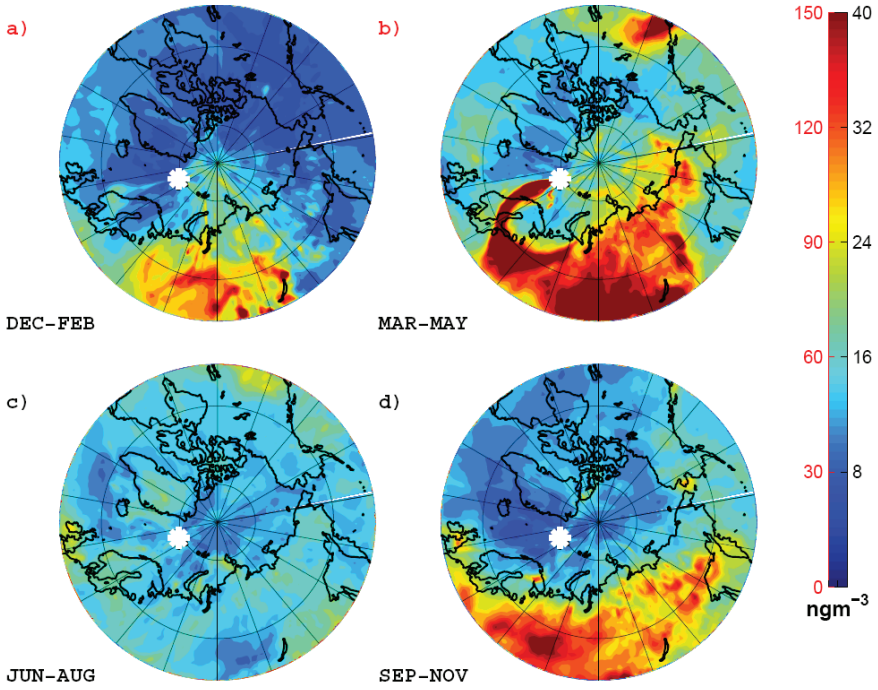

Fig. A3. The complete set of calculated emission sensitivity fields, each weighted with the associated EBC concentrations measured at Zeppelin during the years 2002–2007, for December–February (upper left), March–May (upper right), June–August (lower left) and September–November (lower right). The left colour bar applies to panels **(a)** and **(b)**, right scale applies to panels **(c)** and **(d)**. The white asterisk marks the location of the Zeppelin station.

for Summit and for ice core sites drilled at similar altitudes are distinctly different from those for the surface stations.

– Equivalent black carbon: at Zeppelin, Alert and Barrow, the top decile of EBC concentrations originate from high-latitude Eurasia throughout the year. Only during summer, there is also evidence for transport of emissions from boreal forest fires in North America to Barrow and Alert and from Siberia to Zeppelin. Furthermore, in summer EBC concentrations are enhanced when the air descends from the free troposphere. This point toward boreal forest fires injecting emissions higher into the atmosphere or aged air masses from unresolved sources beyond the 20-day time scale considered in this study. However, we find no direct evidence that transport from Southern Asia or Southern North America is a source of EBC at the Arctic surface stations.

– Sulphate: As for EBC, the dominant source region for sulphate at Zeppelin, Alert and Barrow is high-latitude Eurasia. There, the sulphate primarily originates from two source regions, Eastern Europe and the metal smelting complexes at Norilsk. At Alert in fall and at Barrow in summer, high sulphate concentrations are also found when the air is transported from Eastern Asia and the North Pacific. This may indicate an anthropogenic source of the sulphate in Eastern Asia, but emissions from volcanoes on Kamchatka and the Aleutian Islands are equally likely sources.

– Light scattering aerosols: Enhanced values of aerosol light scattering at Barrow are associated with boreal forest fires in Alaska and Canada, similar to EBC. Transport from Eurasia also leads to enhanced aerosol light scattering. However, there is no close correspondence between the sources of sulphate and light scattering aerosols. Additional sources of scattering aerosol in Northern Alaska and Canada not seen for sulphate are probably related to organic aerosols from oil drilling activities and/or the Smoking Hills fires.

– Ozone: The annual mean concentrations of O_3 increase systematically with altitude from the lowest station, Barrow, to the highest, Summit. This increase is

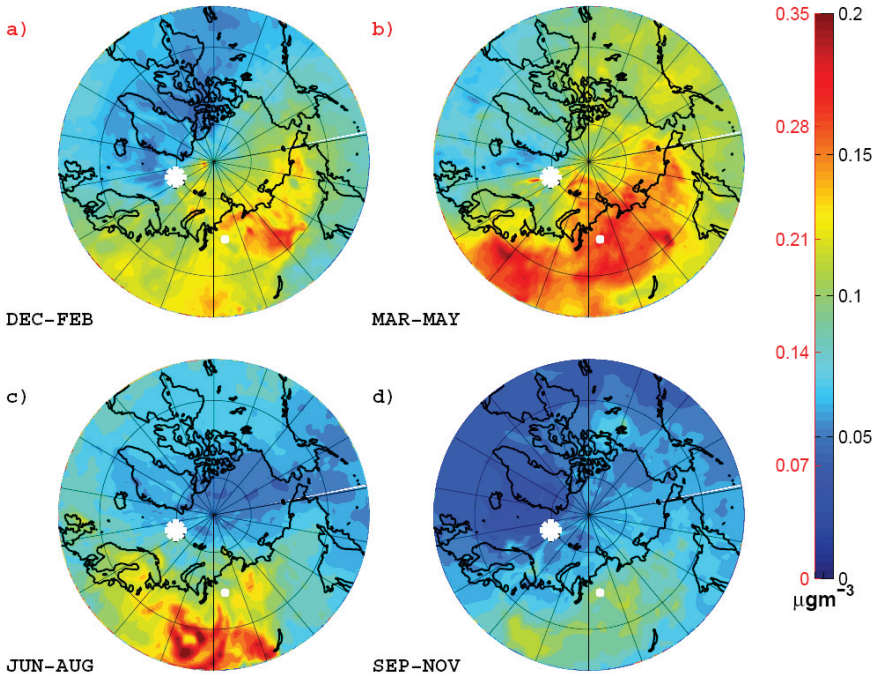

Fig. A4. The complete set of calculated emission sensitivity fields, each weighted with the associated NSS sulphate concentrations measured at Zeppelin during the years 2000–2006, for December–February (upper left), March–May (upper right), June–August (lower left) and September–November (lower right). The left colour bar applies to panels **(a)** and **(b)**, right scale applies to panels **(c)** and **(d)**. The location of the Zeppelin station is marked by a large white asterisk, and a small white dot marks the location of Norilsk.

accompanied by an increasing fraction of air arriving from the stratosphere and increasing positive correlations between this calculated quantity and the observed O_3. Furthermore, at all stations, O_3-rich air masses have little surface contact during the previous 20 days. This indicates that while transport from the stratosphere is slow in the Arctic, it nevertheless has a large impact on observed surface O_3 throughout the year. When transport occurs from Eurasia, all stations show decreased O_3 concentrations in winter (due to titration of O_3 by nitric oxide) but enhanced ozone concentrations in summer (due to photochemical O_3 formation). When air travels across the Arctic Ocean in spring, all stations show decreased O_3 concentrations due to ozone depletion events. Especially for Zeppelin, this pattern continues into summer.

– A harmonization of the sampling instruments and measurements within the Arctic would simplify data comparison significantly and therefore aid similar studies in the future.

Appendix A

Our method uses particular percentile thresholds (uppermost and lowermost deciles) to compare transport patterns for high and low measured concentrations, respectively, with the total average transport. One possible concern is that the results are sensitive to changes of the percentile thresholds. Here we show, at the examples of EBC (Fig. A1) and NSS sulphate (Fig. A2) for Zeppelin, that this is not the case by using the uppermost and lowermost quartiles instead of deciles. The R_{75} and R_{25} patterns identified are almost the same as the R_{90} and R_{10} patterns shown in Figs. 3 and 8.

An alternative method was also tested, similar to the one used by Seibert et al. (1994) and Stohl et al. (1996) for trajectory statistics. With this method, S values are weighted by the corresponding measured concentration $c(m)$.

$$C(i,j) = \frac{\sum_{m=1}^{M} c(m) S(i,j,m)}{\sum_{m=1}^{M} S(i,j,m)} \quad \text{(A1)}$$

High values of $C(i,j)$ indicate that transport through grid cell (i,j) is preferentially associated with high measured concentrations and, thus, grid cell (i,j) is a potential source

of the measured parameter. This method has the advantage of not being focussed on the distribution tails. Figures A3 and A4 show that sources identified with this method are similar to those identified with the percentile method.

Acknowledgements. We appreciate discussions with C. Brock and T. Ryerson on Alaskan emissions. We thank the two anonymous reviewers for their comments on our paper. We would like to thank ECMWF and met.no for access to the ECMWF archives. We would also like to thank the Global Monitoring Division at NOAA Earth System Research Laboratory, the Atmospheric Science and Technology Directorate at Environment Canada and SFT Norway for providing data. The Swedish Environmental Protection Agency and the Swedish Research Council have sponsored BC measurements at Zeppelin. Funding for this study was provided by the Norwegian Research Council through the POLARCAT and SUMSVAL projects.

Edited by: J. W. Bottenheim

References

Aas, W., Solberg, S., Manø, S., and Yttri, K. E.: Monitoring of long range transported air pollutants, annual report for 2007, Norwegian Institute for Air Research, Kjeller, 2008.

Anlauf, K., Mickle, R., and Trivett, N.: Measurement of ozone during polar sunrise experiment 1992, J. Geophys. Res., 99, 25345–25353, 1994.

Arnott, W., Hamasha, K., Moosmuller, H., Sheridan, P., and Ogren, J.: Towards aerosol light-absorption measurements with a 7-wavelength aethalometer: Evaluation with a photoacoustic instrument and 3-wavelength nephelometer, Aerosol Sci. Technol., 39, 17–29, 2005.

Ashbaugh, L.: A statistical trajectory technique for determining air-pollution source regions, Journal of the Air Pollution Control Association, 33, 1096–1098, 1983.

Ashbaugh, L., Malm, W., and Sadeh, W.: A residence time probability analysis of sulfur concentrations at grand-canyon-national-park, Atmos. Environ., 19, 1263–1270, 1985.

Barrie, L.: Arctic air-pollution – an overview of current knowledge, Atmos. Environ., 20, 643–663, 1986.

Barrie, L., Bottenheim, J., Schnell, R., Crutzen, P., and Rasmussen, R.: Ozone destruction and photochemical-reactions at polar sunrise in the lower arctic atmosphere, Nature, 334, 138–141, 1988.

Behrenfeldt, U., Krejci, R., Ström, J., and Stohl, A.: Chemical properties of Arctic aerosol particles collected at Zeppelin station during the aerosol transition period in May and June of 2004, Tellus B, 60, 405–415, 2008.

Bodhaine, B. A.: Aerosol absorption measurements at Barrow, Mauna Loa and the South Pole, J. Geophys. Res., 100, 8967–8975, 1995.

Bond, T., Anderson, T., and Campbell, D.: Calibration and intercomparison of filter-based measurements of visible light absorption by aerosols, Aerosol Sci. Technol., 30, 582–600, 1999.

Bond, T. and Bergstrom, R.: Light absorption by carbonaceous particles: An investigative review, Aerosol Sci. Technol., 40, 27–67, 2006.

Bottenheim, J., Barrie, L., Atlas, E., Heidt, L., Niki, H., Rasmussen, R., and Shepson, P.: Depletion of lower tropospheric ozone during Arctic spring – the polar sunrise experiment 1988, J. Geophys. Res., 95, 18555–18568, 1990.

Bottenheim, J., Fuentes, J., Tarasick, D., and Anlauf, K.: Ozone in the Arctic lower troposphere during winter and spring 2000 (Alert2000), Atmos. Environ., 36, 2535–2544, 2002.

Bottenheim, J. W., Netcheva, S., Morin, S., and Nghiem, S. V.: Ozone in the boundary layer air over the Arctic Ocean: measurements during the TARA transpolar drift 2006–2008, Atmos. Chem. Phys., 9, 4545–4557, 2009, http://www.atmos-chem-phys.net/9/4545/2009/.

Brock, C. A., Radke, L. F., Lyons, J. H., and Hobbs, P. V.: Arctic hazes in summer over Greenland and the North American Arctic. I: Incidence and origins, J. Atmos. Chem., 9, 129–148, 1989.

Browell, E. V., Hair, J. W., Butler, C. F., Grant, W. B., Deyoung, R. J., Fenn, M. A., et al.: Ozone, aerosol, potential vorticity, and trace gas trends observed at high-latitudes over North America from February to May 2000, J. Geophys. Res., 108, 8369, doi:10.1029/2002JD003232, 2003.

Carlson, T.: Speculations on the movement of polluted air to the Arctic, Atmos. Environ., 15, 1473–1477, 1981.

Dalsøren, S. B., Endresen, Ø., Isaksen, I. S. A., Gravir, G., and Sørgård, E.: Environmental impacts of the expected increase in sea transportation, with a particular focus on oil and gas scenarios for Norway and northwest Russia, J. Geophys. Res., 112, D02310, doi:10.1029/2005JD006927, 2007.

Delene, D. and Ogren, J.: Variability of aerosol optical properties at four North American surface monitoring sites, J. Atmos. Sci., 59, 1135–1150, 2002.

Devore, J. and Farnum, N.: Applied statistics for engineers and scientists, in, Duxbury Press, 315–318, 1999.

Eleftheriadis, K., Vratolis, S., and Nyeki, S.: Aerosol black carbon in the European Arctic: Measurements at Zeppelin station, Ny-Ålesund, Svalbard from 1998–2007, Geophys. Res. Lett., 36, L02809, doi:10.1029/2008GL035741 2009.

Eneroth, K., Kjellstrom, E., and Holmen, K.: A trajectory climatology for Svalbard; investigating how atmospheric flow patterns influence observed tracer concentrations, Phys. Chem. Earth., 28, 1191–1203, 2003.

Eneroth, K., Holmen, K., Berg, T., Schmidbauer, N., and Solberg, S.: Springtime depletion of tropospheric ozone, gaseous elemental mercury and non-methane hydrocarbons in the european arctic, and its relation to atmospheric transport, Atmos. Environ., 41, 8511–8526, 2007.

Engvall, A.-C., Ström, J., Tunved, P., Krejci, R., Schlager, H., and Minikin, A.: The radiative effect of an aged, internally-mixed Arctic aerosol originating from lower-latitude biomass burning, Tellus B, 61, 677–684, 2009.

Flanner, M. G. and Zender, C. S.: Linking snowpack microphysics and albedo evolution, J. Geophys. Res., 111, D12208, doi: 10.1029/2005JD006834, 2006.

Flanner, M. G., Zender, C. S., Randerson, J. T., and Rasch, P. J.: Present-day climate forcing and response from black carbon in snow, J. Geophys. Res., 112, D11202, doi:10.1029/2006JD008003, 2007.

Forster, C., Wandinger, U., Wotawa, G., James, P., Mattis, I., Althausen, D., et al.: Transport of boreal forest fire emissions from Canada to Europe, J. Geophys. Res., 106, 22887–22906, 2001.

Forster, C., Cooper, O., Stohl, A., Eckhardt, S., James, P., Dunlea, E., et al.: Lagrangian transport modell forecasts and a trans-

port climatology for the Intercontinental Transport and Chemical Transformation 2002 (ITCT 2k2) measurement campaign, J. Geophys. Res., 109, D07S92, doi:10.1029/2003JD003589, 2004.

Forster, C., Stohl, A., and Seibert, P.: Parameterization of convective transport in a lagrangian particle dispersion model and its evaluation, J. Appl. Meteorol. Climatol., 46, 403–422, 2007.

Fromm, M., Bevilacqua, R., Servranckx, R., Rosen, J., Thayer, J., Herman, J., and Larko, D.: Pyro-cumulonimbus injection of smoke to the stratosphere: Observations and impact of a super blowup in northwestern Canada on 3–4 august 1998, J. Geophys. Res., 110, D08205, doi:10.1029/2004JD005350, 2005.

Garrett, T. and Zhao, C.: Increased arctic cloud longwave emissivity associated with pollution from mid-latitudes, Nature, 440, 787–789, 2006.

Garrett, T. and Verzella, L.: An evolving history of Arctic aerosols, B. Am. Meteorol. Soc., 89, 299–302, 2008.

Gautier, D. L., Bird, K. J., Charpentier, R. R., Grantz, A., Houseknecht, D. W., Klett, T. R., et al.: Assessment of undiscovered oil and gas in the Arctic, Science, 324, 1175–1179, 2009.

Granier, C., Niemeier, U., Jungclaus, J. H., Emmons, L., Hess, P., Lamarque, J.-F., et al.: Ozone pollution from future ship traffic in the Arctic northern passages, Geophys. Res. Lett., 33, L13807, doi:10.1029/2006GL026180, 2006.

Greenaway, K. R.: Experiences with Arctic flying weather, Royal Meteorological Society Canadian Branch, Toronto, 1950.

Han, Y., Holsen, T., Hopke, P., and Yi, S.: Comparison between back-trajectory based modeling and lagrangian backward dispersion modeling for locating sources of reactive gaseous mercury, Environ. Sci. Technol., 39, 1715–1723, 2005.

Hansen, J. and Nazarenko, L.: Soot climate forcing via snow and ice albedos, P. Natl. Acad. Sci. USA, 101, 423–428, 2004.

Helmig, D., Oltmans, S., Carlson, D., Lamarque, J., Jones, A., Labuschagne, C., et al.: A review of surface ozone in the polar regions, Atmos. Environ., 41, 5138–5161, 2007a.

Helmig, D., Oltmans, S., Morse, T., and Dibb, J.: What is causing high ozone at Summit, Greenland?, Atmos. Environ., 41, 5031–5043, 2007b.

Hirdman, D., Aspmo, K., Burkhart, J. F., Eckhardt, S., Sodemann, H., and Stohl, A.: Transport of mercury in the Arctic atmosphere: evidence for a spring-time net sink and summer-time source, Geophys. Res. Lett., 36, L12814, doi:10.1029/2009GL038345, 2009.

Honrath, R., Owen, R., Val Martin, M., Reid, J., Lapina, K., Fialho, P., et al: Regional and hemispheric impacts of anthropogenic and biomass burning emissions on summertime co and o3 in the North Atlantic lower free troposphere, J. Geophys. Res., 109, D24310, doi:10.1029/2004JD005147, 2004.

Hoyle, C. R., Berntsen, T., Myhre, G., and Isaksen, I. S. A.: Secondary organic aerosol in the global aerosol – chemical transport model Oslo CTM2, Atmos. Chem. Phys., 7, 5675–5694, 2007, http://www.atmos-chem-phys.net/7/5675/2007/.

Iversen, T. and Joranger, E.: Arctic air-pollution and large-scale atmospheric flows, Atmos. Environ., 19, 2099–2108, 1985.

Iversen, T.: Numerical modelling of the long range atmospheric transport of sulphur dioxide and particulate sulphate to the Arctic, Atmos. Environ., 23, 2571–2595, 1989.

Kahl, J. D. W., Martinez, D. A., Kuhns, H., Davidson, C. I., Jaffrezo, J.-L., and Harris, J. M.: Air mass trajectories to Summit, Greenland: A 44-year climatology and some episodic events, J. Geophys. Res., 102, 26861–26875, 1997.

Kasischke, E. S., Hyer, E. J., Novelli, P. C., Bruhwiler, L. P., French, N. H. F., Sukhinin, A. I., et al.: Influence of boreal fire emissions on Northern Hemisphere atmospheric carbon and carbon monoxide, Global Biogeochem. Cycles, 9, GB1012, doi:10.1029/2004GB002300, 2005.

Khokhar, M. F., Frankenberg, C., Van Roozendael, M., Beirle, S., Kühl, S., Richter, A., et al.: Satellite observations of atmospheric SO2 from volcanic eruptions during the time-period of 1996–2002, Adv. Space Res., 36, 879–887, 2005.

Klonecki, A., Hess, P., Emmons, L., Smith, L., Orlando, J., and Blake, D.: Seasonal changes in the transport of pollutants into the Arctic troposphere-model study, J. Geophys. Res., 108, 8367, doi:10.1029/2002JD002199, 2003.

Koch, D. and Hansen, J.: Distant origins of arctic black carbon: A Goddard Institute for Space Studies modelE experiment, J. Geophys. Res., 110, D04204, doi:10.1029/2004JD005296, 2005.

Krecl, P., Strom, J., and Johansson, C.: Carbon content of atmospheric aerosols in a residential area during the wood combustion season in Sweden, Atmos. Environ., 41, 6974–6985, 2007.

Lack, D., Lerner, B., Granier, C., Baynard, T., Lovejoy, E., Massoli, P., et al.: Light absorbing carbon emissions from commercial shipping, Geophys. Res. Lett., 35, L13815, doi:10.1029/2008GL033906, 2008.

Law, K. and Stohl, A.: Arctic air pollution: Origins and impacts, Science, 315, 1537–1540, 2007.

McConnell, J., Edwards, R., Kok, G., Flanner, M., Zender, C., Saltzman, E., et al.: 20th-century industrial black carbon emissions altered Arctic climate forcing, Science, 317, 1381–1384, 2007.

Mitchell, J. M.: Visual range in the polar regions with particular reference to the Alaskan Arctic, J. Atmos. Terr. Phys., 17, 195–211, 1957.

Morin, S., Savarino, J., Frey, M., Yan, N., Bekki, S., Bottenheim, J., and Martins, J.: Tracing the origin and fate of NOx in the Arctic atmosphere using stable isotopes in nitrate, Science, 322, 730–732, 2008.

Nansen, F.: Blant sel og bjørn, H. Aschehoug & CO, Oslo, 1961.

Nordenskiöld, A. E.: Nordenskild on the inland ice of Greenland, Science, 2, 732–739, 1883.

Oltmans, S. J., Lefohn, A. S., Harris, J. M., Galbally, I., Scheel, H. E., Bodeker, G., et al.: Long-term changes in tropospheric ozone, Atmos. Environ., 40, 3156–3176, 2006.

Paris, J.-D., Stohl, A., Nédélec, P., Arshinov, M. Yu., Panchenko, M. V., Shmargunov, V. P., Law, K. S., Belan, B. D., and Ciais, P.: Wildfire smoke in the Siberian Arctic in summer: source characterization and plume evolution from airborne measurements, Atmos. Chem. Phys., 9, 9315–9327, 2009, http://www.atmos-chem-phys.net/9/9315/2009/.

Polissar, A., Hopke, P., Paatero, P., Kaufmann, Y., Hall, D., Bodhaine, B., et al.: The aerosol at Barrow, Alaska: Long-term trends and source locations, Atmos. Environ., 33, 2441–2458, 1999.

Polissar, A., Hopke, P., and Harris, J.: Source regions for atmospheric aerosol measured at Barrow, Alaska, Environ. Sci. Technol., 35, 4214–4226, 2001.

Quinn, P., Shaw, G., Andrews, E., Dutton, E., Ruoho-Airola, T., and Gong, S.: Arctic haze: Current trends and knowledge gaps,

Tellus series B-Chemical and Physical Meteorology, 59, 99–114, 2007.

Quinn, P. K., Bates, T. S., Baum, E., Doubleday, N., Fiore, A. M., Flanner, M., Fridlind, A., Garrett, T. J., Koch, D., Menon, S., Shindell, D., Stohl, A., and Warren, S. G.: Short-lived pollutants in the Arctic: their climate impact a nd possible mitigation strategies, Atmos. Chem. Phys., 8, 1723–1735, 2008, http://www.atmos-chem-phys.net/8/1723/2008/.

Raatz, W. and Shaw, G.: Long-range tropospheric transport of pollution aerosols into the alaskan arctic, J. Clim. Appl. Meteorol., 23, 1052–1064, 1984.

Radke, L. F. and Hobbs, P. V.: Arctic hazes in summer over Greenland and the North American Arctic. III: A contribution from natural burning of carbonaceous materials and pyrites, J. Atmos. Chem., 9, 161–167, 1989.

Rahn, K., Borys, R., and Shaw, G.: Asian source of Arctic haze bands, Nature, 268, 713–715, 1977.

Rahn, K.: Relative importances of North-America and Eurasia as sources of Arctic aerosol, Atmos. Environ., 15, 1447–1455, 1981.

Rahn, K. A. and McCaffrey, R. J.: On the origin and transport of the winter Arctic aerosol, University of Rhode Island, 486–503, 1980.

Rahn, K. A.: On the causes, characteristics and potential environmental effects of aerosol in the Arctic atmosphere, The Arctic Ocean, the Hydrographic Environment and Fate of Pollutants, 163–195, 1982.

Seibert, P., Kromp-Kolb, H., Baltensperger, U., Jost, D. T., Schwikowski, M., Kasper, A., and Puxham, H.: Trajectory analysis of aerosol measurements at high alpine sites, in: Transport and Transformation of Pollutants in the Troposphere, edited by: Borrell, P., Cvitaš, T., and Seiler, W., 689–693, Academic Publishing, Den Haag, 1994.

Seibert, P. and Frank, A.: Source-receptor matrix calculation with a Lagrangian particle dispersion model in backward mode, Atmos. Chem. Phys., 4, 51–63, 2004, http://www.atmos-chem-phys.net/4/51/2004/.

Sharma, S., Lavoue, D., Cachier, H., Barrie, L., and Gong, S.: Long-term trends of the black carbon concentrations in the Canadian Arctic, J. Geophys. Res., 109, D15203, doi:10.1029/2003JD004331, 2004.

Sharma, S., Andrews, E., Barrie, L., Ogren, J., and Lavoue, D.: Variations and sources of the equivalent black carbon in the high Arctic revealed by long-term observations at Alert and Barrow: 1989–2003, J. Geophys. Res., 111, D14208, doi:10.1029/2005JD006581, 2006.

Sharma, S., Ishizawa, M., Chan, D., Lavoué, D., Leaitch, R., Worthy, D., et al: Synoptic Transport of Anthropogenic BC to the Arctic, NOAA annual meeting, Boulder, Colorado, 2009.

Sheridan, P. J., Delene, D. J., and Ogren, J. A.: Four years of continuous surface aerosol measurements from the Department of Energy's Atmespheric Radiation Measurement Program Southern Great Plains Cloud and Radiation Testbed site, J. Geophys. Res., 106, 20735–20747, 2001.

Shindell, D.: Local and remote contributions to Arctic warming, Geophys. Res. Lett., 34, L14704, doi:10.1029/2007GL030221, 2007.

Shindell, D. T., Chin, M., Dentener, F., Doherty, R. M., Faluvegi, G., Fiore, A. M., et al.: A multi-model assessment of pollution transport to the Arctic, Atmos. Chem. Phys., 8, 5353–5372, 2008, http://www.atmos-chem-phys.net/8/5353/2008/.

Simpson, W. R., von Glasow, R., Riedel, K., Anderson, P., Ariya, P., Bottenheim, J., et al.: Halogens and their role in polar boundary-layer ozone depletion, Atmos. Chem. Phys., 7, 4375–4418, 2007, http://www.atmos-chem-phys.net/7/4375/2007/.

Sirois, A. and Barrie, L.: Arctic lower tropospheric aerosol trends and composition at alert, Canada: 1980–1995, J. Geophys. Res., 104, 11599–11618, 1999.

Solberg, S., Schmidbauer, N., Semb, A., Stordal, F., and Hov, Ø.: Boundary-layer ozone depletion as seen in the Norwegian Arctic in spring, J. Atmos. Chem., 23, 301–332, 1996.

Stohl, A.: Trajectory statistics – A new method to establish source-receptor relationships of air pollutants and its application to the transport of particulate sulfate in Europe, Atmos. Environ., 30, 579–587, 1996.

Stohl, A.: Computation, accuracy and applications of trajectories – a review and bibliography, Atmos. Environ., 32, 947–966, 1998.

Stohl, A., Hittenberger, M., and Wotawa, G.: Validation of the lagrangian particle dispersion model FLEXPART against large-scale tracer experiment data, Atmos. Environ., 32, 4245–4264, 1998.

Stohl, A., Eckhardt, S., Forster, C., James, P., Spichtinger, N., and Seibert P.: A replacement for single back trajectory calculations in the interpretation of atmospheric trace substance measurements, Atmos. Environ., 36, 4635–4648, 2002.

Stohl, A., Forster, C., Frank, A., Seibert, P., and Wotawa, G.: Technical note: The Lagrangian particle dispersion model FLEXPART version 6.2, Atmos. Chem. Phys., 5, 2461–2474, 2005, http://www.atmos-chem-phys.net/5/2461/2005/.

Stohl, A.: Characteristics of atmospheric transport into the arctic troposphere, J. Geophys. Res., 111, D11306, doi:10.1029/2005JD006888, 2006.

Stohl, A., Andrews, E., Burkhart, J., Forster, C., Herber, A., Hoch, S., et al.: Pan-arctic enhancements of light absorbing aerosol concentrations due to North American boreal forest fires during summer 2004, J. Geophys. Res., 111, D22214, doi:10.1029/2006JD007216, 2006.

Stohl, A., Berg, T., Burkhart, J. F., Fjae'raa, A. M., Forster, C., Herber, A., Hov, Ø., Lunder, C., McMillan, W. W., Oltmans, S., Shiobara, M., Simpson, D., Solberg, S., Stebel, K., Strm, J., Trseth, K., Treffeisen, R., Virkkunen, K., and Yttri, K. E.: Arctic smoke – record high air pollution levels in the European Arctic due to agricultural fires in Eastern Europe in spring 2006, Atmos. Chem. Phys., 7, 511–534, 2007, http://www.atmos-chem-phys.net/7/511/2007/.

Uppala, S., Kallberg, P., Simmons, A., Andrae, U., Bechtold, V., et al.: The ERA-40 re-analysis, Q. J. Roy. Meteorol. Soc, 131, 2961–3012, 2005.

Vasconcelos, L., Kahl, J., Liu, D., Macias, E., and White, W.: A tracer calibration of back trajectory analysis at the Grand Canyon, J. Geophys. Res., 101, 19329–19335, 1996a.

Vasconcelos, L., Kahl, J., Liu, D., Macias, E., and White, W.: Spatial resolution of a transport inversion technique, J. Geophys. Res.-Atmos., 101, 19337–19342, 1996b.

Warneke, C., Bahreini, R., Brioude, J., Brock, C. A., de Gouw, J. A., Fahey, D. W., et al.: Biomass burning in Siberia and Kazakhstan as an important source for haze over

Alaskan Arctic in April 2008, Geophys. Res. Lett., 36, L02813, doi:10.1029/2008GL036194, 2009.

Warren, S. and Wiscombe, W.: Dirty snow after nuclear-war, Nature, 313, 467–470, 1985.

Watanabe, K., Nojiri, Y., and Kariya, S.: Measurements of ozone concentrations on a commercial vessel in the marine boundary layer over the northern North Pacific Ocean, J. Geophys. Res., 110, D11310, doi:10.1029/2004JD005514, 2005.

Weingartner, E., Saathoff, H., Schnaiter, M., Streit, N., Bitnar, B., and Baltensperger, U.: Absorption of light by soot particles: Determination of the absorption coefficient by means of aethalometers, J. Aerosol Sci., 34, 1445–1463, 2003.

White, P. W.: ECMWF, IFS Documentation, ECMWF, Reading, 2002.

Worthy, D. E. J., Trivett, N. B. A., Hopper, J. F., and Bottenheim, J. W.: Analysis of long-range transport events at Alert, Northwest Territories, during the Polar Sunrise Experiment, J. Geophys. Res., 99, 25329–25344, 1994.

Worthy, D. E., Platt, J. A., Kessler, R., Ernst, M., and Racki, S.: The greenhouse gases measurement program, measurement procedures and data quality, in: Canadian baseline program; summery of progress to 2002, edited by: Canada, M. S. O., 97–120, 2003.

Wotawa, G. and Trainer, M.: The influence of Canadian Forest Fires on Pollutant Concentrations in the United States, Science, 288, 1367–1377, 2000.

concentrations
cluster
al
Barrow
EBC
trend
Zeppelin
transport
Alert
et
sulphate
Fig
trends
stations
Arctic
time
mean
period
source
frequency
regions
atmospheric
Eurasia
influence
three
Ocean
also
values
emissions
data
clusters
measurements
measured
changes
decrease
annual
BC
NE
NAO
Hirdman
Stohl
associated
significant
measurement
index
summer
absorption
aerosol
analyses
NA
FLEXPART
interannual
analysis
reported
winter
consistent
variability
PSAP
high
patterns
studies
Table
frequencies
identified
therefore
concentration
small
decreasing
since
light
SCF
PA
seen
use
see
local
may
region
overall
total
derived
find
constant
shows
downward
Russia
spring
influenced
Atlantic
made
two
change
seasonal
last
aethalometer
Eleftheriadis
series
highest
parts
Greenland
used
mainly
frequent
calculations
AO
long-term
show
circulation
station
earlier
four
years
followed
strong
ngm-3yr-1
respectively
shown
WNE
Northern
statistically
lower
However
North
later
Quinn
results
sensitivity
observed
using
large
ENE
cases
model
Sharma
different
similar
well
study
section
yr-1
changing
emission
first
due
footprint
contributions
periods
available
part
increased

Long-term trends of black carbon and sulphate aerosol in the Arctic: Changes in atmospheric transport and source region emissions

D. Hirdman[1], J.F. Burkhart[1], H. Sodemann[1], S. Eckhardt[1], A. Jefferson[2,3], P.K. Quinn[4], S. Sharma[5], J. Ström[6], and A. Stohl[1]

[1] Norwegian Institute for Air Research (NILU), Norway

[2] National Oceanic & Atmospheric Administration (NOAA) Earth System Research Laboratory (ESRL) Global Monitoring Division, United States of America (USA)

[3] Cooperative Institute for Research in Environmental Sciences, University of Colorado, United States of America (USA)

[4] National Oceanic & Atmospheric Administration (NOAA) Pacific Marine Environmental Lab (PMEL), United States of America (USA)

[5] Environment Canada, Science and Technology Branch, Climate Research Division, Canada

[6] Norwegian Polar Institute, Tromsø, Norway

Correspondence to: D. Hirdman (dhi@nilu.no)

Abstract:

As a part of the IPY project POLARCAT (Polar Study using Aircraft, Remote Sensing, Surface Measurements and Models, of Climate, Chemistry, Aerosols and Transport) and building on previous work (Hirdman et al., 2010), this paper studies the long-term trends of both atmospheric transport as well as equivalent black carbon (EBC) and sulphate for the three Arctic stations Alert, Barrow and Zeppelin. We find a general downward trend in the measured EBC concentrations at all three stations, with a decrease of -2.1±0.4 ng m^{-3} yr^{-1} (for the years 1989-2008) and -1.4±0.8 ng m^{-3} yr^{-1} (2002-2009) at Alert and Zeppelin respectively. The decrease at Barrow is, however, not statistically significant. The measured sulphate concentrations show a decreasing trend at Alert and Zeppelin of -15±3 ng m^{-3} yr^{-1} (1985-2006) and -1.3±1.2 ng m^{-3} yr^{-1} (1990-2008) respectively, while the trend at Barrow is unclear.

To reveal the influence of different source regions on these trends, we used a cluster analysis of the output of the Lagrangian particle dispersion model FLEXPART run backward in time from the measurement stations. We have investigated to what extent variations in the atmospheric circulation, expressed as variations in the frequencies of the transport from four source regions with different emission rates, can explain the long-term trends in EBC and sulphate measured at these stations. We find that the long-term trend in the atmospheric circulation can only explain a minor fraction of the overall downward trend seen in the measurements of EBC (0.3-7.2%) and sulphate (0.3-5.3%) at the Arctic stations. The changes in emissions are dominant in explaining the trends. We find that the highest EBC and sulphate concentrations are associated with transport from Northern Eurasia and decreasing emissions in this region drive the downward trends. Northern Eurasia (cluster: NE, WNE and ENE) is the dominant emission source at all Arctic stations for both EBC and sulphate during most seasons. In wintertime, there are indications that the EBC emissions from the eastern parts of Northern Eurasia (ENE cluster) have increased over the last decade.

1 Introduction

Short-lived pollutants have recently received much attention as climate forcers, particularly in the Arctic (Quinn et al., 2008). Black carbon (BC) has gained the greatest interest due to its strong effects on the radiative balance in the Arctic, both as an Arctic haze aerosol absorbing short-wave radiation in the atmosphere (Polissar et al., 1999) as well as by decreasing the albedo if deposited on ice or snow (Hansen and Nazarenko, 2004; Flanner and Zender, 2006; Flanner et al., 2007). Like other aerosols, BC may also influence the microphysical properties of clouds (Garrett et al., 2002, Bréon et al., 2002). To fully understand past and present effects of BC on the Arctic climate, it is necessary to know the long-term changes of BC concentrations. Furthermore, it is important to know where the source regions of BC are located and how their contributions to BC in the Arctic have changed over time. A recent ice-core study by McConnell et al. (2007) presented a historical BC record, which showed that BC concentrations over the ice cap of Greenland peaked around 1910 and thereafter decreased steadily. Continuous measurements of aerosol light absorption (which can be converted to equivalent BC (EBC) concentrations) at Alert and Barrow started in the late 1980s. These records are now long enough for meaningful trend analysis. Previous studies using these data sets have shown – in agreement with the ice-core study of McConnell et al. (2007) – a general decrease of EBC since the start of the measurements (Sharma et al., 2004,

2006; Quinn et al., 2007). However, small increases of EBC were reported for both stations for the last years of each study (Sharma et al., 2006; Quinn et al., 2007). The two parallel EBC measurement time series available from Zeppelin are both still relatively short but for one a decreasing trend over the last decade was reported (Eleftheriadis et al., 2009).

The major BC source region for the Arctic surface stations has repeatedly been identified as Northern Eurasia (Polissar et al., 2001; Sharma et al., 2004, 2006; Stohl, 2006; Eleftheriadis et al., 2009; Hirdman et al., 2010), at least in winter and spring. In the past, these sources have been assumed to be anthropogenic but several recent case studies show that agricultural as well as boreal forest fires in central and western Eurasia may in fact, for periods of time, dominate the aerosol concentrations in large parts of the Arctic troposphere in spring (Stohl et al., 2007; Treffeisen et al., 2007; Engvall et al., 2009; Warneke et al., 2009, 2010). The BC source locations in summer are still debated. Neither Polissar et al (2001) nor Sharma et al. (2006) found any specific source regions for Alert in summer while the later study identified Western China and the Pacific to be associated with enhanced EBC concentrations at Barrow. Iziomon et al. (2006) on the other hand pointed out that Barrow in summer was influenced by emissions from anthropogenic sources as well as from forest fires originating in the central and eastern parts of Russia. The studies of EBC measured at Zeppelin agree in that the continental influence on the station is limited during summertime but the results are inconclusive with regard to specific source regions (Eleftheriadis et al., 2009; Hirdman et al., 2010). Eleftheriadis et al. (2009) pointed out the countries around the Baltic Sea as potential source regions together with Scotland/Ireland and regions in Russia (North-West corner and Norilsk). Other studies have emphasized the importance of emissions from yearly reoccurring boreal forest fires at high latitudes to the EBC concentrations not only at Zeppelin but for the whole Arctic troposphere in summer (Stohl, 2006; Stohl et al., 2006; Hirdman et al., 2010). Model results indicate that source regions for BC in the middle and upper troposphere are markedly different, with a stronger influence from source regions further south (Koch and Hansen, 2005; Stohl, 2006; Hirdman et al., 2010).

Several studies have attempted to estimate to what extent the observed trends in the Arctic EBC concentrations can be attributed to changes in atmospheric transport compared to the emission changes in the source regions. A study by Sharma et al. (2004) concluded that the trends in EBC seen at Alert are mainly due to changed emissions in Russia while a later study pointed out the importance of the interaction between atmospheric transport and variable emissions to explain the trends in EBC concentrations seen at Alert and Barrow (Sharma et

al., 2006). However, a recent study by Gong et al. (2010) concluded that the trends in EBC and sulphate seen at Alert were strongly correlated to the anthropogenic emissions of Northern Eurasia and North America and consistent with their documented reductions.

Most aerosols predominantly scatter, not absorb light (Charlson et al., 1992). Even though trends of aerosol light scattering will not be studied here specifically, it is still of interest to know how its trend correlates to the EBC trends. Measurements of the aerosol light scattering coefficient at Barrow have been made since May of 1976. Bodhaine and Dutton (1993) reported that the spring-time values were stable for the first three years, and then experienced two years of lower values before they reached a maximum in 1982 and decreased strongly thereafter until 1992. From 1997 until 2006, the data show a significant increase in March but no trend at all later in spring (Quinn et al., 2007). Thus, both EBC and aerosol light scattering show a strong decrease during the 1980s and until the late 1990s' but a slight increase or no trend since then. One important light scattering component of the Arctic aerosol is sulphate, for which in situ measurements are available as far back as the late 1970s. Sirois and Barrie (1999) and Sharma et al. (2004) reported that there was no trend in the measured sulphate concentrations at Alert between 1980 and 1991, but they observed a significant decrease of up to 56% thereafter which was speculated to reflect the reduced emissions from Russia. This negative trend was confirmed at several stations around the Arctic (Quinn et al., 2007), and Quinn et al. (2009) reported a 60% decrease over the past three decades.

In a previous paper we investigated the current sources and sinks of several short-lived species for four Arctic stations (Hirdman et al., 2010). For our statistical analysis, we combined the measurement data with transport model calculations. We took advantage of the superior performance of the model calculations of a Lagrangian particle dispersion model (LPDM) compared with trajectory calculations which ignore atmospheric turbulence and convection (Stohl et al., 2002; Han et al., 2005). Here we extend the work of Hirdman et al. (2010) by applying the LPDM for the entire time period for which Arctic measurements of EBC and sulphate are available.

We present climatologies of atmospheric transport from the mid-latitudes to the three Arctic observatories Alert (Canada), Barrow (Alaska), and Zeppelin (Svalbard, Norway) and assess the relative importance of changing transport patterns and changing source region emissions on measured concentrations of EBC and sulphate. The paper is structured as follows: In section 2, the methods used are described. Subsequently, in section 3.1, the climatologies of atmospheric transport towards the three Arctic observatories are presented. In section 3.2, the

potential source regions of the clustered transport are identified and thereafter characterized for trends. In the following sections 3.3 and 3.4, the EBC and sulphate mean concentrations are investigated in association to the different clusters. Section 3.5 separates the influence of changing transport patterns from the changes in clustered source region emissions and quantifies the contribution of each on the overall trend. Thereafter follows a discussion of the implications of the results. Conclusions will be drawn in section 4.

2 Methods

2.1 Measurements

2.1.1 Sites

The measurement data used in this study have been collected at three different sites: Alert, Canada (62,3^{O}W, 82,5^{O}N, 210 m.a.s.l.), Barrow, Alaska (156,6^{O}W, 71,3^{O}N, 11 m.a.s.l.) and Zeppelin on Svalbard, Norway (11,9°E, 78,9°N, 478 m.a.s.l.). The Alert station is located on the north-eastern tip of Ellesmere Island (Hopper et al., 1994; Helmig et al., 2007a). The surroundings, both land and ocean, are mainly ice or snow covered 10 months of the year. The Barrow station lies 8 km northeast from a small settlement, and it is surrounded by the Arctic Ocean except for the south where there is Arctic tundra (Helmig et al., 2007a, 2007b). It is therefore influenced by both maritime and continental air. The Zeppelin station is situated on a mountain ridge on the western coast of Spitsbergen, Svalbard. Contamination from the small nearby community of Ny Ålesund located at the coast is minimal, due to the usually stable stratification of the atmosphere and the location of the station 400 m above the community. Air masses can arrive either from the ice-free North Atlantic Ocean or from the generally ice-covered Arctic Ocean.

2.1.2 Data

Table 1 summarizes the measurement data used here. The EBC data derived from aerosol light absorption measurements from all three stations have a time resolution of 1 hour. Data were averaged to match the model time resolution of 3 hours (see section 2.2). For the daily sulphate measurements from Zeppelin, the 3-hourly model results were averaged to daily values. The sample duration of sulphate measurements at Alert and Barrow varied and was, therefore put on a common daily mean basis together with the model data.

Aerosol light absorption measurements with aethalometers have been made at Barrow since 1988 and at Alert since 1989. In October 1997, as a part of the standard NOAA/ESRL/GMD aerosol optical measurements system design (Delene and Ogren, 2002), the aerosol instrumentation at Barrow was upgraded and since then a particle soot absorption photometer (PSAP) has been used to measure the light absorption. At Zeppelin, measurements have been performed since 2002 using a custom built PSAP that is based on the same measurement principle. The BC study by Eleftheriadis et al. (2009) used data from an aethalometer running in parallel with the PSAP. The responses of both aethalometers and PSAPs depend on the loading of particles on the filter and on the amount of light that the particles scatter (Bond et al., 1999; Weingartner et al., 2003; Arnott et al., 2005). No corrections for this have been made for the aethalometer measurements, neither at Alert nor at Barrow. However, the PSAP data taken at Barrow and Zeppelin were corrected for these dependencies according to the procedure described by Bond et al. (1999). The aethalometer output is reported directly as BC concentrations through an internal conversion using an assumed mass absorption efficiency. The PSAP measurements are reported as the particle light absorption coefficient σ_{ap}. Conversion between σ_{ap} and BC is not straightforward and requires the assumption that all the light absorption measured is from BC. It is also assumed that all BC has the same light absorption efficiency. The PSAP data will therefore be reported as EBC, where σ_{ap} values have been converted approximately to BC mass concentration using a value of $10\mathrm{m}^2\mathrm{g}^{-1}$, typical of aged BC aerosol (Bond and Bergstrom, 2006). The conversion to BC in the aethalometers is done internally but relies on the same assumptions. Therefore, we will also refer to the aethalometer data as EBC. At Alert, the EBC data were further corrected based on a comparison with elemental carbon measurements based on a thermal method (Sharma et al., 2004).

An inter-comparison between the aethalometer and PSAP measurements at Barrow was made for a period of overlapping measurements during 1998. The results indicated that the calculated mean and median values of the aethalometer measurements were, 19.9% and 19.5%, respectively, higher than the PSAP measurements (e.g. see Fig. 16). Unfortunately, the differences in the datasets are not systematic. Thus, it may be misleading to join the two time series and we will report trends separately for the aethalometer and PSAP measurements at Barrow.

To avoid local contamination by emissions from the town of Barrow, EBC values at Barrow were only used when the wind direction fell within the "clean-air sector" from 0-130° (Bodhaine, 1995). This screening likely also affects how representative these data are when analyzing potential source regions such as the influence from the North American continent on this part of the Arctic as discussed more thoroughly in Hirdman et al. (2010).

Measurements of sulphate and other inorganic ions at Alert, Barrow and Zeppelin were analyzed using ion chromatographic analyses on filter samples taken at daily or longer intervals (Table 1). The stations sample different particle size ranges. At Zeppelin, particles smaller than about 10 μm are collected, at Alert, the total suspended particulates (TSP) are sampled; and at Barrow, sub- and super-micron particles are collected separately but in this study only the submicron measurements are used. Measured sulphate concentrations at Alert and Barrow were corrected for the influence from sea-salt by using measurements of sodium on the same filters and a ratio of sulphate to sodium in seawater. At Zeppelin, the sodium content in the filters has only been measured since 1999. In order to use all the data since 1990, the sulphate measurements at Zeppelin were not corrected for the influence of sea-salt sulphate. Due to the high altitude location of the Zeppelin station, the sea salt contribution is only 16-22ng/m^3 or 9-18% of the measured annual mean concentrations since 1999.

For interpretation of our results, we also used various indices for atmospheric circulation patterns. Daily North Atlantic Oscillation (NAO) index data used were provided by the Climate Analysis Section, NCAR, Boulder, USA, (Hurrell 1995). The seasonal values of the atmospheric circulation indices NAO, Pacific-North American pattern (PNA) and Arctic Oscillation (here abbreviated as AOI in order not to confuse it with a later defined transport cluster), used in this study were derived from monthly values provided by the Climate Prediction Center (CPC) at the National Weather Service (NWS), USA. The monthly NAO and PNA index values were derived using principal component analysis (Barnston and Livezey, 1987), while the AOI index was derived using empirical orthogonal functions (EOF) (Higgins et al., 2000).

2.2 Model calculations

In our trend analyses we make use of the FLEXPART LPDM (Stohl et al., 1998; Stohl et al., 2005; Forster et al., 2007). FLEXPART calculates the trajectories of so-called tracer particles using the mean winds interpolated from the analysis fields plus parameterizations representing turbulence and convective transport. These processes, which are not included in

standard trajectory models, are important for a realistic simulation of the transport of trace substances (Stohl et al., 2002). As shown in Han et al. (2005) and discussed in Hirdman et al. (2010), this leads to more accurate results even though the calculations become more computationally demanding and the statistical analysis of the model results more challenging.

FLEXPART was run backward in time using operational analyses from the European Centre for Medium-Range Weather Forecasts (ECMWF, 2002) with 1°x1° resolution for the period 2002-2008. For earlier years, the ERA-40 re-analysis data (Uppala et al., 2005) were used also with 1°x1° resolution. Analyses at 0, 6, 12 and 18 UTC and 3-hour forecasts at 3, 9, 15 and 21 UTC were used. During every 3-hour interval, 40000 particles were released at the measurement point and followed backward for 20 days. The reported global mean atmospheric lifetimes of BC range widely in different studies, from 3-4 days (Liu et al., 2005) to 4-8 days (Park et al., 2005). In the Arctic, the lifetimes may be as long as several weeks to a month during winter (Sharma et al., 2006). The 20 days of our transport simulations should therefore be long enough to capture transport from the most relevant source regions.

In backward mode, FLEXPART calculates an emission sensitivity function *S*, called source-receptor-relationship by Seibert and Frank (2004). The *S* value (in units of $\mathrm{s\,m^{-3}}$) in a particular grid cell is proportional to the particle residence time in that cell and measures the simulated concentration at the receptor that a source of unit strength (1 $\mathrm{kg\,s^{-1}}$) in the cell would produce for an inert tracer which is not affected by chemical or other removal processes. The distribution of *S* close to the surface is of particular interest, as most emissions occur near the ground. Thus, *S* values are calculated for a so-called footprint layer 0-100 m above ground. *S* can be folded with emission distributions of any species to calculate receptor concentrations of that species ignoring loss processes. However, here concentrations are not calculated but instead *S* is used directly for our statistical analyses.

2.3 Statistical methods

We used a cluster analysis (see, e.g., Kalkstein et al., 1987) to semi-objectively classify the emission sensitivities from FLEXPART into distinctly different groups. The classifications, done separately for the three stations, allow studying how the frequency of the different clusters has changed over time and, thus, how atmospheric transport to a station has changed. We will also investigate how the measured EBC and sulphate concentrations have changed for every transport cluster. These changes are likely due to changes of the emissions in the respective source regions associated with a transport cluster. This allows separating the

effects of changes in atmospheric transport to the Arctic from effects of emission changes in a few important source regions, on the Arctic EBC and sulphate concentrations.

In principle, the gridded FLEXPART footprint emission sensitivities *S(i,j,n)* could have been clustered directly. Here, *i* and *j* are the indices of the latitude/longitude grid and *n* runs over the total number of cases *N*. However, due to the large number of grid cells, this is not feasible. Instead, following the approach used by Paris et al. (2009), we divided the Earth into 9 different geographical regions (Fig. 1). We then sum *S(i,j,n)* within each of these 9 regions and use these 9 values, subsequently called $S_T(l,n)$ for the clustering. Here, *l* runs over the 9 geographical regions and replaces the grid indices *i* and *j*. To avoid that relatively small changes in transport over regions close to the station have a too large influence on the clustering result, S_T was standardized (Eq. 1):

$$S_{ST}(l,n) = \frac{S_T(l,n) - \overline{S_T(l)}}{\sigma(l)} \tag{1}$$

where $\overline{S_T(l)}$ and $\sigma(l)$ are the mean value and standard deviation of S_T within each region.

S_{ST}, was then used to identify *M* different transport clusters. The clustering was done using a two-phase iterative algorithm that minimizes the point-to-centroid distances summed over all *M* clusters, where each of the values in S_{ST} was treated as a point in parameter space. In the first phase, the S_{ST} values are simultaneously reassigned to their nearest cluster centroid until convergence of cluster membership is achieved. The result from the first phase serves as an approximate solution and starting point for the second phase. In the second phase, each S_{ST} value is individually reassigned if this reduces the sum of distances. After each reassignment the cluster centroids are recalculated in order to find a local and hopefully a global minimum of the sum of all point-to-centroid distances (Seber, 1984; Spath, 1985).

The number of clusters chosen for further analysis is always subjective (Kalkstein et al., 1987). Here, it is a compromise between a desired large number of clusters to clearly separate differences in major transport patterns and the necessity to have a large enough number of cases in each cluster, so that seasonal averages over these cases are suitable for trend analyses. We successively varied the number of clusters (M=2,..,8). Using visual analysis and applying the silhouette technique (Kaufman and Rousseeuw, 1990) we chose to use M=4 clusters for all three stations. Since the first centroids are chosen in a random way, the clustering was repeated several times and the most persistent patterns were selected for further analysis.

For displaying our results, we first calculate the mean footprint sensitivity S_{MF}:

$$S_{MF}(i,j) = \frac{1}{N}\sum_{n=1}^{N} S(i,j,n) \tag{2}$$

S_{MF} indicates where, on a climatological basis, surface sources can potentially influence the measurements during the last 20 days of transport. Similarly, we calculate the mean footprint emission sensitivity for each individual cluster m:

$$S_{CM}(i,j,m) = \frac{1}{N_m}\sum_{n=1}^{N_m} S(i,j,n) \tag{3}$$

Here n runs over all N_m cases in cluster m. Finally, for displaying our results, we normalize S_{CM} with S_{MF}:

$$S_{CF}(i,j,m) = \frac{1}{M}\frac{S_{CM}(i,j,m)}{S_{MF}(i,j)} \tag{4}$$

to show, for every cluster, the cluster-mean footprint emission sensitivity relative to the total mean footprint sensitivity. Since we chose $M = 4$ clusters, $S_{CF}(i,j,m) > 0.25$ indicates an above-average footprint sensitivity for cluster m in grid cell (i,j). For instance, a value of 1 indicates that influence from that region is four times as strong for cluster m as for the total mean situation. On the other hand $S_{CF}(i,j,m) < 0.25$ indicates a below-average footprint sensitivity in grid cell (i,j) for cluster m. This is similar to methods where the grouping is done based on measurement data (Ashbaugh, 1983; Ashbaugh et al. 1985; Hirdman et al. 2009, 2010).

A linear regression approach was applied in order to analyze the overall trends in a) cluster frequencies showing changes in atmospheric transport to the stations, and b) the measured concentrations of the different species at each station. The linear regression used here is part of a statistical toolbox which makes use of a least-squares approach to find a solution to the system, where the norm of the residual vector is minimized (Chatterjee and Hadi, 1986). The confidence intervals are computed using a QR (orthogonal, triangular) decomposition of the predictor variable (Goodall, 1993). In trend figures, trends statistically significantly (at the 90% level) different from zero are plotted with a solid line, insignificant lines with a dashed line.

3 Results

3.1 Transport climatologies

As explained by Hirdman et al. (2010), plots of S_{MF} (Eq. 2) can be interpreted as flow-climatologies where high values indicate frequent transport reaching the station from that region. To highlight overall trends in transport, we initially focus on the years 1990-1994 when most of the measurements discussed in this paper were started, and on the last five years (2004-2008) for which measurements data were available for most data sets. We show difference plots of S_{MF} for these periods to the mean for the period 1985-2009 (Fig. 2-4).

Alert: For Alert, during winter (DJF), transport from western Russia was enhanced in the earlier period (1990-1994) (Fig. 2a), while transport from the north-eastern parts of Russia, Greenland and Quebec and the neighbouring parts of the Arctic Ocean was more pronounced during the period 2004-2008 (Fig. 2c). In summer (JJA), the influence from Northern Eurasia and the North Pacific Ocean was more pronounced during the first five years (Fig. 2d), whereas transport from the Arctic Ocean, the north-western North Atlantic Ocean and Greenland was strong during the last five years (Fig. 2f).

Barrow: In the winters of 1990-1994, Barrow saw more atmospheric transport from Kazakhstan, eastern Russia and the East Siberian Sea (Fig. 3a), whereas during the winters of 2004-2008, the station was more influenced by transport from north-western Eurasia, Greenland and the Canadian Arctic (Fig. 3c). In summer, the first period was characterized by enhanced transport from the remote parts of the Arctic Ocean, the North Atlantic Ocean and their coastal regions (Fig. 3d), whereas the later period was more influenced by local transport from the Beaufort Sea (Fig. 3f).

Zeppelin: For Zeppelin, in the winters of 1990-1994, transport from Russia was more frequent (Fig. 4a), while transport from Europe, Greenland and eastern Canada was more frequent during the winters of 2004-2008 (Fig. 4c). In summer, the first period was characterized by enhanced influence from North-Central Eurasia and more remote influences from North Atlantic Ocean and North Pacific Ocean (Fig. 4d), whereas the later period was more influenced by transport from within the Arctic Ocean, Greenland and North-Eastern Canada (Fig. 4f).

These differences are associated with the overall difference in the mean circulation. The early period was characterized by a stronger Icelandic low, with influence extending well across

the Eurasian Arctic, and a weaker Siberian high (Fig. 5). The Pacific storm track was also weaker than on average. In the later period, the North Atlantic storm track was somewhat weaker than normal, and the Siberian high more pronounced. This change in the mean circulation may also be identified with the NAO index (Hurrell and Deser, 2010), which was more strongly positive during the winters of 1990-1994 (average PC-based NAO index of 1.28) than during the winters of 2004-2008 (average of 0.51). A pronounced shift from higher to lower NAO index values occurred in the late 1980s and early 1990s (Fig. 6). Related changes can also be seen in the AOI and PNA indices (Fig.6). Thus, monitoring of EBC started during a period with sustained high values of the NAO index. As shown by Eckhardt et al. (2003), transport from mid-latitude pollution source regions and particularly from Eurasia is enhanced for high phases of the NAO. Burkhart et al. (2006) have also shown positive correlation between NAO and nitrate concentrations in Greenland ice cores. These findings are in agreement with our result of more frequent transport from lower-latitude continental regions during the first five years of the measurements than during the last five years, for all three stations.

The influence of transport from the North Atlantic Ocean on the Arctic weakens with distance but even for Barrow, its influence exceeds that of transport from the North Pacific Ocean (Dickson et al., 2000). This explains the strong correlation of transport with NAO even for Barrow. The fact that similar differences in the atmospheric flow patterns exist for the summers (Fig. 2-4d & 2-4f) corroborates well with the picture that the NAO influence is significant also during summer (Folland et al., 2009). The use of ERA-40 reanalysis data up until 2001 and operational analyses data thereafter does not seem to have caused any discontinuities in simulated transport.

3.2 Cluster analysis results: seasonalities of transport

For each of the three stations one set of four unique clusters was identified by the cluster analysis spanning the entire time period of available measurements (1985-2009). The clusters represent unique transport pathways (see section 2.3). The four unique clusters identified for Barrow and Alert have similar characteristics, therefore we give them the same names for the purposes of discussion. For Zeppelin, only two of the four clusters are similar to clusters found for the other stations; the other two represent unique transport pathways to Zeppelin. Below we describe the six clusters relevant to the three stations.

The 1st cluster is common for all three stations and features enhanced S_{CF} values over the Arctic Ocean (and the oceans beyond for Barrow and Zeppelin). It will therefore be referred to as the Arctic Ocean (AO) cluster (panels a in Fig. 7-9). The 2nd cluster is also common for all three stations and will be referred to as North American (NA) cluster since it is associated with high S_{CF} values over the North American continent and to some extent also over the North Atlantic Ocean (panels b in Fig. 7-9). The 3rd cluster, influencing Alert and Barrow (panels' c in Fig. 7 & 8), shows high S_{CF} values over Northern Eurasia and especially over its western parts. We subsequently refer to this cluster as the Northern Eurasia (NE) cluster. The 4th and 5th clusters are unique to Zeppelin and essentially form a separation of the NE cluster into a western and eastern part. The 4th cluster shows high S_{CF} values mainly over western Eurasia (Fig. 9c) and will therefore be referred to as WNE, while the 5th cluster shows high S_{CF} values over eastern Eurasia and will consequently be referred to as ENE (Fig. 9d). Finally, the 6th cluster (Fig. 7d & 8d), only relevant for Alert and Barrow, shows high S_{CF} values over the North Pacific Ocean and South-East Asia and will thus be referred to as the Pacific-Asian (PA) cluster.

Alert: At the Alert station, on an annually averaged basis, AO is the dominant cluster, accounting for over 61% of all cases (Fig. 10). Its frequency is similar from spring to autumn with a maximum of 70% in autumn. In winter, its frequency is only 45%. The reduction in AO frequency during winter is compensated by an increased frequency of the NE cluster which has the largest seasonal variation; 33% in winter, but less than 1% in summer. This is consistent with the fact that atmospheric transport from continental source regions into the Arctic is stronger in winter than in summer (Stohl, 2006). The frequencies of the NA and the PA clusters vary less with season, accounting for 19-24% and 5-8% of all cases, respectively.

Barrow: At Barrow, the AO cluster is also most frequent (62% of all cases), with a maximum frequency in late summer and early autumn (over 80%) and a minimum in winter (39%) (Fig. 10). As for Alert, the NE cluster has the strongest seasonal cycle at Barrow with a maximum frequency of over 34% during the winter and a minimum of less than 1% in summer. Also consistent with Alert, the frequencies of the NA and PA clusters are fairly constant throughout the year (13-18% and 8-13%) except for summer when the NA frequency decreases significantly (to less than 2%) while the PA frequency peaks at 22%.

Zeppelin: At Zeppelin, there is a stronger seasonality of cluster frequencies than for Alert or Barrow (Fig. 10). The AO cluster dominates also at Zeppelin and accounts for 52% of all cases, with a frequency maximum in spring of 57% and a wintertime minimum of 38%. NA

accounts for 25% of all cases and is most frequent in summer (40%) and least frequent in winter (17%). The frequencies of the two Eurasian clusters, WNE and ENE, both peak in winter (18% and 28% respectively) and have a minimum during summertime (6% and 1%).

3.3 Cluster analysis results: trends of transport

Trends were calculated over the periods for which measurement data were available for the different stations. These periods are slightly different for the three stations.

Alert: The cluster frequencies at Alert show large interannual variability but also strong long-term trends for two of the four clusters. The AO cluster's frequency was 60-70% at the beginning of the time period but it decreased by about 11% (or -0.5±0.2 %yr^{-1}) during the 24 year period (Fig. 11a). The frequency of the NA cluster, on the other hand, shows a similar but opposite trend increasing by 12% (or +0.5±0.3 %yr^{-1}) over the same time period.

Barrow: The cluster frequencies at Barrow also experience large interannual variability, but their trends are not as clear as for Alert and the rates of change are smaller (Fig. 11b). The NA influence has increased by 6.2% (±4.0%), while the NE influence decreased by 5.2% (±4.4%). The changes for AO and PA are not statistically significant.

Zeppelin: At Zeppelin none of the four clusters has a statistically significant trend in frequency because of large interannual variations and the shorter time period considered for this station (Fig.11c).

The variations in atmospheric transport may, as mentioned above, be related to circulation changes expressed by the NAO index. The strongest correlation between the seasonal NAO index and the frequency of each cluster is found for Alert and Barrow where the frequency of the NE and NA clusters are reasonably well positively respectively negatively correlated to the NAO index (Table 2). The correlation between the frequency of the transport clusters identified for Zeppelin only show significant correlation to the NAO index in the summer (not shown).

3.4 Equivalent Black Carbon: Cluster means and trends

The annual geometrical mean EBC concentration differ between the stations where Alert is associated with the highest values, followed by Barrow and thereafter Zeppelin (Fig. 12). At all three stations, the highest measured EBC mean concentrations for all seasons but summer are associated with the Northern Eurasian clusters NE, WNE and ENE (Fig. 12). This result is consistent with earlier studies (Hopper et al., 1994; Polissar et al., 1999, 2001; Sharma et

al., 2004, 2006; Hirdman et al., 2010; Gong et al., 2010) which concluded that Northern Eurasia is the main source of EBC for the Arctic near the surface.

Alert: At Alert, the mean EBC concentrations corresponding to the other transport clusters are much lower (by ~45-110 ngm^{-3} or 220-375%), than the NE EBC concentrations and are not significantly different from each other (Fig. 12a). The annual mean EBC concentrations measured at Alert have a clear negative trend of -3.8%yr^{-1}, in accordance with earlier studies (Sharma et al., 2006; Quinn et al., 2007)(Fig. 13a). The largest decreasing EBC concentration trend is seen for cluster NE (Table 3), whereas the weakest decrease is associated with the NA cluster (Table 3) (Fig. 13a).

Barrow: At Barrow, on an annual basis, the NE cluster is associated with the highest and the PA cluster generally is associated with the lowest EBC concentrations (Fig. 12b). In summer, however, the highest EBC concentrations are related to the NA and PA clusters. This result corresponds well with earlier findings indicating that regional sources (including forest fires) are most important for the EBC concentrations in that part of the Arctic in summer (Barrie, 1986; Brock et al., 1989; Stohl, 2006; Hirdman et al., 2010). Due to the change of instrumentation at Barrow in 1998 (as discussed earlier in section 2.1.2), all statistical calculations with this data set are made separately for the two time periods 1988-1997 and 1998-2008 (Fig. 13b). As a result of the shorter continuous time periods and large interannual variations, EBC trends observed in the different clusters as well as for the entire data set are not statistically significant.

Zeppelin: At Zeppelin, the highest annual mean EBC concentrations are associated with the ENE cluster followed by the WNE cluster (Fig. 12c)., while the lowest EBC concentrations occur with cluster NA. However, in spring, cluster WNE has, in some years, the highest EBC mean values due to the influence from the agricultural fires in Eastern Europe in springtime (Stohl et al., 2007; Treffeisen et al., 2007) while the EBC concentrations associated with cluster ENE are more stable. The annual EBC concentrations decrease at a rate of -9%yr^{-1} (-1.44±0.8 $ngm^{-3}yr^{-1}$)(Fig. 13c), which is more than the -0.95 $ngm^{-3}yr^{-1}$ reported by Eleftheriadis et al. (2009) for the time period 2001-2007. The decrease is consistent and significant for all clusters but ENE, which shows a statistically significant increase in winter (+9.4%yr^{-1} or 4.1±3.3 $ngm^{-3}yr^{-1}$) and this increase might be related to emission increases in China.

Comparing these results to previous trend studies, we find that the annual mean EBC concentration measured at Alert (1989-2008) show an even larger decreasing trend than previously presented (-72% against -54% during 1989-2006 (Sharma et al., 2006)). Also the EBC at Zeppelin (2002-2009) showed a stronger negative trend (-1.44±0.8 $ngm^{-3}yr^{-1}$), than the decrease of -0.95 $ngm^{-3}yr^{-1}$ reported by Eleftheriadis et al. (2009) for the time period 2001-2007. For the EBC concentrations measured at Barrow, there were no significant trends observed due to the change in instrumentation and the inconsistency between these measurements (see section 2.1.2). Previous studies have merged the two time series and derived long-term trends (Sharma et al., 2006; Quinn et al., 2007). However, the uncertainties associated with this are large.

3.5 Sulphate aerosol: cluster means and trends

In accordance with EBC, the annual geometrical mean sulphate concentration for Alert once again is associated with the highest values, followed by Barrow and Zeppelin (Fig. 15). As for EBC, the highest sulphate concentrations are associated with the Northern Eurasian clusters NE, WNE and ENE for all three stations (Fig. 14), further confirming this area as the major source region for sulphate in Arctic near-surface air (Raatz and Shaw, 1984; Quinn et al., 2007, 2009; Hirdman et al., 2010). There are, however, prominent seasonal differences between the three stations.

Alert: The highest annual mean sulphate values measured at Alert are systematically associated with the NE cluster (Fig. 14a). This holds true for all seasons except for summer when the sulphate concentrations for all clusters are low and similar. For the other three clusters, the interannual variation of sulphate concentrations is large and no systematic difference between the clusters is found. The annual trend in sulphate at Alert is negative for all clusters and for all seasons. Between 1985 and 2006, the sulphate concentrations decreased by 63.9% (see Fig. 15a). The negative relative trends are similar for the AO, NE and PA clusters, all displaying a decrease of 66-68% while the NA decrease is less than 53% (see Table 3).

Barrow: At Barrow, the highest sulphate concentrations are also associated with the NE cluster followed by the NA cluster (Fig. 14b). The lowest concentrations are related to the PA cluster, except in the year of 2006 when it is instead related to the overall highest concentrations. No significant trends were seen in the measured sulphate at Barrow over the time period of this study, neither for the entire data set nor for any of the clustered subsets

(Fig. 15b). This is due mainly to the short time period with available data. The Alert data show that the trends at this station were stronger for the earlier years than for the period for which data are available at Barrow.

Zeppelin: The highest sulphate concentrations at Zeppelin are associated with the ENE clusters, followed by the WNE cluster (Fig. 14c). The smelting industry in Norilsk is situated in the region where the ENE cluster is most sensitive to emissions, again confirming the importance of this source region (Khokhar et al., 2005; Hirdman et al., 2010). The lowest concentrations are associated with the NA cluster. There was a general, statistically significant, decrease of sulphate concentrations at Zeppelin of 21.5% over the whole time period (see Fig. 15c). This decreasing trend is most pronounced for the WNE cluster (-52.6%) and least so for the NA cluster (-9.7%) (for more details see Table 3).

The long-term trend of the annual mean sulphate aerosol concentrations measured at the three stations agrees quite well (although somewhat lower) with what has been previously reported for springtime by Quinn et al. (2007). Alert shows a clear decrease of -64% (1985-2006) compared with -66-71% in springtime (1981-2003) as reported by Quinn et al (2007). The reduction in measured sulphate of -22% (1990-2008) at Zeppelin well compares with -27-33% in spring 1990-2003) reported by Quinn et al. (2007). In agreement with Quinn et al. (2007), we find no significant trends for Barrow.

3.6 The relative importance of changing transport and changing emissions for the overall trends

So far, we have investigated the mean EBC and sulphate concentrations and their trends for every cluster individually and this comparison was made using geometric mean concentrations. The following section use arithmetic mean concentrations to enable a contribution calculation. The contribution of a particular cluster to the total annual mean concentration also depends on its frequency. To quantify the annual contributions of the four clusters, we multiplied the cluster arithmetic mean concentrations with the respective cluster's frequency. The resulting time series includes the effects of both changing transport pathways and changing emissions on the four clusters' contributions to the total concentration. When summing up the contributions from all four clusters, the original measurement time series is obtained. To investigate the effect of changing transport pathways on the cluster contributions alone, we also calculated the contributions when holding the cluster mean concentrations constant over time. For this, we arbitrarily used the cluster-mean

concentrations derived from the first three years of the time series. In this case, the sum of the cluster contributions is influenced only by changes in cluster frequencies. Comparison of trend estimates with constant and varying cluster-mean concentrations thus allow quantification of the fraction of the total trend that is due to circulation changes. Notice that this fraction is actually a lower estimate because the classification into four clusters cannot fully capture the circulation-related variability. The reason for choosing the first three years of data is arbitrary but the results when using mean values over the whole period were consistent with this approach (not shown).

3.6.1 Equivalent Black Carbon

Alert: At Alert, the largest contribution to the measured EBC is from the AO cluster (see Fig. 16a), due to the high frequency of this cluster, which more than compensates for the below-average concentrations associated with it. The second largest contributor is cluster NE followed by clusters NA and PA. The EBC concentrations decreased rapidly in the 1990s but remained nearly constant since 1998. While there is a large observed trend over the whole period, -3.7±0.9 $ngm^{-3}yr^{-1}$, there is no trend at all (0.0±0.2$ngm^{-3}yr^{-1}$) when holding the cluster-mean concentrations constant. This is explained by the fact that the mean EBC concentrations of clusters AO and NA, which show the largest and opposing trends in frequency, are very similar (see Fig. 11). This shows that at Alert, changes in the EBC concentrations are driven mainly by emission changes, not by circulation changes, despite the trend of the NAO indices towards lower values during the period of available measurement data, which is consistent with the findings of Gong et al., (2010).

Barrow: At Barrow, the interannual variability of the annual mean EBC concentrations is larger than at Alert and none of the trends is statistically significant at a 90% confidence level (Fig. 16b). The variability is driven mainly by changing contributions from the dominant AO cluster. However, in some years (e.g., 1994) cluster NE is the largest contributor. Trend estimates at Barrow are complicated by the break in the measurement record but it appears that the trend since 1998 was very small: -0.06 $ngm^{-3}yr^{-1}$. There was a much larger downward trend of -2.07 $ngm^{-3}yr^{-1}$ during the first period, however. When holding the cluster mean concentrations constant, there is still a small downward trend of -0.15 $ngm^{-3}yr^{-1}$ over the entire time period, which is driven mainly by a decreasing frequency of the EBC-rich NE cluster. This can be well understood by its relationship with the NAO. The circulation-related fraction of the measured trend is relatively small (7.2%) during the first part of the

measurement time series. However, during the second period, the circulation-driven trend is actually 233% of the observed trend, so that it seems possible that emissions in regions influencing Barrow have slightly (but insignificantly) increased during the second period.

Zeppelin: Even though the EBC data record is rather short at Zeppelin (Fig. 16c), mean concentrations have been decreasing during that period and about 4.9% of that decrease can be explained by circulation changes, the larger part is driven by emission reductions. The overall decreasing trend runs counter to a recent BC emission inventory for the Svalbard area, which reports small but strongly increasing emissions between the year 2000 and 2007, which are mostly driven by increased shipping emissions (Vestreng et al., 2009). Obviously, the EBC concentrations at Zeppelin are still more influenced by emission sources outside the Svalbard area than by the relatively small local emissions. However, further increases in local emissions would eventually also increase local concentrations.

3.6.2 Sulphate Aerosol

Alert: The cluster contribution to the measured sulphate shows strong similarities with the EBC at Alert, with relatively small interannual variability (Fig. 17a) but a strong and consistent downward trend. While only 5.3% of the total observed trend can be explained by the trend in the transport, variability of the transport does explain a lot of the year-to-year variation of the measured sulphate, with observed local maxima or minima mostly corresponding to maxima and minima of the time series with fixed cluster concentrations. A strong decrease of the measured sulphate concentrations can be observed especially in the early 1990s, after the break-down of the former Soviet Union.

Barrow: At Barrow, the total observed change, $+4.6\pm11.8$ $ngm^{-3}yr^{-1}$, is insignificant (Fig. 17b). When holding the cluster mean concentrations constant, there is a small downward trend of -1.6 ± 1.1 $ngm^{-3}yr^{-1}$, which is mainly driven by the decreasing frequency of the NE cluster. This is similar to EBC where the circulation-related trend also runs counter to the observed trend, suggesting that emissions may have actually increased over the time period considered. However, the time period is too short to reveal any significant trend.

Zeppelin: At Zeppelin, the overall observed trend is -3.4 ± 1.7 $ngm^{-3}yr^{-1}$, whereas when holding the cluster mean concentrations constant the overall trend is insignificant and small, -0.01 ± 0.49 $ngm^{-3}yr^{-1}$ (Fig. 17c). Only 0.3% of the decreasing trend can be explained by the changes in the circulation.

4 Conclusions

In this paper we have presents trend calculations for equivalent black carbon and sulphate for three Arctic stations, Alert, Barrow, and Zeppelin. We have also investigated which source regions have determined the overall concentrations and their long-term trends. Finally, we have quantified the impact of variations in atmospheric transport on the long-term trends. Listed below are the main findings of this study.

1. There is a general downward trend in the measured EBC concentrations at all stations, with an annual decrease of -2.1±0.4 ngm^{-3} yr^{-1} (for the years 1989-2008) and -1.4±0.8 ngm^{-3} yr^{-1} (2002-2009) at Alert and Zeppelin respectively. The decrease at Barrow is not statistically significant.
2. The measured sulphate concentrations show a decreasing trend at Alert and Zeppelin of -15±3 ngm^{-3} (1985-2006) and -1.3±1.2 ngm^{-3} (1990-2008) per year respectively, while the trend at Barrow is unclear.
3. Northern Eurasia (clusters NE, WNE and ENE) is the dominant emission source region for both EBC and sulphate at all Arctic stations.
4. There are indications that the EBC emissions from ENE in wintertime have increased over the last decade, probably reflecting emission increases in China and other East Asian countries. Emissions associated with the other clusters (AO, NA, PA, and WNE) have been stable or decreasing over the time periods in this study, thus driving the overall trend.
5. Transport explains a major part of the interannual variability of EBC and sulphate concentrations at the stations. At the same time, however, only a minor part of the long-term trends in EBC (0.3-7.2%) and sulphate (0.3-5.3%) can be explained by changes in transport patterns.
6. The interannual variation of the cluster frequency is relatively well correlated to the annual NAO index, which shows a downward trend since most of the measurements started. However, the circulation changes are not large enough to cause substantial long-term trends of EBC and sulphate.
7. The large interannual variability in the measured EBC and sulphate concentrations at all stations and can mask trends over shorter periods, which points out the importance of continuous monitoring in the Arctic over long time periods.
8. The change of instrumentation at Barrow in 1998 severely affects our capability to derive EBC trends for periods overlapping this point in time. While previous studies

have reported longer-term trends, based on a comparison of measurements during overlapping period, we have low confidence in longer-term trend estimates at Barrow.

Acknowledgement

We thank ECMWF and met.no for access to the ECMWF archives. We would also like to thank the Global Monitoring Division at NOAA Earth System Research Laboratory, the Atmospheric Science and Technology Directorate at Environment Canada and KLIF Norway for providing data. The Swedish Environmental Protection Agency and the Swedish Research Council have sponsored EBC measurements at Zeppelin. Funding for this study was provided by the Norwegian Research Council through the POLARCAT and SUMSVAL projects.

References

Aas, W., Solberg, S., Manø, S., and Yttri, K. E.: Monitoring of long range transported air pollutants, annual report for 2007, Norwegian Institute for Air Research, Kjeller, 2008.

Ambaum, M.H.P., Hoskins, B.J., and Stephenson, D.B: Arctic Oscillation or North Atlantic Oscillation?, Journal of Climate, 14, 3495-3507, 2001.

Arnott, W., Hamasha, K., Moosmuller, H., Sheridan, P., and Ogren, J.: Towards aerosol light-absorption measurements with a 7-wavelength aethalometer: Evaluation with a photoacoustic instrument and 3-wavelength nephelometer, Aerosol Sci. Technol., 39, 17-29, 2005.

Ashbaugh, L.: A statistical trajectory technique for determining air-pollution source regions, Journal of the Air Pollution Control Association, 33, 1096-1098, 1983.

Ashbaugh, L., Malm, W., and Sadeh, W.: A residence time probability analysis of sulfur concentrations at grand-canyon-national-park, Atmos. Environ., 19, 1263-1270, 1985.

Barnston, A.G., and Livezey, R.E.: Classification, seasonality and persistence of low-frequency atmospheric circulation patterns. Mon. Wea. Rev., 115**,** 1083-1126, 1987.

Barrie, L.: Arctic air-pollution - an overview of current knowledge, Atmos. Environ., 20, 643-663, 1986.

Bodhaine, B.A. and Dutton, E.G.: A long-term decrease in Arctic Haze at Barrow, Alaska, Geophys. Res. Lett., 20, 947-950, 1993.

Bond, T., Anderson, T., and Campbell, D.: Calibration and intercomparison of filter-based measurements of visible light absorption by aerosols, Aerosol Sci. Technol., 30, 582-600, 1999.

Bond, T., and Bergstrom, R.: Light absorption by carbonaceous particles: An investigative review, Aerosol Sci. Technol., 40, 27-67, 2006.

Bréon, F.-M., Tanré, D., and Generosso, S.: Aerosol Effect on Cloud Droplet Size Monitored from Satellite, Science, 295, 5556, doi: 10.1126/science.1066434, 2002.

Brock, C.A., Radke, L.F., Lyons, J.H., and Hobbs, P.V.: Arctic Hazes in summer over Greenland and the North American Arctic. I: Incidence and Origins, J. Atmos. Chem., 9, 129-148, 1989.

Burkhart, J. F., Bales, R. C., McConnell, J. R., and Hutterli, M. A.: Influence of North Atlantic Oscillation on anthropogenic transport recorded in northwest Greenland ice cores, J. Geophys. Res., 111, D22309, doi:10.1029/2005JD006771, 2006.

Charlson, R.J., Schwartz, S.E., Hales, J.M., Cess, R.D., Coakley, J.A., Hansen, J.E., and Hofmann, D.J.: Climate Forcing by Anthropogenic Aerosols, Science, 255, 423-430, 1992.

Chatterjee, S., and Hadi. A. S.: Influential Observations, High Leverage Points, and Outliers in Linear Regression, Statistical Science, 1, 379–416, 1986.

Delene, D., and Ogren, J.: Variability of aerosol optical properties at four North American surface monitoring sites, J. Atmos. Sci., 59, 1135-1150, 2002.

Dickson, R.R., Osborn, T.J., Hurrell, J.W., Meincke, J., Blindheim, J., Adlandsvik, B., et. al.: The Arctic Ocean Response to the North Atlantic Oscillation, Journal of Climate, 13, 2671-2696, 2000.

Eckhardt S., Stohl, A., Beirle, S., Spichtinger, N., James, P., Forster, C., et. al.: The North Atlantic Oscillation controls air pollution transport to the Arctic, Atmos. Chem. Phys., 3, 1769-1778, 2003.

Eleftheriadis K., Vratolis S., Nyeki S.: Aerosol black carbon in the European Arctic: Measurements at Zeppelin station, Ny-Ålesund, Svalbard from 1998-2007, Geophys. Res. Lett., 36, L02809, doi: 10.1029/2008GL035741, 2009.

Engvall, A.-C., Ström, J., Tunved, P., Krejci, R., Schlager, H., and Minikin, A.: The radiative effect of an aged, internally-mixed Arctic aerosol originating from lower-latitude biomass burning, Tellus B, 61, 677-684, 2009.

Flanner, M.G. and Zender, C.S.: Linking snowpack microphysics and albedo evolution, J. Geophys. Res., 111, D12208, doi: 10.1029/2005JD006834, 2006.

Flanner, M.G., Zender, C.S., Randerson, J.T., Rasch, P.J.: Present-day climate forcing and response from black carbon in snow, J. Geophys. Res., 112, D11202, doi: 10.1029/2006JD008003, 2007.

Folland C.K., Knight, J., Linderholm, H.W., Fereday, D., Ineson, S., and Hurrell, J.W.: The Summer North Atlantic Oscillation: Past, Present and Future, Journal of Climate, 22, 1082-1103, 2009.

Forster, C., Stohl, A., and Seibert, P.: Parameterization of convective transport in a lagrangian particle dispersion model and its evaluation, J. Appl. Meteorol. and Climatology, 46, 403-422, 2007.

Garrett T.J., Radke, L.F., and Hobbs, P.V.: Aerosol Effects on Cloud Emissivity and Surface Longwave Heating in the Arctic, J. Atmos. Sci., 59, 769-778, 2002.

Gong, S.L., Zhao, T.L., Sharma, S., Toom-Saunry, D., Lavoué, D., Zhang, X.B., et al.: Identification of trends and interannual variability of sulfate and black carbon in the Canadian High Arctic: 1981-2007, J. Geophys. Res., 115, D07305, doi: 10.1029/2009JD012943, 2010.

Goodall, C. R.: Computation Using the QR Decomposition, Handbook in Statistics, 9, 1993.

Han, Y., Holsen, T., Hopke, P., and Yi, S.: Comparison between back-trajectory based modeling and lagrangian backward dispersion modeling for locating sources of reactive gaseous mercury, Environ. Sci. Technol., 39, 1715-1723, 2005.

Hansen, J., and Nazarenko, L.: Soot climate forcing via snow and ice albedos, Proceedings of the National Academy of Sciences of the United States of America, 101, 423-428, doi: 10.1073/pnas.2237157100, 2004.

Helmig, D., Oltmans, S., Carlson, D., Lamarque, J., Jones, A., Labuschagne, C. et al.: A review of surface ozone in the polar regions, Atmos. Environ., 41, 5138-5161, 2007a.

Helmig, D., Oltmans, S., Morse, T., and Dibb, J.: What is causing high ozone at Summit, Greenland?, Atmos. Environ., 41, 5031-5043, 2007b.

Higgins, R.W., Leetmaa, A., Xue, Y., and Barnston, A.: Dominant factors influencing the seasonal predictability of U.S. precipitation and surface air temperature. J. Climate, 13, 3994-4017, 2000.

Hirdman, D., Aspmo, K., Burkhart J.F., Eckhardt, S., Sodemann, H., Stohl, A.: Transport of mercury in the Arctic atmosphere: evidence for a spring-time net sink and summer-time source, Geophys. Res. Lett., 36, L12814, doi: 10.1029/2009GL038345, 2009.

Hirdman, D., Sodemann, H., Eckhardt S., Burkhart J.F., Jefferson A., Mefford, T., et. al.: Source identification of short-lived air pollutants in the Arctic using statistical analysis of measurement data and particle dispersion model output, Atmos. Chem. Phys., 10, 669-693, 2010.

Hopper, J.F., Worthy, E.J., Barrie, L.A., and Trivell, N.B.A.: Atmospheric observations of aerosol black carbon, carbon dioxide, and methane in the high Arctic, Atmos. Environ., 18, 3047-3054, 1994.

Hurrell, J.W.: Transient Eddy Forcing of the Rotational Flow during Northern Winter, J. Atmos. Sci., 52, 2286-2301, 1995.

Hurrell J.W., and Deser, C.: North Atlantic climate variability: The role of the North Atlantic Oscillation, J. Marine Systems, 79, 231-244, 2010.

Iziomon M.G., Lohmann, U., and Quinn, P.K.: Summertime pollution events in the Arctic and potential implications, J. Geophys. Res., 111, D12206, doi: 10.1029/2005JD006223, 2006.

Kalkstein, L. S., Tan, G., and Skindlov, J. A.: An evaluation of three clustering procedures for use in synoptic climatological classification, J. Climate and Applied Meteorology 26, 717-730, 1987.

Kaufman L., and Rousseeuw, P.J.: Finding Groups in Data: An Introduction to Cluster Analysis. Hoboken, NJ: John Wiley & Sons, Inc., 1990.

Khokhar, M. F., Frankenberg, C., Van Roozendael, M., Beirle, S., Kühl, S., Richter, A. et al.: Satellite observations of atmospheric SO2 from volcanic eruptions during the time-period of 1996-2002, Adv. Space Res., 36, 879-887, 2005.

Koch, D., and Hansen, J.: Distant origins of arctic black carbon: A Goddard Institute for Space Studies modelE experiment, J. Geophys. Res., 110, D18104, doi: 10.1029/2004JD005296, 2005.

Krecl, P., Strom, J., and Johansson, C.: Carbon content of atmospheric aerosols in a residential area during the wood combustion season in Sweden, Atmos. Environ., 41, 6974-6985, 2007.

Liu, X., Penner, J.E., and Herzog, M.: Global modeling of aerosol dynamics: Model description, evaluation, and interactions between sulfate and nonsulfate aerosols, J. Geophys. Res., 110, D18206, doi: 10.1029/2004JD005674, 2005.

McConnell, J., Edwards, R., Kok, G., Flanner, M., Zender, C., Saltzman, E. et al.: 20th-century industrial black carbon emissions altered Arctic climate forcing, Science, 317, 1381-1384, 2007.

Paris J.-D., Stohl, A., Ciais, P., Nédélec, P., Belan, B.D., et. al.: Source-receptor relationship for airborne measurements of CO_2, CO and O_3 above Siberia: a cluster.based approach, Atmos. Chem. Phys. Discuss., 9, 6207-6245, 2009.

Park, R.J., Jacob, D.J., Palmer, P.I., Clarke, A.D., Weber, R.J., Zondlo, M.A., et al.: Export efficiency of black carbon aerosol in continental outflow: Global implications, J. Goephys. Res., 110, D11205, doi: 10.1029/2004JD005432, 2005.

Polissar, A., Hopke, P., Paatero, P., Kaufmann, Y., Hall, D., Bodhaine, B. et al.: The aerosol at Barrow, Alaska: Long-term trends and source locations, Atmos. Environ., 33, 2441-2458, 1999.

Polissar, A., Hopke, P., and Harris, J.: Source regions for atmospheric aerosol measured at Barrow, Alaska, Environ. Sci. Technol., 35, 4214-4226, 2001.

Quinn, P.K., Coffman, D.J., Kapustin, V.N., Bates, T.S., and Covert, D.S.: Aerosol optical properties in the marine boundary layer during ACE 1 and the underlying chemical and physical aerosol properties, J. Geophys. Res., 103, 16547-16563, 1998.

Quinn, P., Shaw, G., Andrews, E., Dutton, E., Ruoho-Airola, T., and Gong, S.: Arctic haze: Current trends and knowledge gaps, Tellus series B-Chemical and Physical Meteorology, 59, 99-114, 2007.

Quinn, P., Bates, T., Baum, E., Doubleday, N., Fiore, A., Flanner, M. et al.: Short-lived pollutants in the arctic: Their climate impact and possible mitigation strategies, Atmos. Chem. Phys., 8, 1723-1735, 2008.

Quinn, P., Bates, T., Schulz, K., and Shaw, G.E.: Decadal trends in aerosol chemical composition at Barrow, Alaska: 1976-2008, Atmos. Chem. Phys., 9, 8883-8888, 2009.

Raatz, W.E., and Shaw, G.E.: Long-Range Tropospheric transport of pollution Aerosols into the Alaskan Arctic, J. Clim. Appl. Meteorol., 23, 1052-1064, 1984.

Seber, G. A. F.: Multivariate Observations. Hoboken, NJ: John Wiley & Sons, Inc., 1984.

Seibert, P., and Frank, A.: Source-receptor matrix calculation with a lagrangian particle dispersion model in backward mode, Atmos. Chem. Phys., 4, 51-63, 2004.

Sharma, S., Lavoue, D., Cachier, H., Barrie, L., and Gong, S.: Long-term trends of the black carbon concentrations in the Canadian Arctic, J. Geophys. Res., 109, D15203, doi: 10.1029/2003JD004331, 2004.

Sharma, S., Andrews, E., Barrie, L., Ogren, J., and Lavoue, D.: Variations and sources of the equivalent black carbon in the high Arctic revealed by long-term observations at Alert and Barrow: 1989-2003, J. Geophys. Res., 111, D14208, doi: 10.1029/2005JD006581, 2006.

Sirois, A., and Barrie, L.: Arctic lower tropospheric aerosol trends and composition at alert, Canada: 1980-1995, J. Geophys. Res., 104, 11599-11618, 1999.

Spath, H.: Cluster Dissection and Analysis: Theory, FORTRAN Programs, Examples. Translated by Goldschmidt, J., New York: Halsted Press, 1985.

Stohl, A.: Computation, accuracy and applications of trajectories - a review and bibliography, Atmos. Environ., 32, 947-966, 1998.

Stohl, A., Eckhardt, S., Forster, C., James, P., Spichtinger, N., and Seibert P.: A replacement for single back trajectory calculations in the interpretation of atmospheric trace substance measurements, Atmos. Environ., 36, 4635-4648, 2002.

Stohl, A., Forster, C., Frank, A., Seibert, P., and Wotawa, G.: Technical note: The lagrangian particle dispersion model FLEXPART version 6.2, Atmos. Chem. Phys., 5, 2461-2474, 2005.

Stohl, A.: Characteristics of atmospheric transport into the Arctic troposphere, J. Geophys. Res., 111, D11306, doi: 10.1029/2005JD006888, 2006.

Stohl, A., Andrews, E., Burkhart, J., Forster, C., Herber, A., Hoch, S. et al.: Pan-arctic enhancements of light absorbing aerosol concentrations due to North American boreal forest fires during summer 2004, J. Geophys. Res., 111, D22214, doi: 10.1029/2006JD007216, 2006.

Stohl, A., Berg, T., Burkhart, J., Fjaeraa, A., Forster, C. et al.: Arctic smoke - record high air pollution levels in the european arctic due to agricultural fires in Eastern Europe in spring 2006, Atmos. Chem. Phys., 7, 511-534, 2007.

Sukhinin, A.I., French, N.H.F., Kasischke, E.S., Hewson, J.H., Soja, A.J., Csiszar, I.A., et al.: AVHRR-based mapping of fires in Russia: New products for fire management and carbon cycle studies, Remote Sensing of Environment, 93, 546-564, 2004.

Tomasi, C., Vitale, V., Lupi, A., Di Carmine, C., Campanelli, M., Herber, A., et. al.: Aerosol in polar regions: A historical overview based in optical depth and in situ observations, J. Geophys. Res., 112, D16205, doi: 10.1029/2007JD008432, 2007.

Treffeisen, R., Tunved, P., Ström, J., Herber, A., Bareiss, J., Helbig, A., et al.: Arctic smoke – aerosol characteristics during a record smoke event in European Arctic and its radiative impact, Atmos. Chem. Phys., 7, 3035-3053, 2007.

Uppala, S., Kallberg, P., Simmons, A., Andrae, U., Bechtold, V. et al.: The ERA-40 re-analysis, Q. J. Roy. Meteor. Soc, 131, 2961-3012, 2005.

Vestreng, V., Kallenborn, R., and Økstad, E.: Climate influencing emissions, scenarios and mitigation options at Svalbard, Rapport from the Climate and Pollution Agency in Norway (KLIF), TA-2552, 2009.

Warneke, C., Bahreini, R., Brioude, J., Brock, C.A., de Gouw, J.A., Fahey, D.W. et al.: Biomass burning in Siberia and Kazakhstan as an important source for haze over Alaskan Arctic in April 2008, Geophys. Res. Lett., 36, L02813, doi: 10.1029/2008GL036194, 2009.

Warneke, C., Froyd, K.D., Brioude, J., Bahreini, R., Brock, C.A., Cozic, J., et al.: An important contribution to springtime Arctic aerosol from biomass burning in Russia, Geophys. Res. Lett., 37, L01801, doi: 10.1029/2009GL041816, 2010.

Weingartner, E., Saathoff, H., Schnaiter, M., Streit, N., Bitnar, B., and Baltensperger, U.: Absorption of light by soot particles: Determination of the absorption coefficient by means of aethalometers, J. Aerosol Sci , 34, 1445-1463, 2003.

White, P. W.: ECMWF, IFS Documentation, in, ECMWF, Reading, 2002.

Table 1. Measurement data used in this study. Further information on the instrumentation and data can be found in the listed references.

Station	Species	Time period	Time resolution	Data availability	References
Alert	EBC	1989-2008	1 h	75.7%	Sharma et al. (2004; 2006)
Alert	NSS sulphate	1985-2006	3-9 days	98.2%	Sirois and Barrie (1999)
Barrow	EBC	1988-2008	1 h	58.8%	Sharma et al. (2006)
Barrow	NSS sulphate	1997-2008	1-5 days	61.1%	Quinn et al. (1998)
Zeppelin	EBC	2002-2009	1h	83.6%	Krecl et al. (2007)
Zeppelin	Total sulphate	1990-2008	24 h	94.7%	Aas et al. (2008)

Table 2. Yearly correlation between cluster frequency and NAO index for Alert, Barrow, and Zeppelin. Statistically significant r-values at a 90% confidence level or higher are shown in bold.

Station	**ALERT**		**BARROW**		**ZEPPELIN**	
Corr. Coef. \ Cluster	**r**	**p-value**	**r**	**p-value**	**r**	**p-value**
AO	0.23	0.28	0.16	0.48	-0.34	0.14
NA	**-0.47**	**0.02**	**-0.65**	**0.00**	0.28	0.23
NE	**0.36**	**0.09**	**0.45**	**0.04**	-	-
WNE	-	-	-	-	0.07	0.78
ENE	-	-	-	-	0.05	0.84
PA	0.19	0.37	-0.07	0.75	-	-

Table 3. Summary of the overall as well as cluster related yearly trends (based on geometric mean conc.) for EBC and sulphate at Alert, Barrow, and Zeppelin. Statistically significant trends at a 90% confidence level are shown in bold.

Station	**ALERT**		**BARROW**		**ZEPPELIN**	
Specie \ Cluster	**EBC** ($ngm^{-3}yr^{-1}$) **1989-2008**	**SO_4** ($ngm^{-3}yr^{-1}$) **1985-2006**	**EBC** ($ngm^{-3}yr^{-1}$) **1988-1997** **1998-2008**	**SO_4** ($ngm^{-3}yr^{-1}$) **1997-2008**	**EBC** ($ngm^{-3}yr^{-1}$) **2002-2009**	**SO_4** ($ngm^{-3}yr^{-1}$) **1990-2008**
AO	**-1.97±0.35**	**-13.9±2.6**	-0.55±1.07 -0.30±0.85	6.9±14.3	**-1.49±1.02**	**-1.5±1.2**
NA	**-1.59±0.48**	**-8.9±5.6**	-1.00±2.63 0.09±1.38	-3.8±16.1	**-1.11±0.70**	0.3±1.3
NE	**-5.45±1.70**	**43.4±14.3**	-0.24±6.61 -1.20±3.89	-20.3±40.3	-	-
WNE	-	-	-	-	**-2.17±1.64**	**-4.8±3.2**
ENE	-	-	-	-	-0.16±3.47	**-5.6±2.7**
PA	**-1.73±0.91**	**14.3±9.1**	-0.23±0.73 -0.28±0.59	2.4±8.0	-	-
Total trend (geometric)	**-2.13±0.42**	**-14.5±2.9**	-0.85±1.14 -0.34±0.87	4.4±13.5	**-1.44±0.8**	**-1.3±1.2**
Total trend (arithmetic)	**-3.66±0.90**	**-27.3±5.4**	-2.07±2.31 -0.06±1.45	4.6±11.8	-4.84±5.13	**-3.4±1.7**
Total trend (transport)	0.01±0.20	-1.4±1.5	**-0.15±0.12**	**-1.6±1.1**	-0.23±0.40	-0.01±0.49

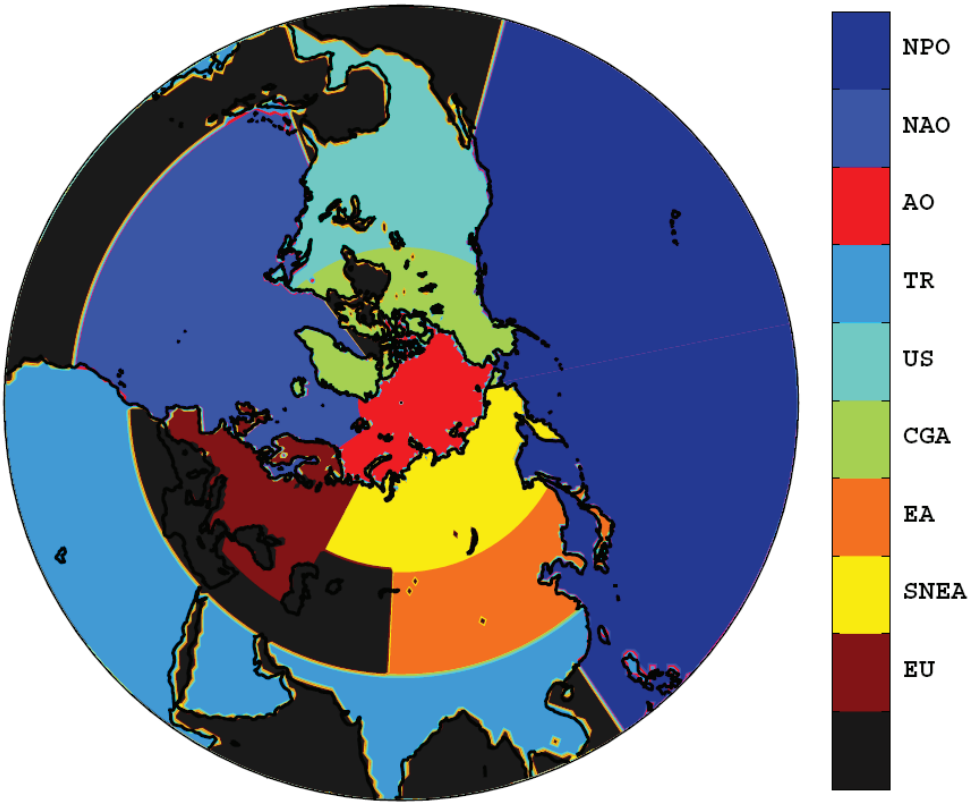

Figure 1. Geographical regions used for the clustering of the footprint emission sensitivities. NPO, NAO and AO represent the North Pacific Ocean, North Atlantic Ocean and Arctic Ocean respectively. TR represents the land masses in the tropics and southern hemisphere. US is USA (except Alaska and Hawaii) and Central America. CGA stands for Canada, Greenland and Alaska. EA, SNEA and EU represent Eastern Asia, Siberia and North-East Asia and Europe respectively.

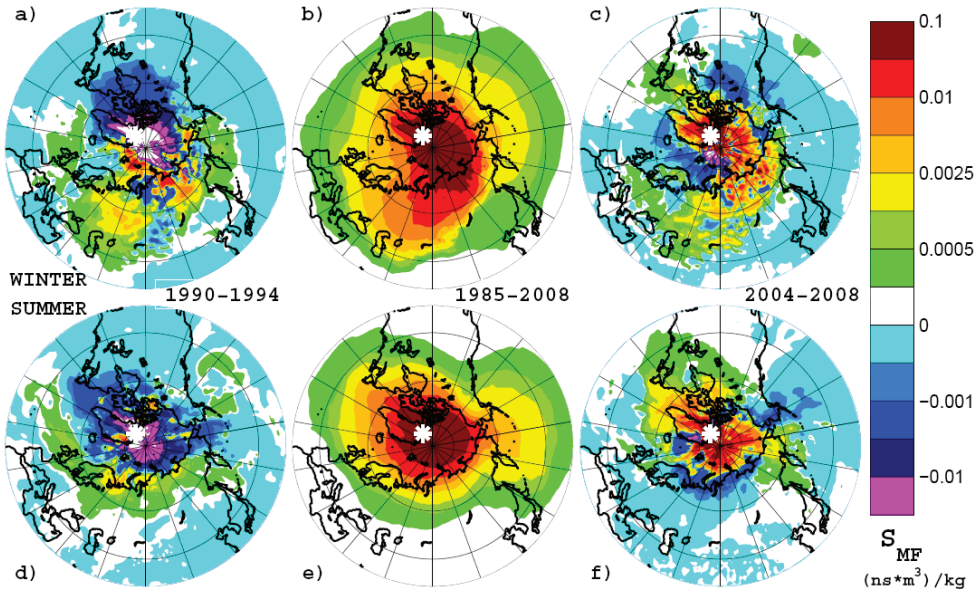

Figure 2. Transport climatologies ($\boldsymbol{S_{MF}}$) at Alert during winter (upper row of panels) and summer (lower row). The middle column shows the mean $\boldsymbol{S_{MF}}$, averaged over the whole time period (1985-2008). The left column of panels illustrates the difference from the mean flow for the early period 1990-1994, and the right column illustrates the difference from the mean for the late period 2004-2008. The station's location is marked with a white asterisk.

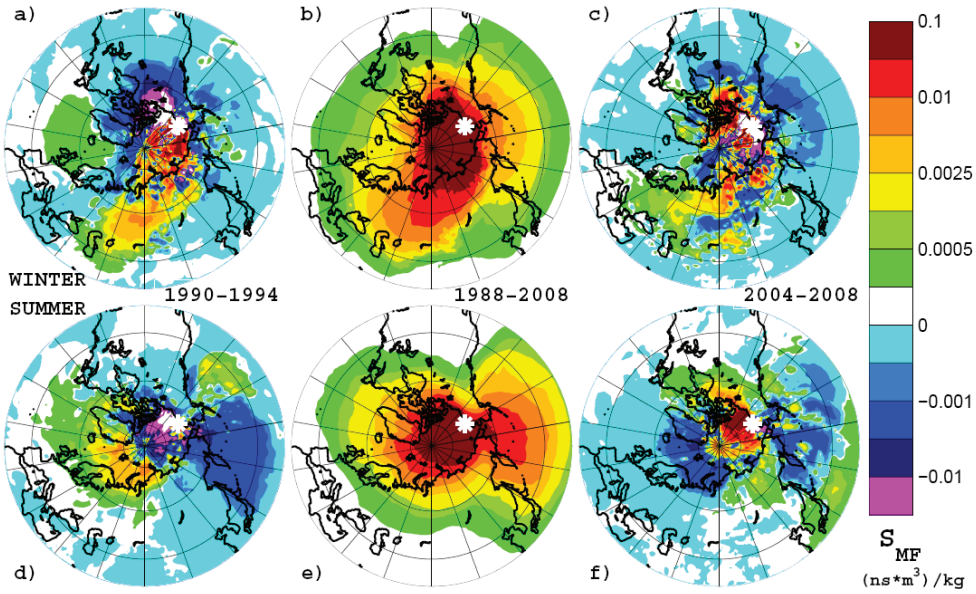

Figure 3. Transport climatologies ($\boldsymbol{S_{MF}}$) at Barrow during winter (upper row of panels) and summer (lower row). The middle column shows the mean $\boldsymbol{S_{MF}}$, averaged over the whole time period (1988-2008). The left column of panels illustrates the difference from the mean flow for the early period 1988-1992, and the right column illustrates the difference from the mean for the late period 2004-2008. The station's location is marked with a white asterisk.

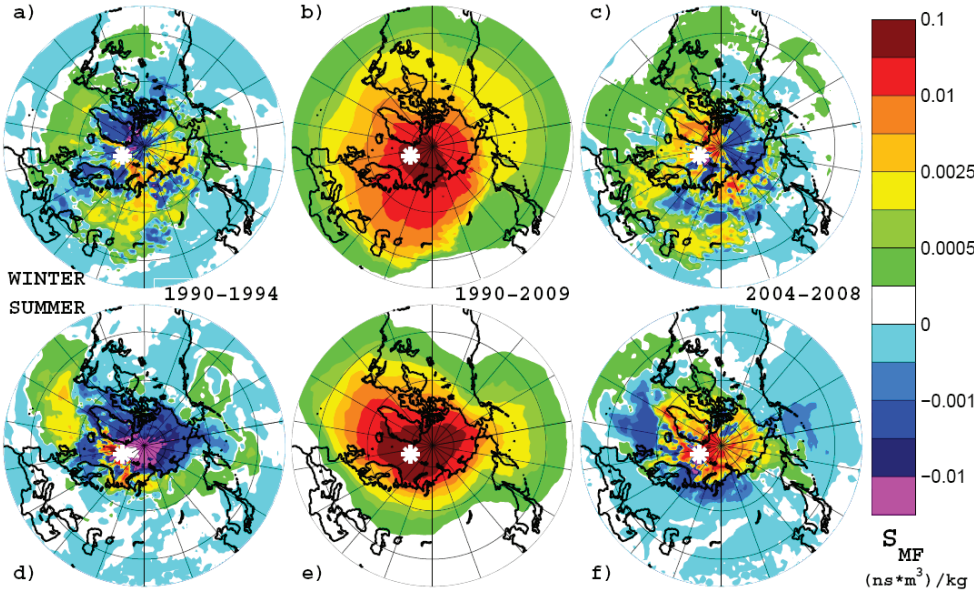

Figure 4. Transport climatologies ($\boldsymbol{S}_{MF}$) at Zeppelin during winter (upper row of panels) and summer (lower row). The middle column shows the mean $\boldsymbol{S}_{MF}$, averaged over the whole time period (1990-2008). The left column of panels illustrates the difference from the mean flow for the early period 1990-1994, and the right column illustrates the difference from the mean for the late period 2004-2008. The station's location is marked with a white asterisk.

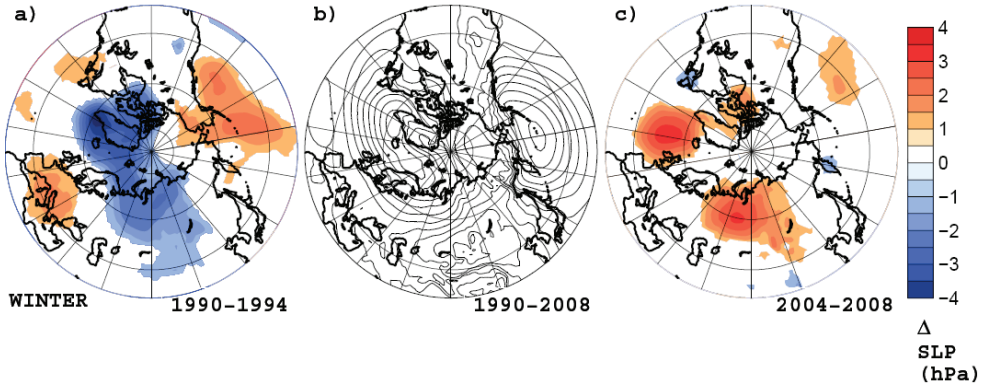

Figure 5. Mean sea level pressure (SLP) during winter over the Arctic. The middle panel shows the mean SLP with contours at 3hPa interval (1990-2008). The left and right panels show the mean SLP for the period of interest (1990-1994, left; 2004-2008, right) minus the mean SLP over the entire time period. Blue and red areas display, respectively, lower and higher SLP than averaged over the whole period.

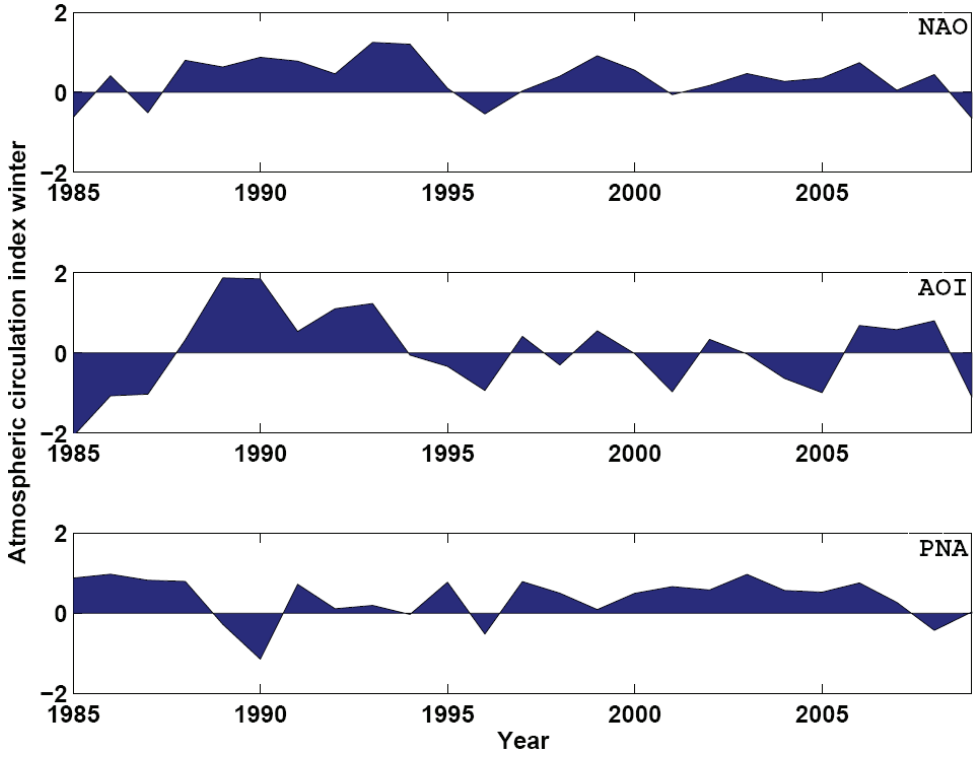

Figure 6. Annual variation of the atmospheric circulation indices NAO, AOI, and PNA during the winter season.

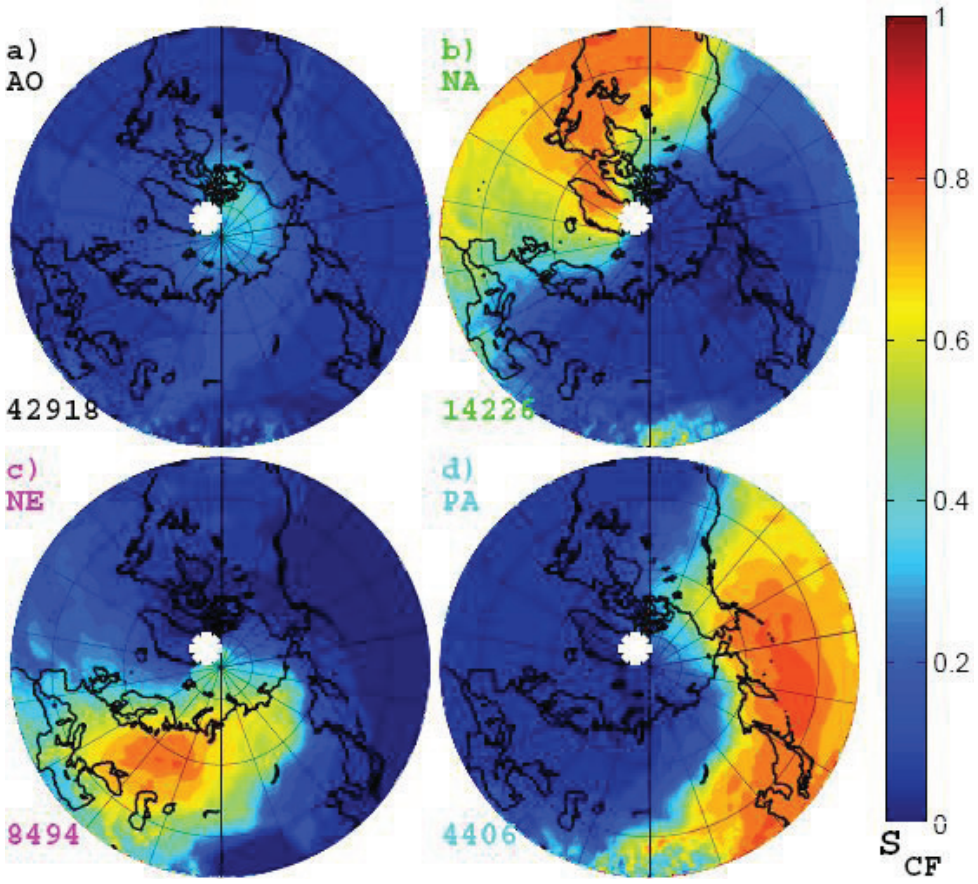

Figure 7. Annual normalized emission sensitivity S_{CF} for clusters a) AO, b) NA, c) NE and d) PA for Alert 1985-2008 (see Eq. 4). The number of cluster members is reported in the bottom left corner of each panel. The location of the Alert station is marked by a white asterisk. AO, Arctic Ocean cluster; NA, North American cluster; NE, Northern Eurasian cluster; and PA, Pacific and South-East Asian cluster.

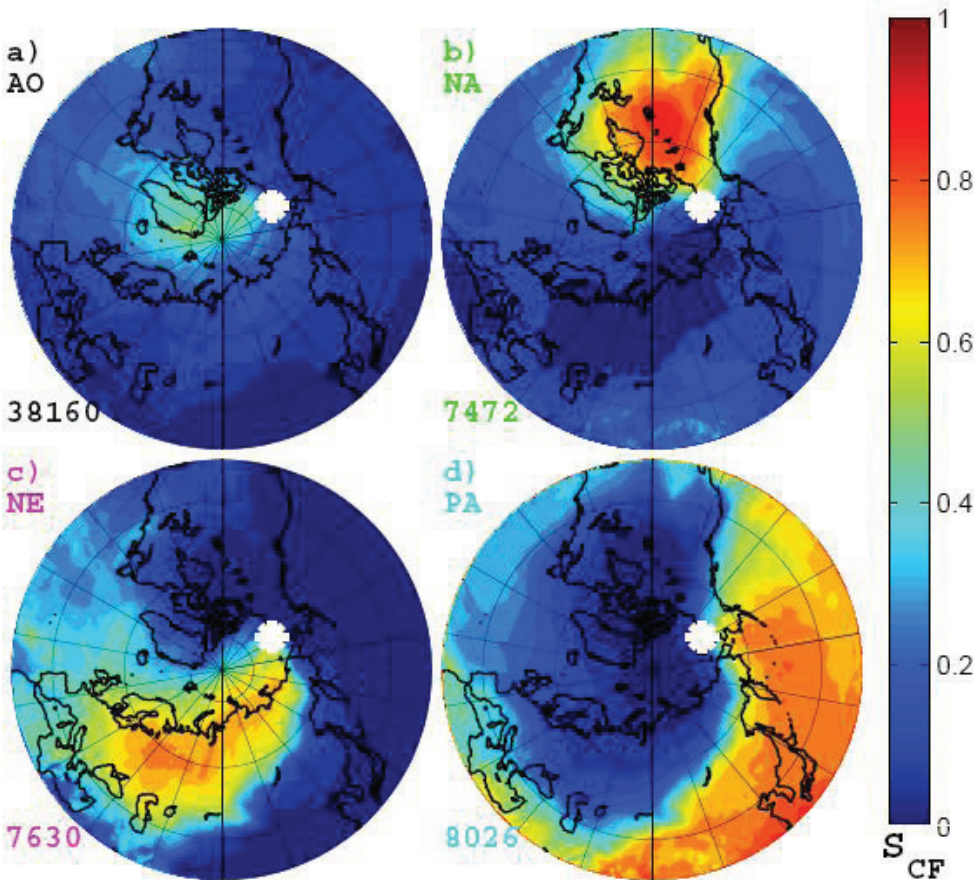

Figure 8. Same as Fig. 7 for Barrow 1988-2008 (see Eq. 4). The location of the Barrow station is marked by a white asterisk.

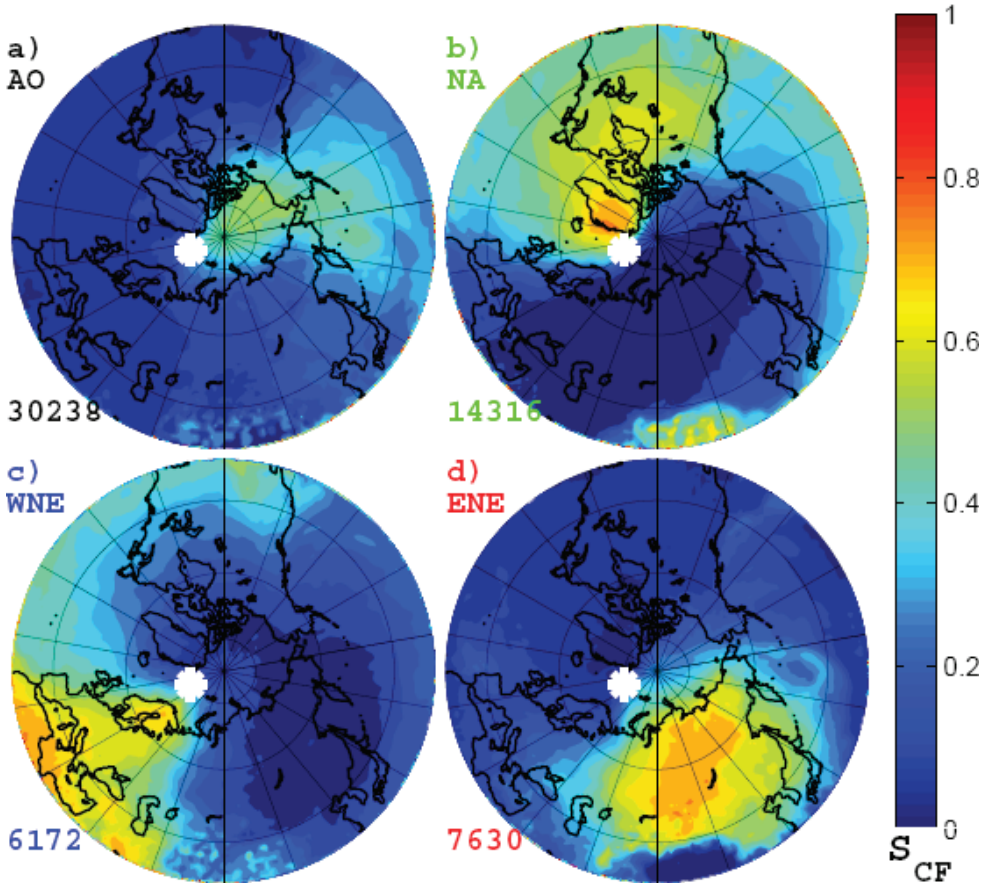

Figure 9. Same as Fig. 7 but for clusters a) AO, b) NA, c) WNE and d) ENE for Zeppelin 1990-2009 (see Eq. 4). The location of the Zeppelin station is marked by a white asterisk. AO, Arctic Ocean cluster; NA, North American cluster; WNE, Western Northern Eurasian cluster; and ENE, Eastern Northern Eurasian cluster.

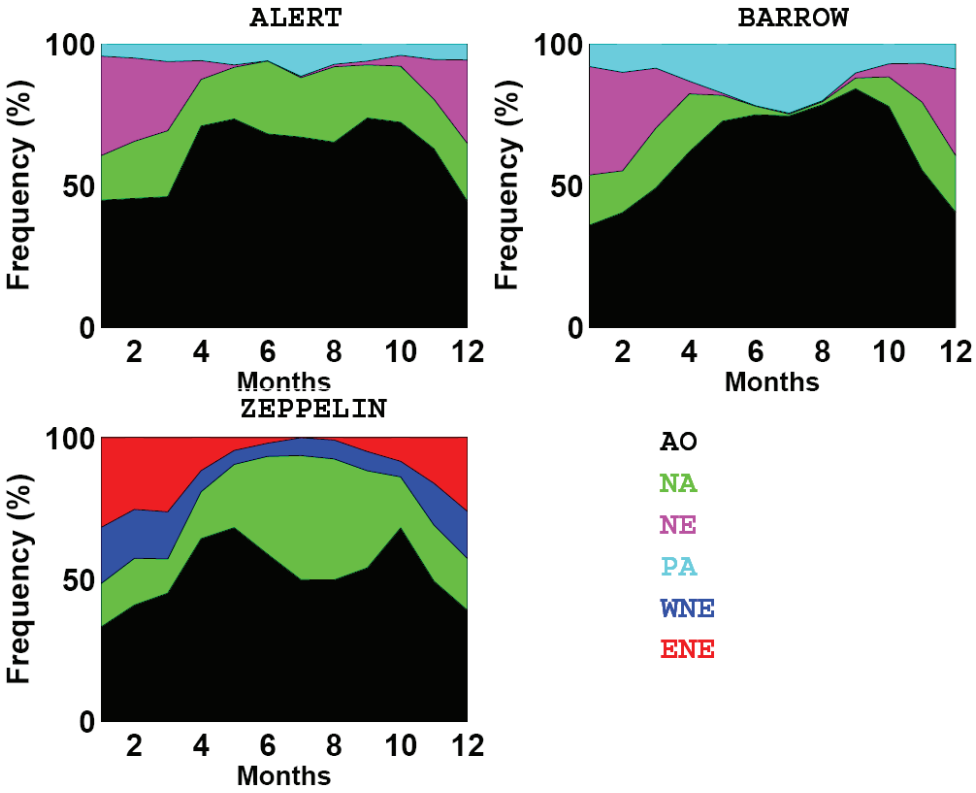

Figure 10. The frequencies of the transport clusters as function of the month of the year for Alert (upper left), Barrow (upper right), and Zeppelin (bottom left).

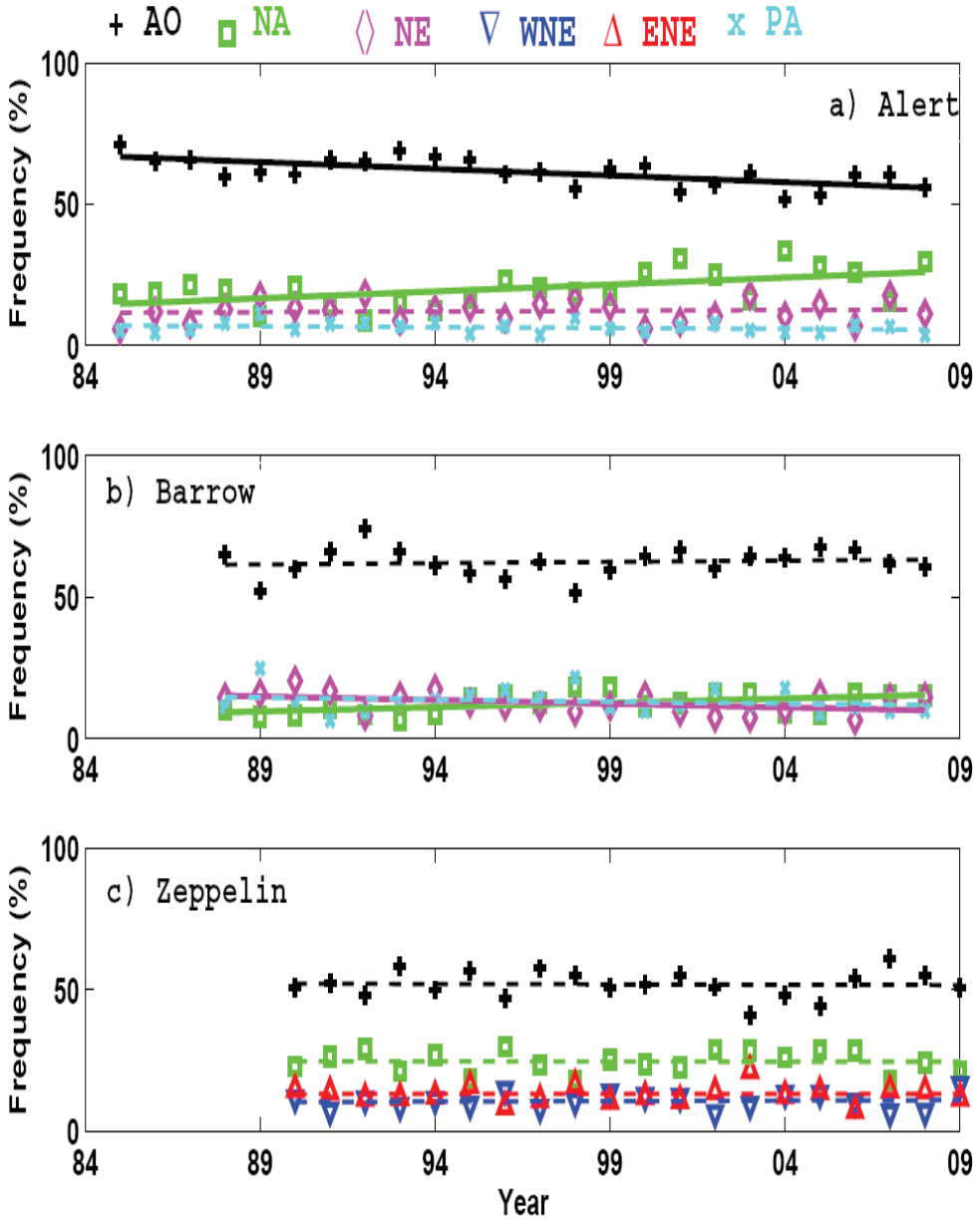

Figure 11. Annual mean cluster frequency as a function of time at Alert (a), Barrow (b), and Zeppelin (c). The colour codes are indicated at the top. Linear trends are also shown, as solid lines when statistically significant with a minimum confidence of 90% and as dashed lines when the confidence is lower.

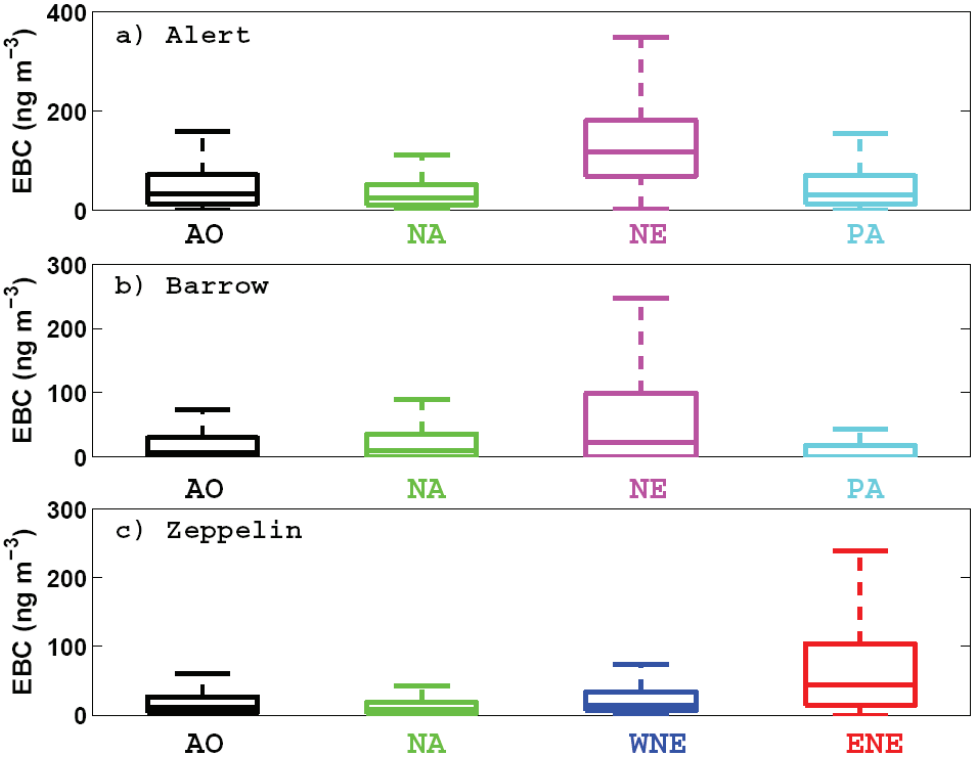

Figure 12. Box-whisker plots of the EBC concentrations associated with each cluster at Alert (a), Barrow (b), and Zeppelin (c), where the box boundaries mark the 25th and 75th percentile of the data and the whiskers includes 99% of the data.

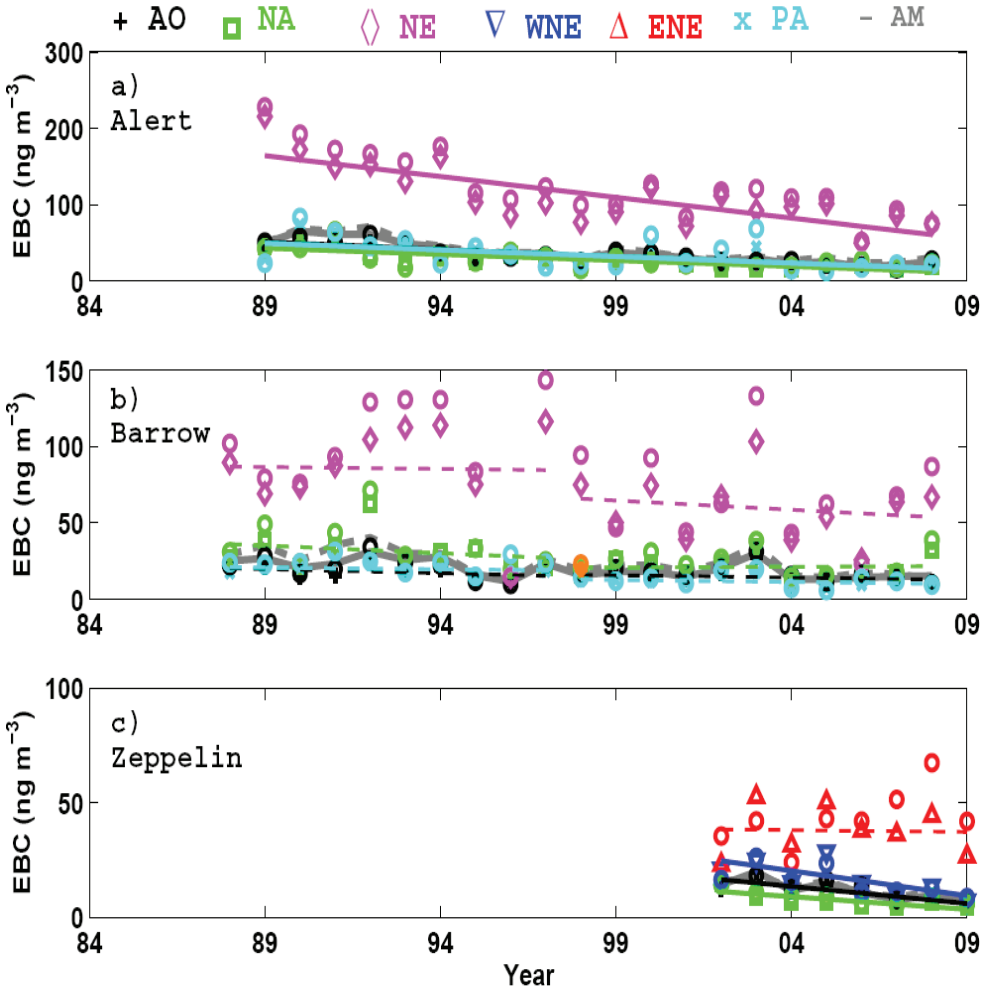

Figure 13. Annual geometrical mean and median values of the EBC concentrations for all measurements (solid gray and dashed gray respectively) as well as associated to the four different clusters at Alert (a), Barrow (b), and Zeppelin (c). Medians are marked with circles and geometric means with unique symbols according to the legend at the top. Trend lines are shown with solid lines for trends with a statistical significance on the 90% confidence level, other trends are shown with dashed lines. Due to change in instrumentation at Barrow, this data set was divided in the sub-periods 1988-1997 and 1998-2008 for which linear trends were calculated separately. The mean and median values measured with the old instrument in 1998 are shown in orange.

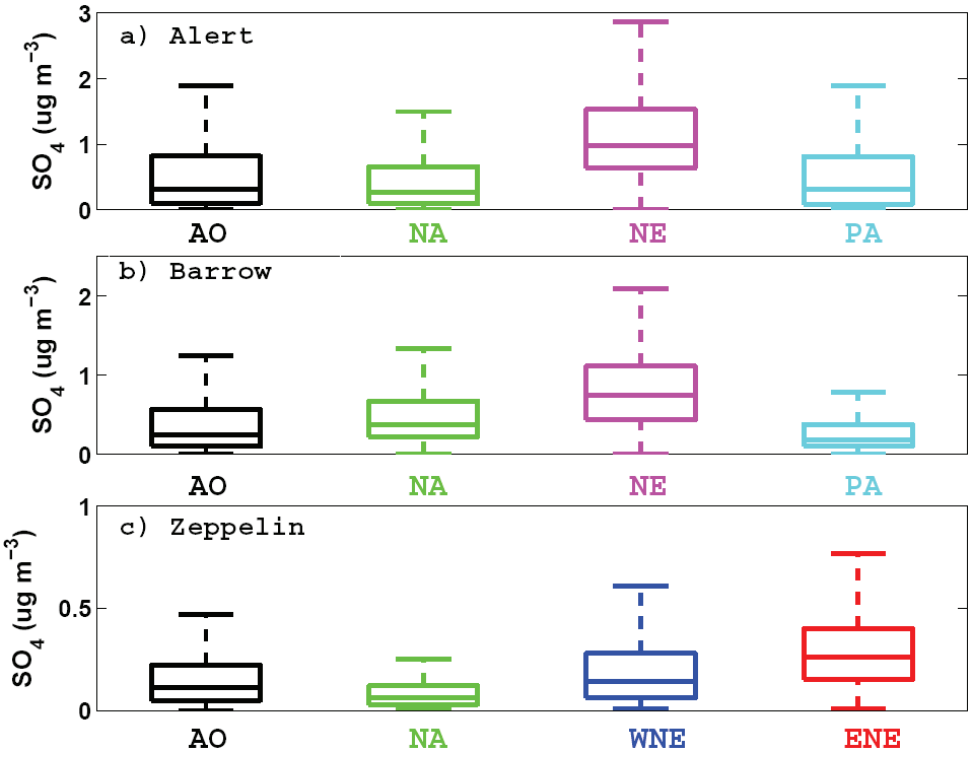

Figure 14. Box-whisker plots over the sulphate concentration associated to each cluster at Alert (a), Barrow (b), and Zeppelin (c), where the box boundaries are set to mark the 25th and 75th percentile of the data whereas the whiskers includes up to 99% of the data. Outliers outside this have not been plotted in order to emphasis the difference between the different clusters. The horizontal line in each box marks the median value.

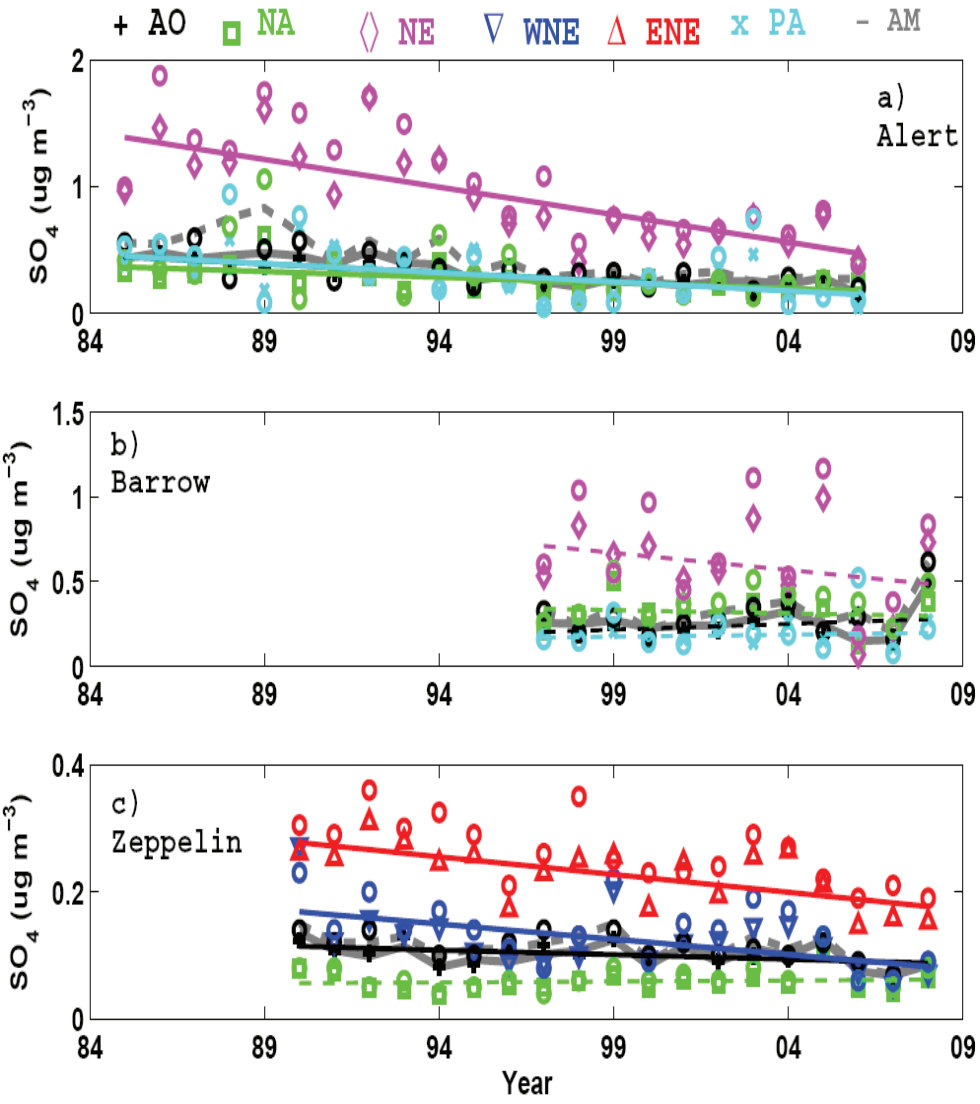

Figure 15. Annual geometrical means and medians of the sulphate concentrations for all measurements (solid gray and dashed gray respectively) and for the four different clusters at Alert (a), Barrow (b), and Zeppelin (c). Medians are marked with circles and geometric means with unique symbols according to the legend at the top. Trend lines are shown with solid lines for trends with a statistical significance on the 90% confidence level, other trends are shown with dashed lines.

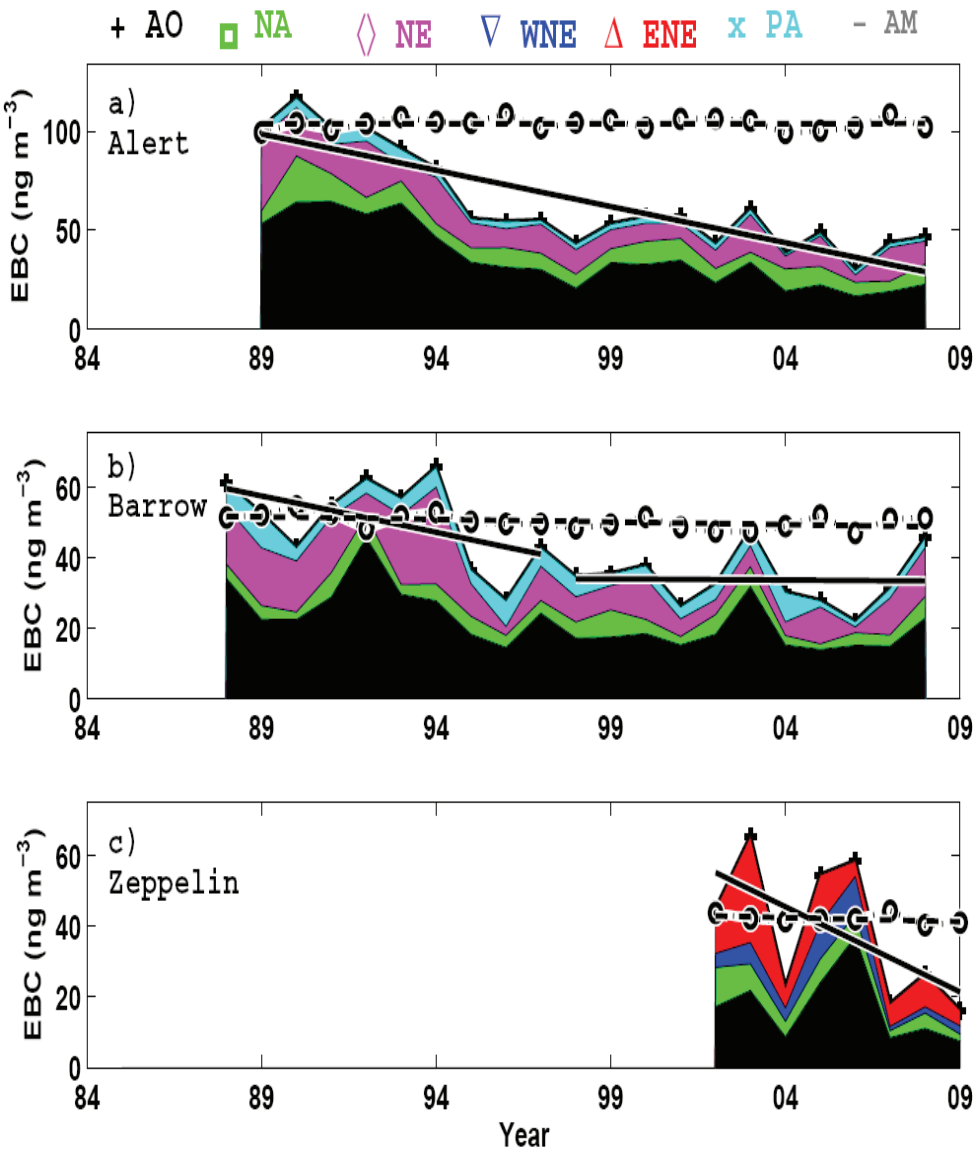

Figure 16. The annual mean EBC concentrations measured at Alert (a), Barrow (b), and Zeppelin (c) and split into contributions from the four transport clusters. The solid line shows the linear trend through the measured concentrations. The circles show the annual mean EBC concentrations when the cluster-mean concentrations are held constant over time (means over the first three years). This line is influenced only by changes in the frequencies of the four clusters. The dashed line shows the linear trend of these data.

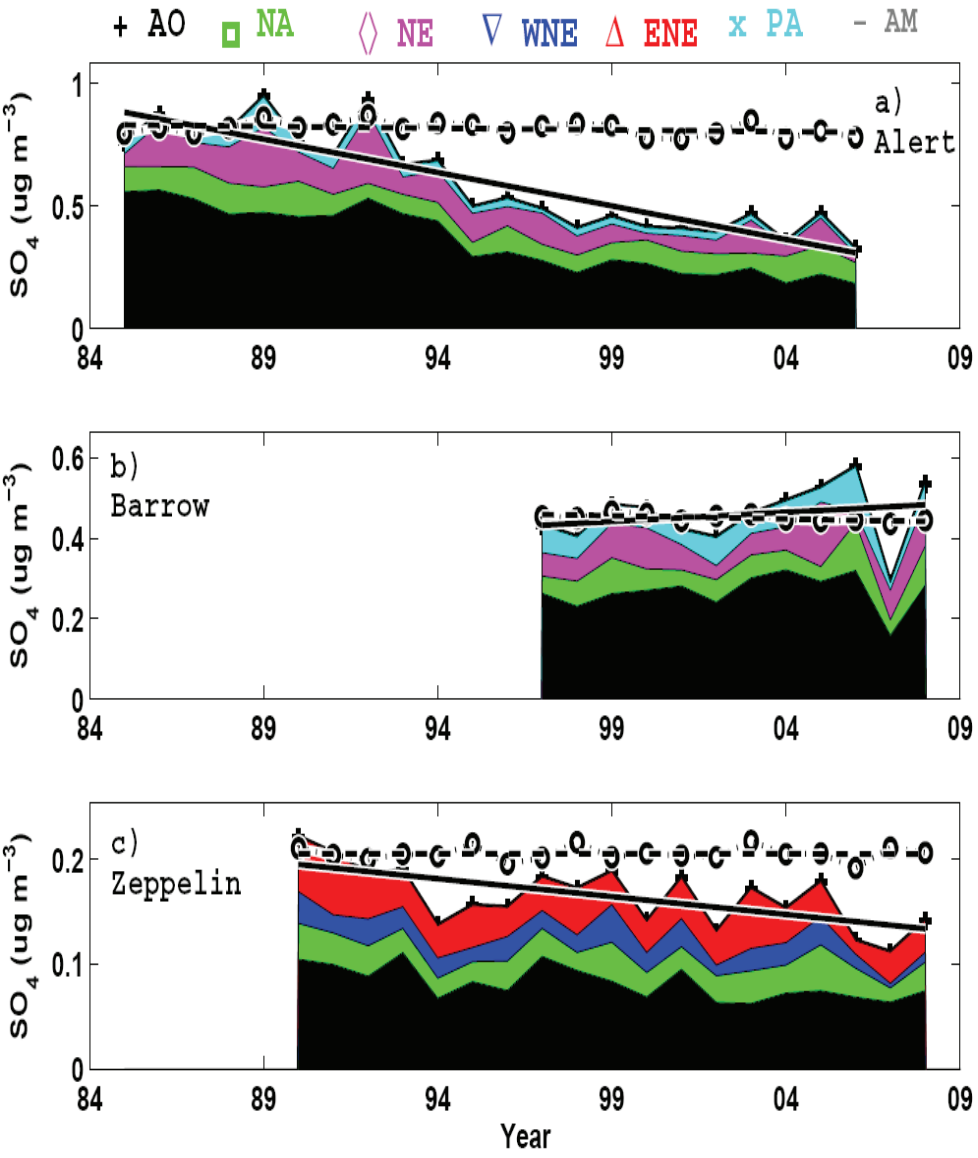

Figure 17. Same as Fig. 16 but for sulphate.